ANALYTICAL EVALUATION OF MODAL LOSS FACTORS AND RADIATION EFFICIENCY FOR RECTANGULAR PLATES

A THESIS

submitted in fulfilment of the
requirements for the award of the degree
of
DOCTOR OF PHILOSOPHY
in
MECHANICAL ENGINEERING

By

S. P. NIGAM

DEPARTMENT OF MECHANICAL AND INDUSTRIAL ENGINEERING
UNIVERSITY OF ROORKEE,
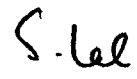ROORKEE (INDIA)

April 1975

C E R T I F I C A T E

Certified that the thesis entitled 'ANALYTICAL EVALUATION OF MODAL LOSS FACTORS AND RADIATION EFFICIENCY FOR RECTANGULAR PLATES' which is being submitted by Sri S.P.Nigam in fulfilment of the requirements for the award of the degree of DOCTOR OF PHILOSOPHY in Mechanical Engineering of the University of Roorkee is a record of candidate's own work carried out by him under the supervision and guidance of the undersigned. The matter embodied in this thesis has not been submitted for award of any other degree.

This is further certified that he has worked for a period of three years from February 1972 to February 1975 for preparing this thesis.

(G.K. Grover)
Associate Professor
Mechanical and Industrial
Engineering Department,
University of Roorkee,
    Roorkee.

(S.Lal)
Professor and Head,
Mechanical and Industrial
Engineering Department,
University of Roorkee,
    Roorkee.

Roorkee
April 11, 1975.

ACKNOWLEDGEMENTS

ABSTRACT

In this thesis, an analytical formulation of the modal loss factor has been done for the case of simply supported rectangular plate subjected to a point harmonic force of constant frequency.An attempt has been made to seeka generalisation for the internal damping of the plate for which the material damping constants J and N are known. Effects of changes in aspect ratio, thickness, material damping constants, and point force location on the modal damping for both the constant force and the constant amplitude excitations have been studied.The higher order modal damping has been correlated with the fundamental mode value in each case. Loss factors when the plate vibrates under complex resonance condition(more than one mode under simultaneous resonance) have also been evaluated. Thus the dependence of modal damping values on the different point excitations has been quantified.

Fundamental mode loss factors have been evaluated for the plates with different combinations of simply supported and clamped edge conditions.

Damping of a simply supported plate with thickness variation in one direction has been obtained with the help of Galerkin's method. Thickness variations of linear and parabolic type have been considered and the loss factor in each case has been correlated with that of uniform thickness case.

Number of practical simplified expressions have been evolved which would be useful in design type estimates of the loss factors for such plates vibrating in the fundamental as well as higher complex resonant modes.

Radiation efficiency and radiated sound power have been defined and analytically obtained for a simply supported plate when it vibrates under complex resonance and non-resonance conditions. This has been done by formulating Rayleigh's integral for the far-field sound pressure and giving due care to the modal phase shift while performing the modal superposition of the pressures.

C O N T E N T S

GLOSSARY

a — length of the plate

A_{11} — coefficient in the one term Galerkin solution for the response of a variable thickness plate

A'_{11}, A'_{21} — coefficients in the two term Galerkin solution for the response of a variable thickness plate

b — width of the plate

B — flexural rigidity $= Eh^3/12(1-\nu^2)$

B_o — $Eh_o^3/12(1-\nu^2)$

c — speed of sound in air

C_1, C_2 — coefficients which are functions of the plate size and taper parameter in the expression for A_{11}

D — unit damping energy of material i.e. energy dissipated per unit volume under uniform stress during one complete cycle of amplitude σ_a

D_{am} — unit damping energy of material at stress amplitude σ_a equal to the maximum value σ_{am}

D_p — total damping energy dissipation in a plate having a total effective volume V_p in which $\sigma_a \ll \sigma_{am} = D.V_p.\alpha$

e — aspect ratio $= a/b$

e' — changed value of aspect ratio

E — modulus of elasticity

g — acceleration due to gravity

G(x) — taper function

G_x, G_y — coefficients in Warburton's frequency equation

h — thickness of plate

h' — changed value of thickness

h_0 — thickness of the variable thickness plate at $x = 0$

H_x, H_y — coefficients in Warburton's frequency equation

i — imaginary quantity

I — far-field acoustic intensity

J — damping constant in the relation $D = J \sigma^N$

J' — damping constant of a different material

J_x, J_y — coefficients in Warburton's frequency equation

k — acoustic wave number $= \omega/c$

k_{mx} — X-component of flexural wave number $= m\pi/a$

k_{ny} — Y-component of flexural wave number $= n\pi/b$

k_1 — force ratio $= P'/P$

k_2 — amplitude ratio $= W'_{mn}/W_{mn}$

K — $(\eta\sigma_{am})_{mn}/(\eta\sigma_{am})_{11}$

m,n — mode numbers along X- and Y-axes

N — damping index

N' — damping index of a different material

p_ω — the far-field acoustic pressure

$P(x,y,t)$ — excitation force

P — amplitude of exciting force

P' — changed value of force

P_{mn} — modal loading coefficient

$r \qquad - \dfrac{JE}{\pi} \cdot \dfrac{\alpha}{\beta}$

$r_1 \qquad - \dfrac{J'E}{\pi} \cdot \dfrac{\alpha'}{\beta'}$

r_{av} — average radiation resistance under complex modes of excitation

R, θ, ϕ — spherical coordinates

S_{av} — average radiation efficiency

S_{mn} — modal radiation efficiency

t — time parameter

U — unit strain energy of a material at the maximum value of strain imposed

U_d — distortional strain energy $= (\dfrac{1+\nu}{3E}) \, \sigma_{ed}^2$

U_v — dilatational strain energy $= (\dfrac{1-2\nu}{6E}) \, \sigma_{ev}^2$

U_{mn} — modal deflection coefficient

U'_{mn} — changed value of the modal deflection coefficient

U_p — total strain energy in plate $= U \cdot V_p \cdot \beta$

V — volume of specimen having an amplitude of stress equal to or less than σ_a

V_p — total effective volume of the plate i.e. volume having a stress amplitude equal to or less than $\sigma_{am} = a.b.h$

V_{mn} — modal velocity coefficient for a resonant mode

V'_{mn} — modal velocity coefficient for a non-resonant mode

$V_\omega(x,y)$ — surface velocity distribution

$W(x,y,t)$ — deflection or the vibration amplitude in the plate

W_{mn} — maximum deflection in the plate vibrating in $(m,n)^{th}$ mode

W'_{mn} – changed value of the maximum deflection

(x,y,z) – cartesian coordinates

(x_1,y_1) – position of the eccentric point force

α – normalized damping energy integral for the plate

$$= \int_{\frac{\sigma_a}{\sigma_{am}}=0}^{1} \frac{D}{D_{am}} \cdot \frac{d(V/V_p)}{d(\sigma_a/\sigma_{am})} \cdot d\left(\frac{\sigma_a}{\sigma_{am}}\right)$$

α_0 – $k.a.\sin\theta.\cos\emptyset$

β – normalized strain energy integral for the plate

$$= \int_{\frac{\sigma_a}{\sigma_{am}}=0}^{1} \left(\frac{\sigma_a}{\sigma_{am}}\right)^2 \cdot \frac{d(V/V_p)}{d(\sigma_a/\sigma_{am})} \cdot d\left(\frac{\sigma_a}{\sigma_{am}}\right)$$

β_0 – $k.b.\sin\theta.\sin\emptyset$

γ_1 – roots of the equation $\tan(\gamma_1/2) + \tanh(\gamma_1/2) = 0$

γ_2 – roots of the equation $\tan(\gamma_2/2) - \tanh(\gamma_2/2) = 0$

Γ – proportional damping parameter in Hooker's formula

δ – linear taper parameter

ε – ratio of ($\eta\ \sigma_{am}$) for variable thickness plate to that of constant thickness plate

η – internal loss factor for the plate

η_{ac} – acoustic loss factor $= \rho_0 c\ S_{mn}/\rho h\omega$

η_c – loss factor for the constant thickness plate

η_{mn} – modal loss factor for $(m,n)^{th}$ mode

η'_{mn} – modal loss factor when a plate parameter changes

η^{*}_{mn} - modal loss factor for a reference plate of particular parameters

η_{T} - total loss factor under complex resonance excitation

η_{v} - loss factor for a variable thickness plate

λ_{mn} - frequency parameter $= \rho h a^{4} \omega^{2}_{mn} / B$

μ - parabolic taper parameter

ν - Poisson's ratio

ξ - ratio of principal stresses $= \dfrac{\sigma_{a_2}}{\sigma_{a_1}}$

ξ_{mn} - ratio of principal stresses at $x=a/2$, $y=b/2$, for $(m,n)^{th}$ mode

ρ - mass density of plate material

ρ_{o} - mass density of acoustic medium i.e. air

σ_{a} - amplitude of cyclic stress

σ_{a_1} - amplitude of larger principal stress

σ_{a_2} - amplitude of smaller principal stress

σ_{am} - amplitude of normal stress at location or position of maximum cyclic stress = maximum value of σ_{e}

σ_{e} - equivalent uniaxial stress that produces same damping energy dissipation as a specified state of multi-axial stress

σ_{ed} - effective stress from distortional energy view point $= (\sigma^{2}_{a_1} + \sigma^{2}_{a_2} - \sigma_{a_1}\sigma_{a_2})^{1/2}$

σ_{ev} - effective stress from dilatational energy view point $= (\sigma_{a_1} + \sigma_{a_2})$

σ_{x} - normal stress along X-axis

σ_y - normal stress along Y-axis

τ_{xy} - shear stress in X-Y plane

$\psi_{mn}(x,y)$ - eigen function or shape function for $(m,n)^{th}$ mode

ω - frequency of the exciting force

ω_{mn} - eigen value or the natural frequency for the plate for $(m,n)^{th}$ mode

π - total average acoustic power radiated from one side of the plate vibrating under complex mode

$\{\ \}$ - larger of the quantity within the braces

$\langle\ \rangle$ - space-time average of the quantity within the sign

∇^2 - Laplacian operator $= \left(\dfrac{\partial^2}{\partial x^2} + \dfrac{\partial^2}{\partial y^2}\right)$

∇^4 $- \nabla^2 \cdot \nabla^2 = \left[\dfrac{\partial^4}{\partial x^4} + 2\dfrac{\partial^4}{\partial x^2 \partial y^2} + \dfrac{\partial^4}{\partial y^4}\right]$.

σ_{eT} - Effective stress from total strain-energy viewpoint.

σ_{eTm} - Maximum value of σ_{eT}

LIST OF FIGURES

LIST OF TABLES

CHAPTER-1

INTRODUCTION

The study of vibration and accompanying sound radiation from a vibrating plate is of considerable interest to acoustical and mechanical engineers. For the case of untreated plate with no external connections, the energy input is partly dissipated in the form of internal losses and the remainder in the form of acoustical radiation. Therefore, the knowledge of internal and acoustical losses in a vibrating plate is of fundamental importance in order to predict and control the resonant response and the sound radiation.

As far as the internal damping of a material is concerned, one of the earliest studies was made by Robertson and Yorgiadis[61]. They studied experimentally the effect of different parameters on the damping capacity and gave an expression for equivalent stress which was in terms of maximum shear stress only. This was based on their proposition that the damping depends on distortion strain energy only. Marin and Stulen[47] developed a useful criterion for the design of resonance members which took into consideration not only the fatigue strength but the damping property as well. This was probably one of the earliest attempts to include damping property in design aspect. It was shown by Lazan and

-1-

Demer [33] that material damping may be sufficiently large to be highly significant as a limiter of resonance vibrations, even when significant structural and aerodynamic damping are present. Myklestad [55] gave the concept of complex damping which helped in the development of mathematical models for internal friction. An important contribution was made by Lazan [34], when he visualized the importance of the inherent damping of materials in limiting the resonant amplitude of the vibrating structures. He developed the longitudinal stress-distribution factor, the material factor and the cross-sectional stress distribution factor and studied the effect of damping constants on these factors. With the help of these factors damping studies for structural members could be undertaken. He lateron built up the normalized energy integrals and correlated them with these factors.

Yorgiadis [83] has obtained the expressions for the resonance stresses in non-uniformly as well as uniformly stressed members. Cochardt [5] has obtained certain functions which are similar to the factors as obtained by Lazan [34]. With the help of the stress distribution function - which depends on material only- Cochardt could obtain the internal damping of machine members. He also studied in a particular case, whether the low or high stress damping is more effective.

Mental and Fu[51] have indicated that in many cases the panel material itself provides the main source of damping energy dissipation, though in some cases the panel supports contribute significantly to the total damping. They have computed the damping of a square plate by using the maximum shear criterion a choice . for which sufficient justification was not given. Lazan[35] has discussed the various energy dissipating mechanisms in structures which contribute to the material damping under different conditions. He also formulated the normalized damping energy integral and the normalized strain energy integral and made use of them in evaluating the damping of a member. It was conjectured by Mentel [52] that in the case of plate vibrations - wherein dilatational straining generally accounts for a much larger share of the total straining action - it might also be found to be significant in material damping production. He proposed the inclusion of dilatational strain by means of a parameter in the equivalent stress expression which, till then, contained terms proportional to distortional strain only.

Whittier [81, 82] calculated the loss factor for a symmetrical circular plate and obtained a spread of 7 to 1 between the two bounding curves based on dilatational energy criterion and on distortional energy criterion for

the multi-axial stress system, considering the maximum

bending stress to be same in both the cases. He observed

the actual test data for the panel to lie within the

bounding regions and suggested an expression for the

equivalent stress which depends on both the effective

dilatational and distortional stresses. He proposed a

qualitative argument in support of the independence of

the energy dissipations based on dilatational and

distortional effects and thence proposed an idea of

limiting bounds in damping values due to these effects.

The manner in which these two effects combine is not

known. Considering the damped flexural vibrations in

beams and plates, Ungar [71] has obtained expressions for

maximum stresses at resonance. Heckl [24] has given a

method of estimating damping of plates- having beams

attached to it or having treatments- by formulating

absorption coefficients on the basis of architectural

acoustics.

It has been conjectured by Mentel and Chi [53]
that damping effects due to dilatational straining, small
enough to be masked by experimental scatter in the
usual test set-up, might be signficant under conditions
of pronounced dilatational straining such as can occur
in plate vibration. With the help of detailed experimenta-
tion they have obtained a small but definite contribution
to the material damping by dilatational straining action.

As a consequence, a modified formula for equivalent stress has been suggested by them.

Lazan[37] has discussed a modified theory for multiaxial stress systems for obtaining the equivalent stress. This is based on the stress-strain hysteretic behaviour of the materials. However, the expressions obtained do not degenerate to conventional expressions for simple combination of biaxial stresses as the derivation involves certain unjustified assumptions.

Hooker[25] has reviewed the work of different investigators [52,53,82,83] who gave different expressions for the equivalent stress which represents material damping in combined stress. He has pointed out that different investigators define the proportional factor, for taking into consideration the distortional and dilatational effects, in different ways. He also considered the two effects to be independent for want of limited experimental evidence. He compared the various expressions of the equivalent stresses as suggested by different investigators. After formulating general rules for such expressions, he proposed a simple expressions for the equivalent stress based on distortional and dilatational strain energies and on shear and dilatational stresses.

The average loss factor of a structure in a frequency band containing a number of resonant modes, has

been discussed in [10,13,14].

Hamme[22] has discussed the different material and techniques for damping vibrating panels. King[31] has described the general causes and remedies of vibration and noise as they occur in mechanisms and machines.

A general criterion in terms of mass, stiffness and damping for considering the effectiveness of a damping treatment was developed by Mead[49,50]. He has also dealt with the various kinds of excitations and discussed the advantages gained by adding damping treatments in different cases. He has shown that at higher frequencies damping may not have any effect on the sound radiation.

The normal mode shapes of a vibrating plate have been studied by Waller[77,78]. She has discussed the possibility of occurrence of 'combined' or 'compounded' normal vibration patterns and of degenerate modes which are mathematically possible. The natural frequencies of a rectangular plate with different boundary conditions are available in the classical work of Warburton [79]. Appl and Byers[1] have computed the natural frequencies of a linearly varying thickness plate for different combinations of the aspect ratio and the taper parameter. Jain and Soni[27] have evaluated the natural frequencies of a rectangular plate having a parabolic thickness variation in one direction.

larger than the sound wavelength in air. In this case, whenever the dimensions of the plate exceed bending wavelength, neither the internal damping nor the dimensions of the plate have any influence on the sound radiations. However, these parameters do have importance in the frequency region where bending wavelength is smaller than sound wavelength in air. Cremer and Schwantke [8] have studied the radiation of a plate when it forms a bounding surface of an enclosure into which the plate is radiating.

Skudrzyk [63,64,65] made an important contribution by his studies of vibration, sound radiation and of noise and vibration insulation of systems with finite or an infinite number of resonances. He gave expressions for sound pressure at different frequency ranges for vibrators with zero nodal lines and with many nodal lines. He also studied the sound radiation of a finite plate with nodal lines in the range of acoustic short circuit and obtained expressions for sound pressure generated by forced vibration of modes with low nodal lines. Beranek [3] has dealt with the problem of acoustic transmission through walls and panels in the audio-frequency range. He has also explained the phenomenon of wave coincidence and the occurrence of critical frequency. Kurtze and Bolt [32] have studied the effect of loading due to a medium of finite or infinite extent on the flexural wave speed in a plate. Heckl [23] has

shown that if an infinite plate is excited at a point, then the exponentially decaying flexural wave near field gives a small finite radiation. He has further shown that the same relation holds for damped plates of finite size, provided the damping is not small.

Lyamshev [39] observed-on the basis of reciprocity principles- that the sound pressure at a point in the fluid due to the motion of a structure subjected to distribution of mechanical forces can be determined from a knowledge of the acoustic pressure on the flexible structure due to a point source placed at the observation point in the presence of the flexible structure. Greene [20] experimentally studied the sound radiation from a freely supported rectangular plate. He obtained the sound pressure at different frequencies and observed that the sound field of a vibrating flat plate at the higher frequencies seems to result primarily from the forced vibration of the lower-order modes. The effect of plate damping on the sound level radiated at different frequencies was also considered.

Lyon and Maidanik [40] calculated the radiation resistance for some of the normal modes of a supported beam by considering the power flow between structural mode and a reverberant acoustic field. The response to

been discussed in [10,13,14].

Hamme[22] has discussed the different material and techniques for damping vibrating panels. King[31] has described the general causes and remedies of vibration and noise as they occur in mechanisms and machines.

A general criterion in terms of mass, stiffness and damping for considering the effectiveness of a damping treatment was developed by Mead[49,50]. He has also dealt with the various kinds of excitations and discussed the advantages gained by adding damping treatments in different cases. He has shown that at higher frequencies damping may not have any effect on the sound radiation.

The normal mode shapes of a vibrating plate have been studied by Waller[77,78]. She has discussed the possibility of occurrence of 'combined' or 'compounded' normal vibration patterns and of degenerate modes which are mathematically possible. The natural frequencies of a rectangular plate with different boundary conditions are available in the classical work of Warburton [79]. Appl and Byers[1] have computed the natural frequencies of a linearly varying thickness plate for different combinations of the aspect ratio and the taper parameter. Jain and Soni[27] have evaluated the natural frequencies of a rectangular plate having a parabolic thickness variation in one direction.

larger than the sound wavelength in air. In this case, whenever the dimensions of the plate exceed bending wavelength, neither the internal damping nor the dimensions of the plate have any influence on the sound radiations. However, these parameters do have importance in the frequency region where bending wavelength is smaller than sound wavelength in air. Cremer and Schwantke[8] have studied the radiation of a plate when it forms a bounding surface of an enclosure into which the plate is radiating.

Skudrzyk[63,64,65] made an important contribution by his studies of vibration, sound radiation and of noise and vibration insulation of systems with finite or an infinite number of resonances. He gave expressions for sound pressure at different frequency ranges for vibrators with zero nodal lines and with many nodal lines. He also studied the sound radiation of a finite plate with nodal lines in the range of acoustic short circuit and obtained expressions for sound pressure generated by forced vibration of modes with low nodal lines. Beranek[3] has dealt with the problem of acoustic transmission through walls and panels in the audio-frequency range. He has also explained the phenomenon of wave coincidence and the occurrence of critical frequency. Kurtze and Bolt[32] have studied the effect of loading due to a medium of finite or infinite extent on the flexural wave speed in a plate. Heckl[23] has

shown that if an infinite plate is excited at a point, then the exponentially decaying flexural wave near field gives a small finite radiation. He has further shown that the same relation holds for damped plates of finite size, provided the damping is not small.

Lyamshev[39] observed-on the basis of reciprocity principles- that the sound pressure at a point in the fluid due to the motion of a structure subjected to distribution of mechanical forces can be determined from a knowledge of the acoustic pressure on the flexible structure due to a point source placed at the observation point in the presence of the flexible structure. Greene[20] experimentally studied the sound radiation from a freely supported rectangular plate. He obtained the sound pressure at different frequencies and observed that the sound field of a vibrating flat plate at the higher frequencies seems to result primarily from the forced vibration of the lower-order modes. The effect of plate damping on the sound level radiated at different frequencies was also considered.

Lyon and Maidanik[40] calculated the radiation resistance for some of the normal modes of a supported beam by considering the power flow between structural mode and a reverberant acoustic field. The response to

sound and consequent sound radiation for one linear
resonant mode of a part of a larger structure were analysed
by Smith Jr. [66]. He also established a modal reciprocity
relation between the modal radiation resistance and the
transfer function which relates incident sound pressure
to modal force in the absence of motion. He has shown that
the response is governed by internal damping and radiation
resistance and gave a qualitative analysis.

Maidanik [42] made an important contribution by
his studies on the response of ribbed panels to rever-
berant acoustic fields. Following a statistical method,
it was shown by him, that the acceleration spectrum of the
vibrational field is related to the pressure spectrum by
a coupling factor which is a simple function of the
radiation and mechanical resistances of the structure.
Therefore, to predict the response of structure one
requires the values of both these resistances which consti-
·tute the total resistance. Maidanik considered the modal
resonant vibrations and the radiation resistance was
determined by calculating the power radiated by a vibrat-
ing panel by means of transform method. He also gave a
physical picture and concept of the corner, edge and
surface modes of radiation.

Lyon [41] computed the radiated sound power and the

radiation resistance of the acoustically slow waves in a plate which are scattered by a beam. Nikiforov[58] used integral transforms to calculate the energy radiated by a plate of finite dimensions with arbitrary boundary conditions as a function of the impedances loading the plate edges. Coupling of panel vibration and sound waves below critical frequency has been studied by Smith Jr.[67]. He has obtained the sound power and the radiation effi- ciency from clamped edges and from other boundaries as well. Manning and Maidanik[46] have shown that the radiation efficiencies of cylindrical shells and of plate could be adequately estimated from simple physical arguments based on considerations of the shape of typical modal patterns. They determined the radiation efficiencies on the basis of piston, strips and surface modes of panel vibrations. They also developed the overall radiation efficiency of the panel in a frequency band containing several resonant modes by means of simple averages and sums.

Gutin[21] has studied the sound radiation from an infinite plate excited by a normal point force but at low frequencies only. Maidanik and Kerwin Jr.[43] have considered the influence of fluid loading on the radiation from infinite plate driven by a normal point and by a normal line force, below the critical frequency.Feit[16]

has obtained the acoustic pressure radiated by an infinit
elastic plate excited by a harmonic point force or by a
moment for low as well as high frequency ranges. He has
made use of Timoshenko-Mindlin thick plate theory for
the case of frequencies above the coincidence frequency.
Maidanik[44] has studied the influence of fluid loading
on the radiation from orthotropic plates. He has distin-
guished between the fluid loading due to the subsonic
wave motion - appearing as an additional mass- and super-
sonic wave motion - occuring as an acoustic damping. While
investigating the latter part he has critically discussed
the 'free-field' and the 'forced field'. The effect of
internal and acoustic damping on propagating free radiat-
ing waves and non-propagating forced waves have also been
studied. Near sound field of an infinite plate driven by
a point force has been studied by Plakhov [59].

The problem of acoustic radiation from an infinite
plate with a baffle normal to its surface has been studied
by Mazzola [48]. Rao, et al.[60] experimentally studied
the near field sound pressures and vibrations from a
clamped plate and fixed-free beam. It was shown that these
measurements match well with the approximate theoretical
evaluations and the modal patterns and the resonant fre-
quencies could be predicted. Advantages associated with
acoustical measurement in regard to the prediction of
mode shape and frequency was pointed out. Sound pressures
from the thin, infinite plate excited by a point, line

and moment source have been studied by Ivanov and
Romanov [26] and by Gomperts [17]. Bailey and Fahy[2]
have studied the radiation from cylindrical beams which
are excited by sound waves.

Radiation resistances of a baffled beam and of
a simply supported rectangular panel have been theoretic-
ally determined by Wallace [75,76]. These have been
obtained for single modes from the total energy radiated
to the far field. Asymptotic solutions for the low frequency
region have been derived and curves covering the entire
frequency range for various mode shapes and aspect ratios
have been obtained through numerical integration. Approxi-
mate matching of his results with those obtained by
Maidanik has been indicated.

Chan and Anderton [4] have obtained a simple relation-
ship between the radiated noise and the mean square surface
averaged vibration level of cast machine structures.
Donato [11] and Dym[12] have obtained the radiation resis-
tance of a rectangular panel by direct application of
Rayleigh's radiation f ormula.

Mangirotty [45] explained the importance of the
internal damping which is due to hysteresis losses in the
material and the acoustic damping which results from the
reaction forces of the surrounding fluid on the radiating
surfaces of a structure. The acoustic damping of a single
flexible panel forming part of an otherwise rigid plane

baffle was predicted theoretically and measured experimentally by three different methods.

Johnston and Barr [28] conducted theoretical and experimental studies for the determination of damping at different frequencies for the case of freely supported beam specimens. Internal and acoustic damping were obtained by conducting tests in air and in vacuum and they showed that above a certain frequency the acoustic damping is responsible for a considerable frequency dependency of the overall loss factor. Crocker and Price [9] have studied the problem of sound transmission by using statistical energy analysis. They have brought out the importance of resonant and non-resonant transmission which depends upon the variation of internal and radiation resistance with frequency. They have shown, that, at low frequencies, where the radiation resistance is small, the resistance of the panel is mostly due to the internal resistance. At the critical frequency the resistance is mostly due to the radiation resistance, but well above coincidence the total resistance again normally becomes dominated by the internal resistance. The acoustically slow and fast modes of a vibrating panel have been well explained.

Crandall [6] has shown the general importance and applications of the internal dissipation and acoustic radiation damping. Fahy [15] has dealt in detail the

subject of structural-acoustic interaction. The effect of fluid loading, the acoustic and mechanical excitation of flat plates and cylindrical shells have been discussed by him. It has been pointed out that it is necessary to assess the relative importance of flexural near-field sound radiation and free-wave radiation because this factor decides the appropriate choice of methods of radiation reduction from mechanically excited structures. The most important parameter in this respect is the ratio of radiation resistance to the internal resistance.

A survey of the literature explicitly indicates the significant role of the internal and radiation resistance in the control of the resonant response and the sound radiation from a vibrating structure. Therefore, it becomes imperative for one to know the values of the internal loss factors and the radiation efficiencies at different excitation frequencies. A further look into the review indicates that no mathematical relationships exist giving the modal loss factors for rectangular plates of different types and sizes under mechanical excitation conditions. Although it is obvious (in view of the dependence of energy dissipation on the stress amplitude) that the modal damping values depend on the excitation distribution, no work is available which quantifies this dependence. No investigator has attempted to evaluate the internal loss factor for plates vibrating under complex resonance conditions. There is almost no literature on the

evaluation of internal loss factors for rectangular plates of variable thicknesses. Though the radiation efficiencies of a rectangular plate simply supported in a baffle-for single mode resonant and non-resonant excitations-have been obtained by different investigators but these efficiencies for the case of complex mode excitations under resonant and non-resonant conditions are not available. The present dissertation is in the direction of fulfilling these requirements.

A simply supported, thin, rectangular plate of homogeneous and isotropic material subject to a central point harmonic force has been considered. Starting from the known damping constants J and N of the material, the modal loss factors for the plate have been evaluated under constant force and constant amplitude excitation conditions. A simplified relationship between loss factors of fundamental and $(m,n)^{th}$ mode has been obtained. The material dampings for complex resonance conditions (those excitation frequencies where more than one mode is under resonance) have also been evaluated. A simple relationship between the total loss factor under this complex resonance condition and individual loss factors has been derived. Effects of changes in thickness, aspect ratio, material damping constants and position of the point force, on the internal loss factor have been studied quantitatively. Simple relations have been derived which correlate the loss factor values with the corresponding values of a known plate.

Effect of clamping the edges of a simply supported

plate, on the fundamental mode loss factors has also been
studied. The fundamental mode loss factors for the
variable thickness plate whose thickness varies in one
direction according to linear and parabolic laws have also
been obtained by Galerkin's method. A relationship has been
established between these values and the damping of plates
of uniform thickness.

The average radiation efficiencies under complex
resonant and non-resonant excitation conditions of a constant
thickness rectangular plate, simply supported in a baffle,
have been obtained by calculating the energy radiated to the
far field. This has been done by performing the modal super-
position of the far-field acoustic pressures. The effect of
superposition of any number of modes on the radiation efficiency
and radiated sound power have been studied. The variations
in average radiation efficiency and sound power with the
excitation frequency below the critical frequency, have also
been studied.

The objectives of the investigation reported here
have been four-fold. First, to study quantitatively the
dependence of the modal damping of rectangular plates on
the excitation distribution and the effect of various para-
meters including the thickness variation on the modal loss
factors. Second, to obtain practical simplified expressions
relating higher mode damping to the fundamental value under
different conditions. Third, to obtain the loss factors and
radiation efficiencies when the plate vibrates under complex
resonance conditions. Fourth, to evaluate the radiation
efficiencies for the plate vibrating under complex non-
resonance excitation conditions.

CHAPTER-2

BASIC THEORY

2.1 EQUATION OF MOTION OF SIMPLY SUPPORTED RECTANGULAR PLATE OF UNIFORM THICKNESS

The classical equation of transverse motion of thin, elastic plates of constant thickness and of isotropic and homogeneous material, is given by [38,74]

$$B \nabla^4 W + \rho h \frac{\partial^2 W}{\partial t^2} = P(x,y,t) \qquad \ldots (2.1.1)$$

For harmonic excitation of the plate, one may write

$$P(x,y,t) = P(x,y) \, e^{i\omega t} \qquad \ldots (2.1.2)$$

Further, assuming a harmonic response, the deflection is given by

$$W(x,y,t) = W(x,y) \, e^{i\omega t} \qquad \ldots (2.1.3)$$

Damping is taken into consideration by allowing the flexural rigidity to take complex form [68,71]. Substituting Eqs.(2.1.2) and (2.1.3) in equation (2.1.1), one gets

$$B(1+i\eta) \nabla^4 W(x,y) - \rho h \omega^2 W(x,y) = P(x,y) \qquad \ldots (2.1.4)$$

It can be shown, that, an eigen function $\psi_{mn}(x,y)$ exists for each eigen value ω_{mn} satisfying

$$B \nabla^4 \psi_{mn} - \rho h \omega_{mn}^2 \psi_{mn} = 0 \qquad \ldots (2.1.5)$$

where the eigen functions and eigen values for various sets of boundary conditions of rectangular plates are obtained from [79].

One could write the load distribution, as

$$P(x,y) = \sum_{m,n=0}^{\infty} P_{mn} \psi_{mn} \qquad \ldots (2.1.6)$$

and the plate deflection, as

$$W(x,y) = \sum_{m,n=0}^{\infty} U_{mn} \psi_{mn} \qquad \ldots (2.1.7)$$

Because of orthogonality of the eigen functions, one gets the expression for P_{mn} as

$$P_{mn} = \frac{\iint P(x,y) \psi_{mn} \, dx dy}{\iint \psi_{mn}^2 \, dx \, dy} \qquad \ldots (2.1.8)$$

Combining Eqs.(2.1.4), (2.1.6) and (2.1.7) one obtains

$$\frac{P_{mn}}{U_{mn}} = B(i+i\eta) \frac{\nabla^4 \psi_{mn}}{\psi_{mn}} - \rho h \omega^2 \qquad \ldots (2.1.9)$$

From Eqs.(2.1.5) and (2.1.9) one gets

$$\frac{P_{mn}}{U_{mn}} = \rho h \left[(1+i\eta)\omega_{mn}^2 - \omega^2 \right] \qquad \ldots (2.1.10)$$
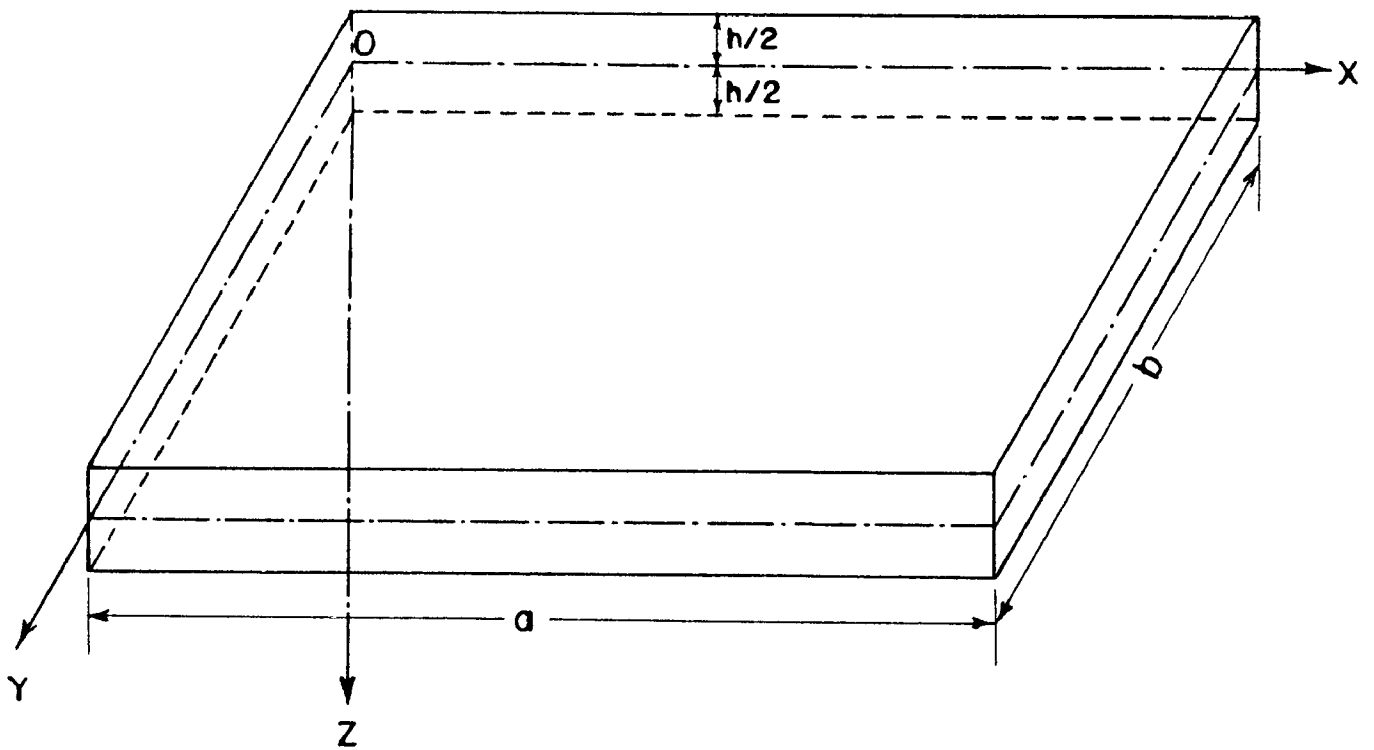
FIG. 2·1 CO-ORDINATE SYSTEM OF RECTANGULAR PLATE

further analysis, since the remainder term in the right hand side gives the amplitude of the displacement at different points, and the amplitude stresses depend upon the amplitude displacement. Also 1/i indicates the 90° phase between the resonant response and the excitation and is dropped hence onwards in the analysis.

Now, the stresses at a point in the plate which depend upon the displacement of the corresponding points can be obtained from

$$- \frac{h^3}{12ZB} \sigma_x = \left[\frac{\partial^2 W}{\partial x^2} + \nu \frac{\partial^2 W}{\partial y^2} \right]$$

$$- \frac{h^3}{12ZB} \sigma_y = \left[\nu \frac{\partial^2 W}{\partial x^2} + \frac{\partial^2 W}{\partial y^2} \right]$$

$$\frac{h^3}{12ZB} \tau_{xy} = (1-\nu) \frac{\partial^2 W}{\partial x \partial y} \qquad \dots (2.1.17)$$

and are as follows

$$\eta_{mn}\sigma_x = \frac{48PZe}{\pi^2 h^3} \left[\frac{(m^2 + \nu e^2 n^2)}{(m^2 + e^2 n^2)^2} \right] \sin\left(\frac{m\pi x}{a}\right) \sin\left(\frac{n\pi y}{b}\right)$$

$$\eta_{mn}\sigma_y = \frac{48PZe}{\pi^2 h^3} \left[\frac{(\nu m^2 + e^2 n^2)}{(m^2 + e^2 n^2)^2} \right] \sin\left(\frac{m\pi x}{a}\right) \sin\left(\frac{n\pi y}{b}\right)$$

$$\eta_{mn}\tau_{xy} = \frac{48PZe^2(1-\nu)}{\pi^2 h^3} \left[\frac{mn}{(m^2 + e^2 n^2)^2} \right] \cos\left(\frac{m\pi x}{a}\right) \cos\left(\frac{n\pi y}{b}\right)$$

$$\dots (2.1.18)$$

The principal stresses can be obtained from

$$\eta_{mn}\sigma_{a_1, a_2} = \frac{|\eta_{mn}\sigma_x| + |\eta_{mn}\sigma_y|}{2} \pm \left[\left(\frac{|\eta_{mn}\sigma_x| - |\eta_{mn}\sigma_y|}{2} \right)^2 + (\eta_{mn}\tau_{xy})^2 \right]^{1/2}$$

... (2.1.19)

Thus, the stress distribution in terms of η_{mn} times principal stresses are obtained when the plate is vibrating under $(m,n)^{th}$ resonance mode.

2.2 CRITERIA FOR EQUIVALENT UNIAXIAL STRESS

The damping of a member subjected to a multi-axial stress system can be obtained from the damping properties of the material of which the member is made of, by incorporating an equivalent uniaxial stress σ_e. This stress is conceptually considered to represent a state of multi-axial stress provided the damping energy dissipation is same in both the cases, such that

$$D(\sigma_e) = D(\sigma_{a_1}, \sigma_{a_2})$$

... (2.2.1)

Number of theories or criteria for determining σ_e have been developed by different investigators [52,53,82,83]. Lazan[37] has reviewed these in detail and Hooker [25] has critically examined them and proposed the following relationship which is based on contributions by distoritional and dilatational strain energies:

$$\sigma_e^N = (1 - \Gamma) \sigma_{ed}^N + \Gamma \sigma_{ev}^N$$

... (2.2.2)

In this expression $\Gamma = 0$ indicates damping dependent on distortional strain energy only and $\Gamma = 1$ indicates the damping dependent on dilatational strain energy only. For a particular problem, Hooker has suggested that Γ is to be estimated experimentally. Whittier [37] argued that the dilatational and distortional effects are independent- a fact which was supported by Hooker [25] for want of proper experimental evidence against it. Under this circumstances $\Gamma = 1$ and $\Gamma = 0$ would lead to upper and lower bounds for the loss factor, respectively.

In the case of rectangular plates, shear effects are known to be small and as such dilatational strain energy criterion for obtaining the equivalent uniaxial stress is made use of in the present work.

The expressions for the equivalent uniaxial stress based on distortional strain energy is given by [37]

$$\sigma_e = \sigma_{a_1} (1 - \xi + \xi^2)^{1/2} \qquad \ldots (2.2.3)$$

and based on dilatational strain energy is given by

$$\sigma_e = \sigma_{a_1} (1 + \xi) \qquad \ldots (2.2.4)$$

2.3 MODAL LOSS FACTOR FOR A RESONANT MODE

Once the equivalent uniaxial stress at every point on the plate is known, the problem of evaluating the modal resonant loss factor of the damped plate which is subjected to multiaxial stress system, reduces to one which is subjected to equivalent uniaxial stress system. The internal damping of the plate can then be evaluated as follows [37]:

The total strain and damping energies of the plate are given by

$$U_p = \sum \frac{\sigma_{eT}^2}{2E}.dv$$

and
$$D_p = \sum J \sigma_e^N.dv$$

where σ_{eT} the effective stress from total strain energy view point is given by

$$\sigma_{eT} = \sigma_{a_1} (1-2\nu\xi + \xi^2)^{1/2} \qquad \qquad \ldots \ (2.3.1)$$

provided the plate is imagined to be constituted of a very large number of small rectangular elements, each of volume dv, and having an equivalent stress σ_e at the center of each element.

The loss factor is given by

$$\eta = \frac{D_p}{2 \pi U_p} \qquad \qquad \text{... (2.3.2)}$$

Observing that Eqs. (2.2.3) or (2.2.4) would give a stress distribution in terms of $\eta \, \sigma_e^-$, one gets

$$\eta = \left(\frac{JE}{\pi}\right)^{\frac{1}{(N-1)}} \left[\frac{\sum (\eta \, \sigma_e^-)^N}{\sum (\eta \, \sigma_{eT}^-)^2} \right]^{\frac{1}{(N-1)}}$$

which for the case of equivalent stress based on dilatational strain energy dissipation becomes

$$\eta = \left(\frac{JE}{\pi}\right)^{\frac{1}{(N-1)}} \left[\frac{\sum (\eta \, \sigma_{a_1})^N (1+\xi)^N}{\sum (\eta \, \sigma_{a_1})^2 (1-2\nu\xi + \xi^2)} \right]^{\frac{1}{(N-1)}} \qquad \text{... (2.3.3)}$$

The loss factor can also be determined by evaluating the integrals α and β. For this, polynomial curve fittings of (V/V_p) vs. (σ_e/σ_{am}) - for evaluating α - and of (V/V_p) vs. $(\sigma_{eT}/\sigma_{eTm})$ - for evaluating β - are to be made.

Thus,

$$\eta = \left(\frac{JE}{\pi}\right) \left(\frac{\alpha}{\beta}\right) \frac{\sigma_{am}^N}{\sigma_{eTm}^2} \qquad \qquad \text{... (2.3.4)}$$

Here, σ_{am}^{-} is the maximum value of σ_{e}^{-} and σ_{eTm}^{-} is the maximum value of σ_{eT}^{-} in the stress distribution of the plate. Above equation modifies as

$$\eta = \left(\frac{JE}{\pi}\frac{\alpha}{\beta}\right)^{\frac{1}{(N-1)}} \left[\frac{(\eta\sigma_{am}^{-})^{N}}{(\eta\sigma_{eTm}^{-})^{2}}\right]^{\frac{1}{(N-1)}} \qquad \dots (2.3.5)$$

2.4 CHOICE OF ELEMENTS

In order to make use of the equations derived in the previous section, one should know the distribution of the equivalent uniaxial stress throughout the plate volume. For this purpose the plate is conceptually thought to be divided into a large number of small rectangular elements. The choice of the elements is dictated by the fact that the waveform of the plate vibrating in any mode (m,n) would be symmetrical about the central lines. Since the stress distribution along the thickness of the plate is triangular about the mid-neutral,plane, it is

(a)

(b)
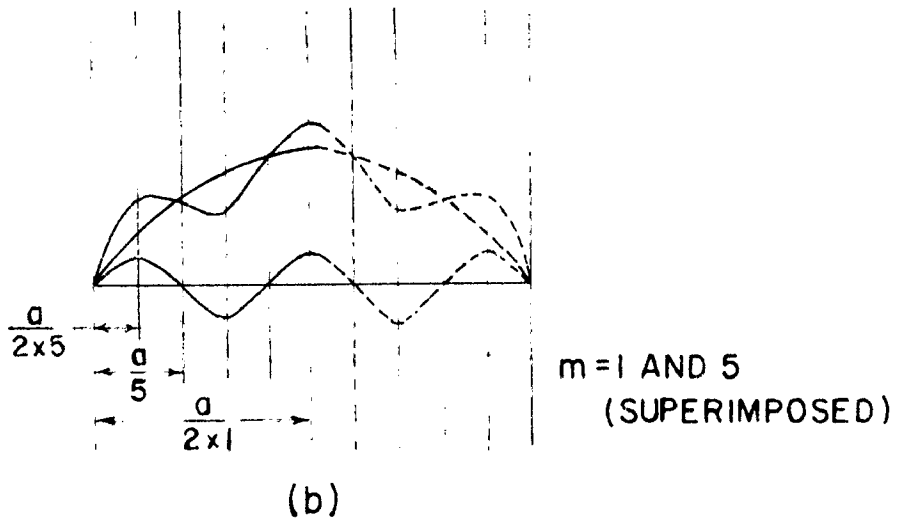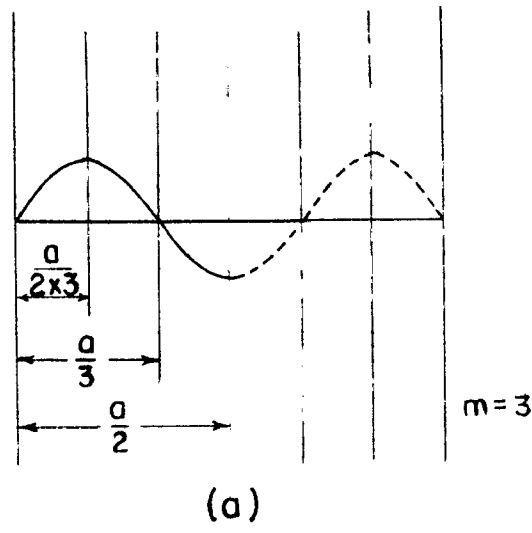
FIG. 2·2 VIBRATION AMPLITUDE WAVE FORMS

must have the same sign in each mode. Hence, the express-
ions, within the summation sign, are to be multiplied by
+1 or -1 as required to ensure correct phases.

The principal stresses and thence the equivalent
uniaxial stress σ_e are obtained as before. The loss factor
η_T under complex resonant mode is now computed from

$$\eta_T = (\frac{JE}{\pi}) \left[\frac{\sum \sigma_e^N}{\sum \sigma_{eT}^2} \right] \qquad \ldots \text{ (2.5.2)}$$

As regards the selection of **element** in this case,
it would be observed from Fig.2.2b, that, due to super-
position of two or more different modal waves, the stress
values are to be calculated upto a/2 and b/2. However,
the overall symmetry in the stress distribution pattern
sould still exist about the central lines of the plate.
The element size would be governed by the largest values
of m and n within the group of (m,n) order modes whose
superposition effect is to be studied. For this analysis
two elements were chosen in a quarter of the wave corres-
ponding to the highest order m i.e. m_{max} and to the highest
order n i.e. n_{max}, giving the element size

$$dv = \frac{a}{4\ m_{max}} \times \frac{b}{4 n_{max}} \times \frac{h}{8}$$

2.6 EQUATION OF MOTION OF SIMPLY SUPPORTED RECTANGULAR PLATE OF VARIABLE THICKNESS

The differential equation of a free, undamped motion of a rectangular plate of isotropic, homogeneous material with no inplane forces and having a variable thickness is given by[1]:

$$B \nabla^4 W + 2 \frac{\partial B}{\partial x} \frac{\partial}{\partial x} \nabla^2 W + 2 \frac{\partial B}{\partial y} \frac{\partial}{\partial y} \nabla^2 W + \nabla^2 B \nabla^2 W - (1-\nu) \left(\frac{\partial^2 B}{\partial x^2} \frac{\partial^2 W}{\partial y^2} \right.$$
$$\left. -2 \frac{\partial^2 B}{\partial x \partial y} \frac{\partial^2 W}{\partial x \partial y} + \frac{\partial^2 B}{\partial y^2} \frac{\partial^2 W}{\partial x^2} \right) + \rho h \frac{\partial^2 W}{\partial t^2} = 0 \qquad \qquad \dots (2.6.1)$$

If thickness varies only in one direction, say X, Fig.2.3, then the plate equation for forced vibration with a forcing function $P(x,y,t)$ reduces to

$$B \nabla^4 W + 2 \frac{dB}{dx} \frac{\partial}{\partial x} \nabla^2 W + \frac{d^2 B}{dx^2} \left[\frac{\partial^2 W}{\partial x^2} + \nu \frac{\partial^2 W}{\partial y^2} \right] + \rho h \frac{\partial^2 W}{\partial t^2} = P(x,y,t)$$
$$\dots (2.6.2)$$

Considering the excitation to be harmonic, postulating the motion W to be of similar type and introducing the damping by permitting rigidity to take complex value, as was done in section 2.1, one gets

$$(1+i\eta) \left[B \nabla^4 W + 2 \frac{dB}{dx} \frac{\partial}{\partial x} \nabla^2 W + \frac{d^2 B}{dx^2} \left(\frac{\partial^2 W}{\partial x^2} + \nu \frac{\partial^2 W}{\partial y^2} \right) \right] - \rho h \omega^2 W = P(x,y)$$
$$\dots (2.6.3)$$

Let the thickness variation in X-direction be given by
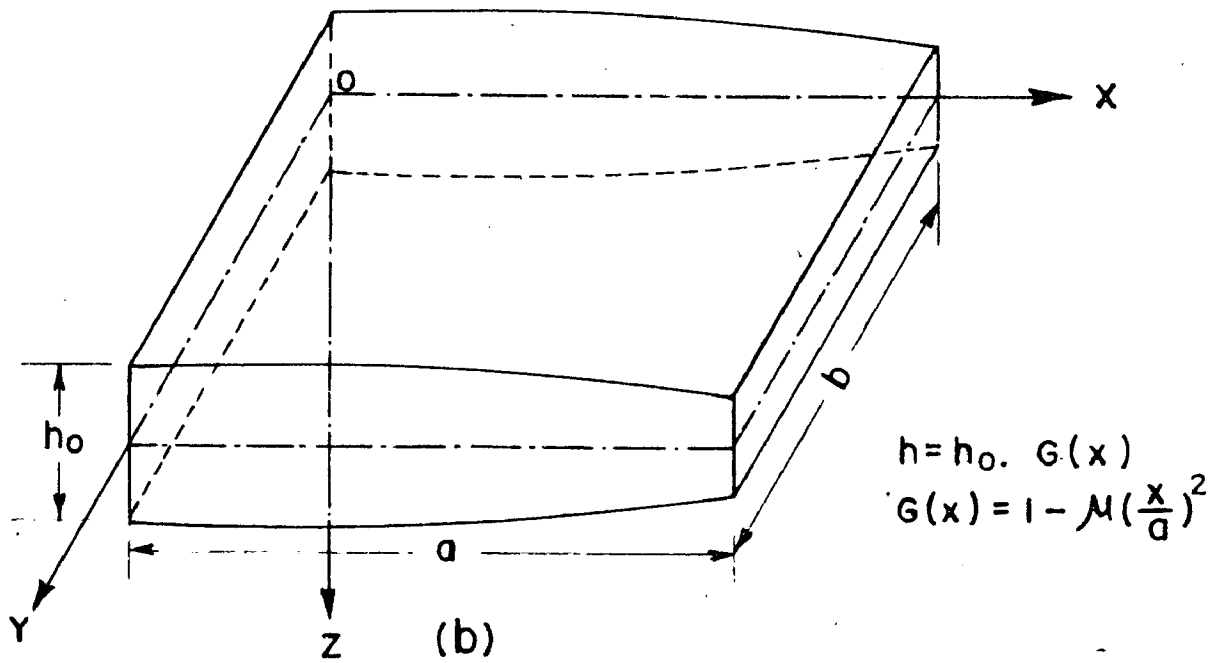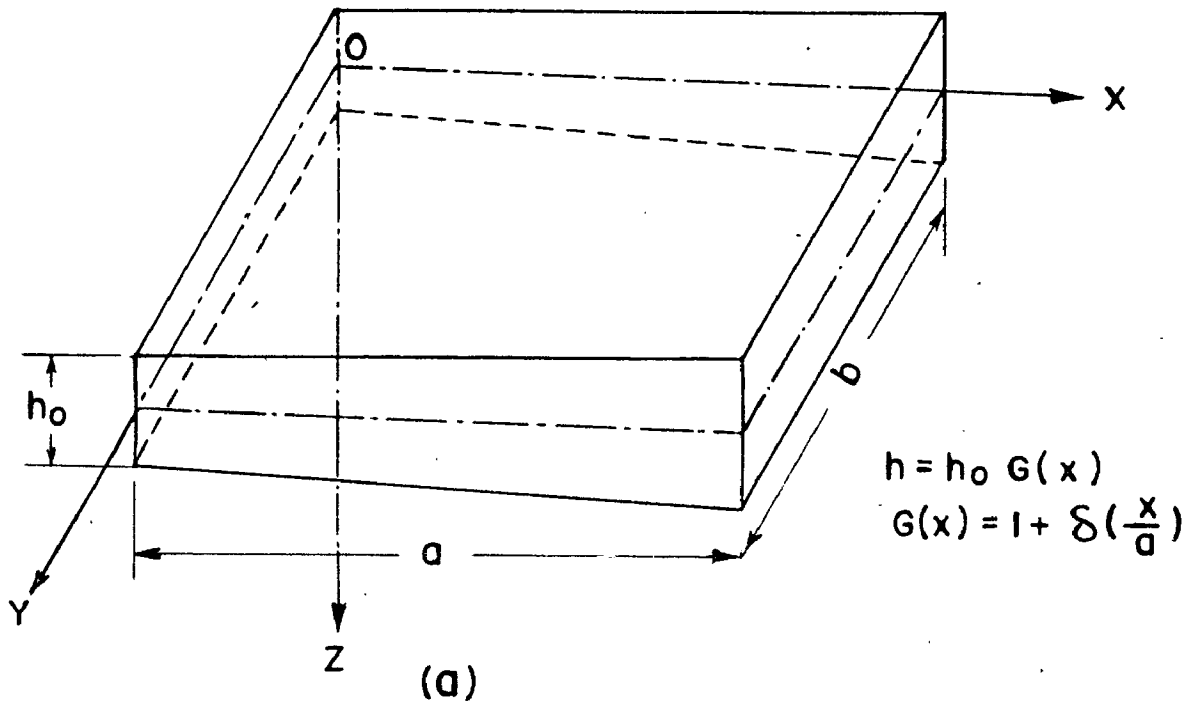
FIG. 2·3 RECTANGULAR PLATE—THICKNESS VARIATION IN X—DIRECTION.

$$h = h_0 G(x) \qquad \qquad \dots (2.6.4)$$

where, for linear thickness variation

$$G(x) = 1 + \delta\left(\frac{x}{a}\right) \qquad \qquad \dots (2.6.5)$$

and, for parabolic thickness variation

$$G(x) = 1 - \mu\left(\frac{x^2}{a^2}\right) \qquad \qquad \dots (2.6.6)$$

Also, the rigidity term is given by

$$B = B_0\left[\, G(x) \,\right]^3 \qquad \qquad \dots (2.6.7)$$

Consider the case of the above plate having all the four edges as simply supported, then the response and the load term are written as,

$$W(x,y) = \left[\sum_{m=1}^{m} A_{m1} \, \mathrm{Sin}\left(\frac{m\pi x}{a}\right)\right] \mathrm{Sin}\left(\frac{\pi y}{b}\right) \qquad \dots (2.6.8)$$

$$P(x,y) = \left[\sum_{m=1}^{m} P_{m1} \, \mathrm{Sin}\left(\frac{m\pi x}{a}\right)\right] \mathrm{Sin}\left(\frac{\pi y}{b}\right) \qquad \dots (2.6.9)$$

since the thickness variation is in X-direction only. For the central point harmonic force of amplitude P, one observes, that

$$\begin{aligned} P_{m1} &= \frac{4P}{ab} \qquad \text{for } m = \text{odd} \\ &= 0 \qquad \text{for } m = \text{even} \end{aligned} \qquad \dots (2.6.10)$$

Let the plate vibrate in its fundamental resonant mode. Using the Galerkin's Method, one obtains approximate one term and two term solutions as,

$$W = A_{11} \, Sin(\tfrac{\pi x}{a}) Sin(\tfrac{\pi y}{b}) \qquad\qquad \text{... (2.6.11)}$$

and $\qquad W' = \left[A'_{11} \, Sin(\tfrac{\pi x}{a}) + A'_{21} Sin(\tfrac{2\pi x}{a}) \right] \, sin(\tfrac{\pi y}{b}) \quad \text{... (2.6.12)}$

Load term in both the cases is assumed as $\tfrac{4P}{ab} \, Sin(\tfrac{\pi x}{a}) \, sin(\tfrac{\pi y}{b})$ which is supposed to excite fundamental mode under resonance condition. After evaluating the Galerkin's coefficients A_{11}, A'_{11} and A'_{21} the one term and two term responses are obtained. The loss factor is then evaluated by following the steps as laid down in previous sections.

2.7 SOUND RADIATION UNDER COMPLEX MODES

The sound power radiated by a vibrating plate depends on the details of surface velocity distribution and the value of the radiation efficiency at that frequency of vibration. These values are available in literature when the plate is vibrating in a single mode whether resonant or non-resonant. For the complex modes of vibration - both resonant and non-resonant - these quantities are to be evaluated by superposing the individual modal contributions after giving due consideration to their phases.

If the plate vibrates in a fluid medium then the fluid exerts a radiation load on the plate which would normally modify the distributed loading and introduce a 'feed-back' fluid-structure coupling. When the fluid medium happens to be the atmosphere, the radiation loading is generally small enough to have a negligible effect on the

structural vibrations, because of the low density of
air as compared to structural materials [29]. Thus, in
such situations, the dynamic response of a structure in
the atmosphere, excited by prescribed driving forces,
can be determined as though the structure were vibrating
in vacuum. Therefore, the eigen shape functions and the
corresponding natural frequencies of the in-vacuo modes
of plate vibration do not get modified when the plate
vibrates in air.

The surface velocity distribution over a rectangular
plate, simply supported in an infinite baffle is given by

$$V_\omega (x,y) = \sum_{m,n=0}^{\infty} V_{mn} \Psi_{mn} (x,y) \qquad \dots (2.7.1)$$

The modal velocity coefficients are related to modal dis-
placement coefficients by the following simple relation

$$V_{mn} = i\omega U_{mn} \qquad \dots (2.7.2)$$

Combining Eqs.(2.1.12), (2.1.15) and (2.7.2) one gets,
for a central point force excitation of a resonant mode,
when $\omega = \omega_{mn}$,

$$V_{mn} = \frac{4P}{ab\rho h \; \eta_{mn}\omega_{mn}} \qquad \dots (2.7.3)$$

From Eqs.(2.1.10), (2.1.15) and (2.7.2) one obtains for
a non-resonant mode (damping being low)

$$V'_{mn} = i \; \frac{4P\omega}{ab\rho h (\omega_{mn}^2 - \omega^2)} \qquad \dots (2.7.4)$$

Now, temporal and spatial average of the square of the surface velocity is given by

$$\langle |V_\omega|^2 \rangle = \frac{1}{ab} \int_o^b \int_o^a \frac{1}{2} |V_\omega|^2 \, dx \, dy \qquad \ldots (2.7.5)$$

For a single mode under resonance,

$$V_\omega = V_{mn} \, Sin(\frac{m\pi x}{a}) \, Sin(\frac{n\pi y}{b}) \qquad \ldots (2.7.6)$$

and, therefore, one obtains

$$\langle |V_\omega|^2 \rangle = \frac{1}{8} V_{mn}^2 \qquad \ldots (2.7.7)$$

For complex resonance excitation condition, one has

$$V_\omega = \sum_{m=1}^{m} \sum_{n=1}^{n} V_{mn} \, sin(\frac{m\pi x}{a}) \, sin(\frac{n\pi y}{b}) \qquad \ldots (2.7.8)$$

and therefore, one gets after neglecting the effect of the cross coupling between the modal damping

$$\langle |V_\omega|^2 \rangle = \sum_{m=1}^{n} \sum_{n=1}^{n} \frac{1}{8} V_{mn}^2 \qquad \ldots (2.7.9)$$

When the effect of large number of non-resonant modes is to be considered, then,

$$V_\omega = \sum \sum V_{mn}' \, Sin(\frac{m\pi x}{a}) \, Sin(\frac{n\pi y}{b})$$

and,

$$\langle |V_\omega|^2 \rangle = \sum_{m=1}^{m} \sum_{n=1}^{n} \frac{1}{8} |V_{mn}'|^2 \qquad \ldots (2.7.10)$$

Finally, for the case of superposition of resonant and non-resonant modes, the velocity distribution is given by,

$$V_\omega = \sum \sum \left[V_{mn} \, \text{Sin}(\tfrac{m\pi x}{a}) \, \text{Sin}(\tfrac{n\pi y}{b}) + V'_{mn} \, \text{Sin}(\tfrac{m\pi x}{a}) \, \text{Sin}(\tfrac{n\pi y}{b}) \right]$$

and, $\langle |V_\omega|^2 \rangle = \sum \sum \tfrac{1}{8}(V_{mn}^2 + |V'_{mn}|^2)$ ... (2.7.11)

Defining the average radiation resistance r_{av} as

$$r_{av} = \frac{\Pi}{\langle |V_\omega|^2 \rangle}$$ ... (2.7.12)

where Π is the total average acoustic power radiated from one side of the panel vibrating under complex resonance or non-resonance condition and the temporal and spatial overage of the square of the surface velocity would be given by Eqs.(2.7.9) or (2.7.10) or (2.7.11) depending upon the nature of modes under consideration, one obtains the average radiation efficiency, S_{av}, as

$$S_{av} = \frac{\Pi}{\rho_o c \, a \, b \, \langle |V_\omega|^2 \rangle}$$ ... (2.7.13)

The far-field acoustic pressure radiated by a baffled plate can be obtained from Rayleigh's integral[29] and is given by

$$p_\omega = -ik\rho_o c \, \frac{e^{ikR}}{2\pi R} \int_0^b \int_0^a V_\omega(x,y) \, \exp\left[-i(\tfrac{\alpha_o x}{a}) - i(\tfrac{\beta_o y}{b})\right] dxdy$$

     ... (2.7.14)

where $V_{\omega}(x,y)$ is as given in Eq.(2.7.8) and the plate coordinate system is shown in Fig.2.4. It is to be noted that while making use of the above equation, the modal pressure contributions are to be summed up after giving due considerations to their individual phases. In this connection, it would be easily observed, that, for the combined case of resonant and non-resonant modes it is the square of the modal pressures which are to be added up. However, for the case of superposition of resonant modes or for non-resonant modes only, the modal pressures can be algebraically added up. This would be evident, if one remembers, that,

$$p^2 = p_1^2 + p_2^2 + 2p_1p_2\cos\theta,$$

where θ is the phase angle between the two superimposing modes.

Starting from p_{ω} one obtains the far-field acoustic intensity I and then the sound power Π. Thus the average radiation efficiency and the total average acoustic power radiated by a plate vibrating under complex modes is obtain and effect of superposition of any number of modes on them, can be studied.
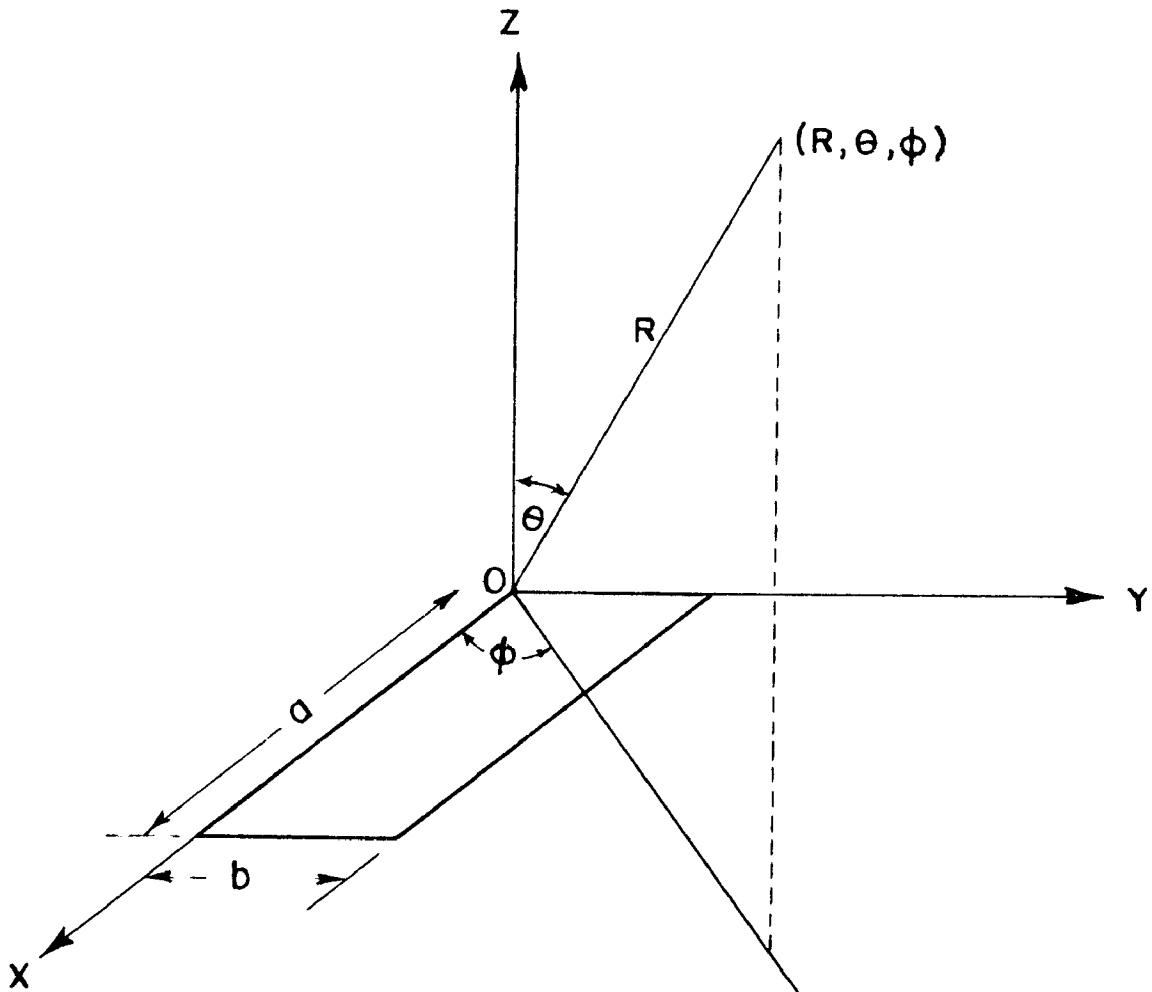
FIG. 2·4 PLATE CO-ORDINATE SYSTEM
FOR SOUND RADIATION.

CHAPTER-3

LOSS FACTOR FOR SIMPLY SUPPORTED
RECTANGULAR PLATE

3.1 MODAL LOSS FACTOR FOR A SINGLE RESONANT
MODE UNDER CONSTANT FORCE EXCITATION

The method discussed in the previous chapter makes
.it possible to evaluate the loss factor for the plate
for any resonant mode (m,n). A factor 'K' has been obtained
which relates the modal damping of any higher order
resonant mode with that of the fundamental mode. With
the help of this factor the higher order mode damping is
obtained directly without going into the cumbersome
computations everytime, once the fundamental mode loss
factor has been computed.

This factor 'K' is defined as the ratio of $(\eta\sigma_{am})^N / (\eta\sigma_{eTm})^2$
for the $(m,n)^{th}$ mode to that of fundamental mode. It is
easily seen from Eqs.(2.1.18), (2.1.19) and (2.2.4), that,
for a mode, the maximum value of the proportional stress
$(\eta\sigma_{am})$ in the plate would be either equal to $(\eta\ \sigma_x)_{max}$ or
$(\eta\sigma_y)_{max}$ depending on which one is larger. Further, it
can be noted from Eq.(2.1.18), that,

$$(\eta_{mn}\sigma_x)_{max} \ \alpha \left[(m^2 + \nu\ e^2 n^2) \ / \ (m^2 + e^2 n^2)^2 \right]$$

and

$$(\eta_{mn}\sigma_y)_{max} \; \alpha \; \left[(v\,m^2 + e^2 n^2) \; / \; (m^2 + e^2 n^2)^2 \right]$$

Combining above equations with Eqs.(2.2.4) and (2.3.1) one obtains

$$K = K_1 \; K_2 \; K_3 \qquad\qquad \ldots (3.1.1)$$

where,

$$K_1 = \left[\frac{\{(m^2 + v\,e^2 n^2) \text{ or } (v\,m^2 + e^2 n^2)\} }{(m^2 + e^2 n^2)^2} \frac{(1+ e^2)^2}{(v + e^2)} \right]^{(N-2)} \qquad \ldots (3.1.2)$$

where, within the braces $\{\;\}$ the larger term is to be taken.

In the above $e > 1.0$. In case $e < 1.0$, the term $(v + e^2)$ is to be replaced by $(1+ e^2 v)$

$$K_2 = \left[\frac{1 - 2v\,\xi_{11} + \xi_{11}^2}{1 - 2v\,\xi_{mn} + \xi_{mn}^2} \right] \qquad\qquad \ldots (3.1.3)$$

$$K_3 = \left[\frac{1+ \xi_{mn}}{1+ \xi_{11}} \right]^N \qquad\qquad \ldots (3.1.4)$$

where,

$$\xi_{mn} = \left(\frac{v m^2 + e^2 n^2}{m^2 + v e^2 n^2} \right) \quad \text{or} \quad \left(\frac{m^2 + v e^2 n^2}{v m^2 + e^2 n^2} \right) \qquad \ldots (3.1.5)$$

whichever is less than or equal to 1.0

Here, $\xi_{11} = \left(\frac{v+e^2}{1+e^2 v} \right)$ or $\left(\frac{1+e^2 v}{v+e^2} \right)$ for $e <$ or > 1.0 $\qquad \ldots (3.1.6)$

Neglecting the modal variation in (β/α), as shown in Table 7.1, one obtains from Eq.(2.3.5)

$$\frac{\eta_{mn}}{\eta_{11}} = K^{(\frac{1}{N-1})} \qquad \qquad \dots (3.1.7)$$

The above relationship correlates the modal loss factor with the fundamental modal value.

For modes m = n, one gets from Eqs.(3.1.2) to (3.1.4),

$$K_2 = K_3 = 1.0 \text{ and}$$
$$K = K_1 = \left[\frac{1}{(mxn)}\right]^{(N-2)}$$

Now, let a particular plate of known material and size be considered and let its modal damping be represented as η_{mn}^x. Let the load be changed to P' such that $P' = k_1 \cdot P$ and loss factor change to η_{mn}', then it is observed from Eqs.(2.1.12) and (2.1.16), that

$$\frac{U_{mn}'}{U_{mn}} = k_1 \left[\frac{\eta_{mn}^x}{\eta_{mn}'}\right] , \qquad \qquad \dots (3.1.8)$$

where, henceforth, the prime represents a changed parameter. Going through Eqs.(2.1.18) and (2.3.5) one obtains

$$\frac{\eta_{mn}'}{\eta_{mn}^x} = (k_1)^{(\frac{N-2}{N-1})} \qquad \qquad \dots (3.1.9)$$

This equation gives the effect of change in the amplitude of constant force excitation on the modal damping of

the plate.

3.2 MODAL LOSS FACTOR FOR A SINGLE RESONANT MODE UNDER CONSTANT AMPLITUDE EXCITATION

Maximum deflection for any mode (m,n) is obtained

from Eq. (2.1.16) as

$$(W_{mn})_{max} = \left[\frac{4a^2}{\pi^4 B} e\right] \frac{P}{(m^2 + e^2 n^2)^2 \eta^*_{mn}} \qquad \ldots (3.2.1)$$

In order that the maximum amplitude of vibration under

any mode (m,n) remains same as that of fundamental mode,

i.e.,

$$(W_{mn})_{max} = (W_{11})_{max}$$

such that condition of constant maximum amplitude excitation

is satisfied for all the modes, one can visualize that the

load has now to change to say P'. This would lead to a new

value of loss factor η'_{mn}, such that,

$$\left[\frac{P'}{\eta'_{mn}}\right] = \frac{P}{\eta^*_{11}} \left[\frac{m^2 + e^2 n^2}{1 + e^2}\right]^2 \qquad \ldots (3.2.2)$$

Substituting this equation in Eq. (2.1.18) and then combin-

ing with Eqs. (2.2.4) and (2.3.1) one obtains a factor K_o

which is similar to K (Eq. (3.1.1)).

Here,

$$K_o = K_{01} K_{02} K_{03} \qquad \ldots (3.2.3)$$

$$\text{where,} \quad K_{01} = \left[\frac{\{(m^2 + \nu e^2 n^2) \text{ or } (\nu m^2 + e^2 n^2)\}}{(\nu + e^2)}\right]^{(N-2)}$$

depending on which one is greater. Also in the above $e \geqslant 1.0$.

When $e < 1.0$, $(\nu + e^2)$ is to be replaced by $(1+e^2\nu)$.

$$K_{02} = K_2 \text{ and } K_{03} = K_3$$

Further, making use of Eq.(2.3.4) one gets

$$\frac{\eta'_{mn}}{\eta^x_{11}} = K_0 \qquad \qquad \ldots \text{ (3.2.4)}$$

This equation correlates the higher mode damping with the fundamental mode value under constant amplitude excitation. Let the maximum constant amplitude of vibration for the mode (m,n) change from W_{mn} to W'_{mn} such that

$$\frac{W'_{mn}}{W_{mn}} = \frac{U'_{mn}}{U_{mn}} = k_2$$

One obtains the relation between the load ratio k_1 and the amplitude ratio k_2 from Eqs.(3.1.9) and (3.2.1) as

$$k_2 = k_1^{(\frac{1}{N-1})} \qquad \qquad \ldots \text{ (3.2.5)}$$

Hence, from Eq.(3.1.9) and the above equation one gets

$$\frac{\eta'_{mn}}{\eta^x_{mn}} = k_2^{(N-2)} \qquad \qquad \ldots \text{ (3.2.6)}$$

This equation gives the effect of change in the constant maximum amplitude of vibration on the modal damping of the plate.

3.3 SIMPLIFIED RELATIONSHIP BETWEEN THE TOTAL LOSS FACTOR UNDER COMPLEX RESONANT MODES AND INDIVIDUAL LOSS FACTORS

The evaluation of the internal loss factor for the plate vibrating under complex resonances (when more than

one mode have identical natural frequencies) has been

dealt with in Section 2.5. A simplified approximate

relationship between the individual modal loss factors and

the total loss factor under complex resonant modes is

derived below:

Let, there be two modes having identical natural

frequencies which are represented by suffix '1' and '2'

and let them vibrate under resonance condition. Let

suffic 'T' represent the total values under such excitation.

Neglecting the effect of cross-coupling between the modal

damping and applying the principle of modal superposition,

the stress relationship can be written as

$$\sigma_{e_T} = \sigma_{e_1} + \sigma_{e_2} \qquad \qquad \dots (3.3.1)$$

Further, the maxima of σ_e's can also be written as

$$\sigma_{am_T} = \sigma_{am_1} + \sigma_{am_2} \qquad \qquad \dots (3.3.2)$$

provided one ensures that phases at the centre of the

vibrating modes are same. Also, one may write the following

aprroximate relationship in terms of σ_{eT} as

$$\sigma_{eTm_T} = \sigma_{eTm_1} + \sigma_{eTm_2} \qquad \qquad \dots (3.3.3)$$

Going through Eqs.(2.3.4) and (3.3.2) and neglecting the

variations in integral ratios one gets,

$$(\eta_T \sigma_{eTm_T}^2)^{1/N} = (\eta_1 \sigma_{eTm_1}^2)^{1/N} + (\eta_2 \sigma_{eTm_2}^2)^{1/N} \qquad \ldots (3.3.4)$$

or

$$(\eta_T \sigma_{eTm_T}^2)^{1/N} = \left\{ \frac{(\eta_1 \sigma_{eTm_1})^2}{\eta_1} \right\}^{1/N} + \left\{ \frac{(\eta_2 \sigma_{eTm_2})^2}{\eta_2} \right\}^{1/N} \qquad \ldots (3.3.5)$$

Hence, σ_{eTm_1} and σ_{eTm_2} can be obtained through Eqs.(2.3.1),
(3.1.5) and observing that

$$\eta \, \sigma_{a_1} \, \alpha \, \left[\frac{vm^2 + e^2 n^2}{(m^2 + e^2 n^2)^2} \right] \text{ or } \left[\frac{m^2 + ve^2 n^2}{(m^2 + e^2 n^2)^2} \right] \text{and}$$

σ_{eTm_T} is given by Eq.(3.3.3).

One can then estimate the loss factor for the plate
vibrating under complex resonance condition from the above
equation thereby avoiding the detailed computational
procedure as given in Section 2.5.

In the above analysis, a constant force excitation
has been assumed for the complex and as well as individual
modal excitations. It is further verified that Eq.(3.1.9)
holds good with the suffix 'T' i.e. for the total loss
factor values for the complex mode as well.

A similar analysis is made for the case when the maximum amplitude of each individual mode of the complex resonance case is same as that of the fundamental mode under a load P, and an expression similar to equation (3.3.5) is derived wherein η_1 and η_2 then are the individual loss factors under constant maximum amplitude excitation. It is also observed that Eq.(3.2.6) holds good for the total loss factor values as well.

Now, instead of maximum amplitude of each individual mode being equal to the fundamental mode value, one may come across a case when the maximum amplitude under complex resonance condition is equal to the fundamental mode value. In such situations, assuming the individual loss factors of the modes under complex resonance to be equal, one can observe that stresses will be reduced to a factor of (1/j) times the value under previous case, where j is the number of modes under a complex resonance. It can be seen then that the loss factor will be $[1/j]^{(N-2)}$ times the previous value.

3.4 EFFECT OF CHANGES IN PLATE THICKNESS AND ASPECT RATIO ON THE MODAL DAMPING

Let, the constant thickness of the plate change from h to h' and the aspect ratio change from e to e', such that the new loss factor for the fundamental mode be η'_{11}. Let, the excitation force remain constant. The variation in β/α is very small as shown in Table 7.8 and

is therefore neglected. Combining Eqs.(2.1.18), (2.2.4), (2.3.1) and (2.3.5) one obtains the relationship between $\eta_{11}^{!}$ and η_{11}^{x} the loss factor value corresponding to thickness h and aspect ratio e, as,

$$\left[\frac{\eta_{11}^{!}}{\eta_{11}^{x}}\right] = C_0^{\frac{1}{(N-1)}} \qquad \qquad \text{... (3.4.1)}$$

where, $\qquad C_0 = C_{01} C_{02} C_{03} \qquad \qquad \text{... (3.4.2)}$

Here,

$$C_{01} = \left[(\frac{e^!}{e}) (\frac{h}{h^!})^2 (\frac{1+e^2}{1+e^{!2}})^2 \frac{\{(\nu+e^{!2}) \text{ or } (1+e^{!2}\nu)\}}{\{(\nu+e^2) \text{ or } (1+e^2\nu)\}} \right]^{(N-2)}$$

where the larger term within the braces is to be taken.

$$C_{02} = (\frac{1-2\nu \, \xi_{11} + \xi_{11}^2}{1-2\nu \, \xi_{11}^! + \xi_{11}^{!2}})$$

$$C_{03} = (\frac{1+\xi_{11}^!}{1+\xi_{11}})^N$$

It is noted, that, for $e = e^!$, $C_{02} = C_{03} = 1$

$$\text{and } C_0 = C_{01} = (\frac{h}{h^!})^{2(N-2)}$$

Equation (3.4.1) gives the ratio of fundamental mode loss factors between two plates of different sizes subjected to constant force excitation. However, the value of the fundamental modal frequency itself changes as h or e changes.

Let us now consider a case when the two plates
of different sizes are vibrating with same maximum
amplitude. Then to attain this condition, the force has
to change to P' and one gets from Eq.(3.2.1)

$$(W_{11})_{max} = (\frac{4a^2 e}{B\pi^4}) \left[\frac{P}{(1+e^2)^2\, \eta_{11}^x} \right] = (\frac{4a^2 e'}{B'\pi^4}) \left[\frac{P'}{(1+e'^2)^2 \eta_{11}'} \right]$$

i.e.,
$$\frac{P'}{\eta_{11}'} = \frac{P}{\eta_{11}^x}\, (\frac{e}{e'})\, (\frac{h'}{h})^3 \left[\frac{1+e'^2}{1+e^2} \right]^2 \qquad \qquad \dots (3.4.3)$$

Substituting this equation in Eq.(2.1.18) and making use of
Eqs.(2.2.4) and (2.3.4) one obtains after neglecting the
variation in (β/α) once again,

$$\left[\frac{\eta_{11}'}{\eta_{11}^x} \right] = C_0' \qquad \qquad \dots (3.4.4)$$

where $C_0' = C_{01}' C_{02}' C_{03}'$

Also,
$$C_{01}' = \left[(\frac{h'}{h})\, \frac{\{(1+\nu e'^2)\ \text{or}\ (\nu+e'^2)\}}{\{(\nu+e^2)\ \text{or}\ (1+\nu e^2)\}} \right]^{(N-2)}$$

$$C_{02}' = C_{02}$$

$$C_{03}' = C_{03}$$

It is seen, that, for $e = e'$

$$C_0' = C_{01}' = (\frac{h'}{h})^{(N-2)}$$

Equation (3.4.4) gives the ratio of fundamental mode loss factors between two plates of different aspect ratios and thicknesses but of same length, subjected to constant maximum amplitude excitations.

3.5 EFFECT OF DAMPING CONSTANTS ON THE LOSS FACTOR

Let η'_{11} be the loss factor corresponding to the damping constants of J' and N' of the material, the elastic properties remaining same. Observing, that, $\xi_{11} = \xi'_{11}$ and $\eta^x_{11}\sigma^x_{a_1} = \eta'_{11}\sigma'_{a_1}$ one obtains with the help of Eqs.(2.1.18), (2.2.4), (2.3.1) and (2.3.5)

$$\eta'_{11} = (\eta^x_{11})^{\left(\frac{N-1}{N-2}\cdot\frac{N'-2}{N'-1}\right)} \cdot R_o^{\left(\frac{N'-2}{N'-1}\right)} \cdot \frac{r_1^{1(N'-1)}}{r^{\left(\frac{N'-2}{N-2}\cdot\frac{1}{N'-1}\right)}} \qquad \dots (3.5.1)$$

WHERE,

$$R_o = R_{01}^{\left(\frac{1}{N-2}-\frac{1}{N'-2}\right)} \cdot R_{02}^{\left(\frac{N'}{N'-2}-\frac{N}{N-2}\right)}$$

$$\dots\dots (3.5.2)$$

$$R_{01} = (1-2\nu\,\xi_{11}+\xi_{11}^2)$$

and $\quad R_{02} = (1 + \xi_{11})$

$$r = \left[\frac{JE}{\pi}\cdot\frac{\alpha}{\beta}\right] \text{and} \quad r_1 = \left[\frac{J'E}{\pi}\cdot\frac{\alpha'}{\beta'}\right]$$

The loss factor for any plate material for which the damping relation $D = J\,\sigma^N$ is assumed to hold good, can be evaluated from the above equation provided the integral

ratios (α/β) and (α'/β') are known. The variation in the Poisson's ratio is taken care of in the term R_o and the variation in E is to be accounted for in r and r_1.

3.6 MODAL DAMPING UNDER ECCENTRIC POINT FORCE

So far in the analysis, a central point harmonic force has been considered to act on the plate which excites only odd-odd mode. Let the force now act at an eccentric point (x_1, y_1) instead of at $(\frac{a}{2}, \frac{b}{2})$. Then it is known [70] that the response term in Eq.(2.1.16) for odd-odd mode will be multiplied by $\sin(\frac{m\pi x_1}{a})\sin(\frac{n\pi y_1}{b})$. Hence, going through the steps as laid down in Sections 2.1, 2.2, and 2.3, one observes that

$$\frac{\eta'_{mn}}{\eta^{x}_{mn}} = \left[|\sin(\frac{m\pi x_1}{a})\,\sin(\frac{n\pi y_1}{b})\,|\,\right]^{(\frac{N-2}{N-1})} \qquad \dots (3.6.1)$$

where η'_{mn} is the loss factor for a mode (m,n) when the force is eccentric and η^{x}_{mn} is the modal loss factor for central point force.

For additional even order modes which are excited when the force is eccentric, one may obtain η'_{mn} (m,n = even or odd) from an equation of the type (3.1.7) where the factor K_1 of Eq.(3.1.2) modifies to

$$K_1 = \left[\frac{\{(m^2+\nu\,e^2n^2)\text{ or }(m^2\nu + e^2n^2)\}}{\{(1+\nu e^2)\quad\text{ or }(\nu + e^2)\}} \cdot (\frac{1+e^2}{m^2+ e^2n^2})^2 \cdot \right.$$
$$\left. \frac{\sin(\frac{m\pi x_1}{a})\sin(\frac{n\pi y_1}{b})}{\sin(\frac{\pi x_1}{a})\sin(\frac{\pi y_1}{b})} \right]^{(N-2)} \qquad \dots (3.6.2)$$

CHAPTER-4

FUNDAMENTAL MODE LOSS FACTOR FOR CLAMPED PLATE

The modal loss factor for a rectangular plate of which all the four edges are simply supported has been dealt with in the previous chapters. The eigen shape functions and the natural frequencies for such plate are given in Eqs.(2.1.13) and (2.1.14), respectively. The effect of clamping in turn of the edges is to change the boundary conditions of the plate. The shape functions and the natural frequencies for different sets of boundary conditions as derived by Warburton are given in Appendix 1. The loss factor for the fundamental resonant mode for four different plate boundary conditions, Fig.4.1, will now be determined and effect of in-turn clamping of the edges on the modal damping of a simply supported rectangular plate will be studied.

4.1 ONE EDGE CLAMPED-CASE 1

The shape function for the plate having the edge x = 0 as clamped and the remaining edges as simply supported is obtained by combining Eqs.(A.1.2) and (A.1.5) as

$$\Psi_{mn}(x,y) = \left[\sin\gamma_2(\frac{x}{2a} - \frac{1}{2}) - \frac{\sin(0.5\gamma_2)}{\sinh(0.5\gamma_2)}\cdot\sinh\gamma_2(\frac{x}{2a} - \frac{1}{2})\right]\sin\frac{n\pi y}{b}$$

$$\ldots (4.1.1)$$

Also, from Eq.(A.1.8) and Table A.1.1 one gets the fundamental mode frequency parameter as
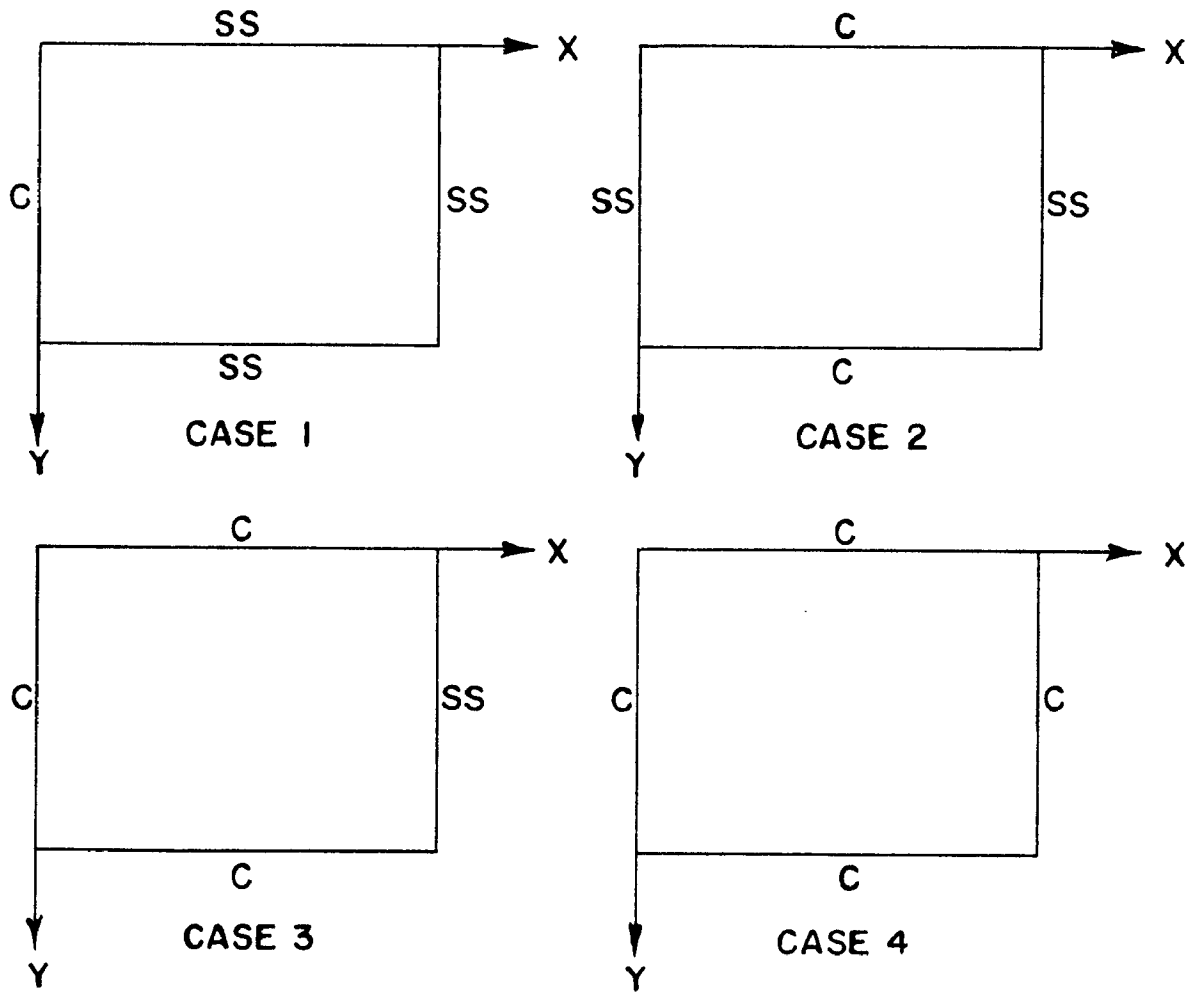
FIG. 4·1 RECTANGULAR PLATE-DIFFERENT BOUNDARY CONDITIONS ON THE EDGES.

$$\lambda_{11} = \pi^4 \left[(1.25)^4 + e^4 + 2e^2 (1.25)^2 \left[1 - \frac{4}{5\pi} \right] \right] \qquad \dots (4.1.2)$$

Since the orthogonality of eigen functions holds good for clamped and simply supported conditions, one gets the modal loading coefficient from Eq.(2.1.8).

It is seen from Eq.(4.1.1), that,

$$\int_0^b \int_0^a \Psi_{mn}^2 \, dx \, dy = \frac{ab}{4} \left[1 - \frac{\sin^2 (0.5 \, \gamma_2)}{\sinh^2 (0.5 \, \gamma_2)} - \frac{2 \, \sin \gamma_2}{\gamma_2} \right] \qquad \dots (4.1.3)$$

Further, one obtains with the help of the procedure given in [70]

$$\int_0^b \int_0^a P(x,y) \, \Psi_{mn}(x,y) \, dx \, dy = P \left[\sin(0.25\gamma_2) \left\{ \frac{\cos(0.25\gamma_2)}{\cosh(0.25\gamma_2)} - 1 \right\} \right]$$

$$\text{for } n = \text{odd} \qquad \dots (4.1.4)$$

Substituting Eqs.(4.1.3) and (4.1.4) into Eq.(2.1.8) one gets for central point force, the value of modal loading coefficient P_{11} as

$$P_{11} = \frac{4P}{ab} \cdot F_1$$

where,

$$F_1 = \left[\frac{\sin(0.25\gamma_2) \left\{ \frac{\cos(0.25\gamma_2)}{\cosh(0.25\gamma_2)} - 1 \right\}}{1 - \frac{\sin^2 (0.5 \, \gamma_2)}{\sinh^2 (0.5\gamma_2)} - 2 \frac{\sin \gamma_2}{\gamma_2}} \right] \qquad \dots (4.1.5)$$

The response when the plate is vibrating in its fundamental

resonant mode is now obtained as in Section 2.1 and is given by

$$W(x,y) = \frac{4Pa^2eF_1}{i\eta_{11}B\lambda_{11}}\left[\sin\gamma_2(\frac{x}{2a} - \frac{1}{2}) - \frac{\sin(0.5\ \gamma_2)}{\sinh(0.5\ \gamma_2)} \cdot \sinh\gamma_2(\frac{x}{2a} - \frac{1}{2})\right]\sin\frac{\pi y}{b}$$

$$\ldots (4.1.6)$$

Stresses are obtained by making use of Eq.(2.1.17). Following the procedure as given in Chapter 2 and using Eqs.(2.2.4) and (2.3.5), the modal loss factor for the fundamental resonant mode is evaluated.

4.2 TWO OPPOSITE EDGES CLAMPED-CASE 2

For the case of a plate with edges $x = 0$ and $x = a$ as simply supported and edges $y = 0$ and $y = b$ as clamped, the shape function is obtained from Eqs.(A.1.2) and (A.1.3) as

$$\psi_{mn}(x,y) = \left[\cos\gamma_1(\frac{y}{b} - \frac{1}{2}) + \frac{\sin(0.5\ \gamma_1)}{\sinh(0.5\ \gamma_1)} \cdot \cosh\gamma_1(\frac{y}{b} - \frac{1}{2})\right]\sin\frac{m\pi x}{a}$$

$$\text{for } n = \text{odd} \qquad \ldots (4.2.1)$$

The modal frequency parameter for the fundamental mode is obtained from Eq.(A.1.8) and Table A.1.1 , as

$$\lambda_{11} = \pi^4\left[1+(1.506)^4e^4+2e^2\times1.248\right] \qquad \ldots (4.2.2)$$

It is seen from Eq.(4.2.1), that

$$\int_0^b \int_0^a \psi_{mn}^2 \, dx \, dy = \frac{ab}{4} \left[1 + \frac{\sin^2(0.5 \, \gamma_1)}{\sinh^2(0.5 \, \gamma_1)} \right] \qquad \dots (4.2.3)$$

Also, for a central point force one obtains [70],

$$\int_0^b \int_0^a P(x,y) \, \psi_{mn}(x,y) \, dx \, dy = P\left[1 + \frac{\sin(0.5 \, \gamma_1)}{\sinh(0.5 \, \gamma_1)} \right] \qquad \dots (4.2.4)$$

Substituting Eqs.(4.2.3) and (4.2.4) in Eq.(2.1.8) one gets the modal loading coefficient, as

$$P_{11} = \frac{4P}{ab} \cdot F_2$$

$$\text{where } F_2 = \frac{\left[1 + \frac{\sin(0.5\gamma_1)}{\sinh(0.5\gamma_1)} \right]}{\left[1 + \frac{\sin^2(0.5 \, \gamma_1)}{\sinh^2(0.5 \, \gamma_1)} \right]} \qquad \dots (4.2.5)$$

The fundamental resonant mode response for the plate, therefore, becomes

$$W(x,y) = \frac{4Pa^2 e F_2}{i\eta_{11} B\lambda_{11}} \left[\cos \gamma_1 \left(\frac{y}{b} - \frac{1}{2} \right) + \frac{\sin(0.5\gamma_1)}{\sinh(0.5\gamma_1)} \cdot \right.$$

$$\left. \cdot \cosh \gamma_1 \left(\frac{y}{b} - \frac{1}{2} \right) \right] \sin \frac{\pi x}{a}$$

$$\dots (4.2.6)$$

Having obtained the response, the fundamental mode loss factor is once again obtained by following the procedure as given in previous section.

4.3 THREE CLAMPED EDGES-CASE 3

In this case the edge x = a of the plate is simply supported whereas all the remaining three edges are clamped. The shape function is obtained with the help of Eqs.(A.1.3) and (A.1.5) and is given by

$$\Psi_{mn}(x,y) = \left[\cos \gamma_1 (\tfrac{y}{b} - \tfrac{1}{2}) + \frac{\sin(0.5\gamma_1)}{\sinh(0.5\gamma_1)} \cosh \gamma_1 (\tfrac{y}{b} - \tfrac{1}{2}) \right] \cdot$$

$$\cdot \left[\sin \gamma_2 (\tfrac{x}{2a} - \tfrac{1}{2}) - \frac{\sin(0.5\gamma_2)}{\sinh(0.5\gamma_2)} \cdot \sinh\gamma_2 (\tfrac{x}{2a} - \tfrac{1}{2}) \right]$$

$$\ldots (4.3.1)$$

The fundamental mode frequency parameter λ_{11} is obtained from Eq.(A.1.8) and Table A.1.1 as

$$\lambda_{11} = \pi^4 \left[(1.25)^4 + (1.506)^4 \ e^4 + 2e^2 1.248 (1.25)^2 \{ 1 - \tfrac{4}{5\pi} \} \right]$$

$$\ldots (4.3.2)$$

One gets from Eq.(4.3.1)

$$\int_0^b \int_0^a \Psi_{mn}^2 dx \, dy = \frac{ab}{4} \left[1 - \frac{\sin^2(0.5\gamma_2)}{\sinh^2(0.5\gamma_2)} - \frac{2 \sin \gamma_2}{\gamma_2} \right] \cdot$$

$$\cdot \left[1 + \frac{\sin^2(0.5\gamma_1)}{\sinh^2(0.5\gamma_1)} \right] \qquad \ldots (4.3.3)$$

Also, for a central point force one gets [70]

$$\int_0^b \int_0^a P(x,y) \ \Psi_{mn}(x,y)dx \, dy = P \left[\sin(0.25\gamma_2) \left\{ \frac{\cos(0.25\gamma_2)}{\cosh(0.25\gamma_2)} - 1 \right\} \right]$$

$$\cdot \left[1 + \frac{\sin(0.5\gamma_1)}{\sinh(0.5\gamma_1)} \right] \qquad \ldots (4.3.4)$$

Substituting Eqs.(4.3.3) and (4.3.4) in Eq.(2.1.8) one gets,

$$P_{11} = \frac{4P}{ab} \cdot F_1 \cdot F_2 \qquad , \qquad \dots (4.3.5)$$

where F_1 and F_2 are given by Eqs.(4.1.5) and (4.2.5), respectively.

The fundamental resonant mode response for the plate, therefore, becomes

$$W(x,y) = \frac{4Pa^2 e F_1 F_2}{i\eta_{11} B\lambda_{11}} \left[\cos \gamma_1 \left(\frac{y}{b} - \frac{1}{2}\right) + \frac{\sin(0.5\gamma_1)}{\sinh(0.5\gamma_1)} \cdot \cosh\gamma_1 \left(\frac{y}{b} - \frac{1}{2}\right) \right] \cdot$$

$$\cdot \left[\sin \gamma_2 \left(\frac{x}{2a} - \frac{1}{2}\right) - \frac{\sin(0.5\gamma_2)}{\sinh(0.5\gamma_2)} \cdot \sinh\gamma_2 \left(\frac{x}{2a} - \frac{1}{2}\right) \right]$$

$$\dots (4.3.6)$$

The fundamental mode loss factor is now evaluated as indicated in previous sections.

4.4 ALL THE FOUR EDGES CLAMPED - CASE 4

The shape function for the rectangular plate of which all the edges are clamped is obtained by combining Eqs.(A.1.3) for X(x) and for Y(y) and is found to be

$$\psi_{mn}(x,y) = \left[\cos \gamma_1 \left(\frac{x}{a} - \frac{1}{2}\right) + \frac{\sin(0.5\gamma_1)}{\sinh(0.5\gamma_1)} \cdot \cosh \gamma_1 \left(\frac{x}{a} - \frac{1}{2}\right) \right]$$

$$\cdot \left[\cos\gamma_1 \left(\frac{y}{b} - \frac{1}{2}\right) + \frac{\sin(0.5\gamma_1)}{\sinh(0.5\gamma_1)} \cosh\gamma_1 \left(\frac{y}{b} - \frac{1}{2}\right) \right]$$

$$\dots (4.4.1)$$

The fundamental mode frequency parameter is obtained from Eq.(A.1.8) and Table A.1.1 as

$$\lambda_{11} = \pi^4\left[(1.506)^4 + e^4(1.506)^4 + 2e^2 \times 1.248 \times 1.248\right] \qquad \cdots (4.4.2)$$

One obtains from Eq.(4.4.1)

$$\int_0^b \int_0^a \psi_{mn}^2 \, dx \, dy = \frac{ab}{4}\left[1 + \frac{\sin^2(0.5\gamma_1)}{\sinh^2(0.5\gamma_1)}\right]^2 \qquad \cdots (4.4.3)$$

For a central point force one gets [27]

$$\int_0^b \int_0^a P(x,y) \, \psi_{mn}(x,y) dx \, dy = P\left[1 + \frac{\sin(0.5\gamma_1)}{\sinh(0.5\gamma_1)}\right]^2 \qquad \cdots (4.4.4)$$

Substituting Eqs.(4.4.3) and (4.4.4) in Eq.(2.1.8) one obtains the modal loading coefficient for the fundamental mode as

$$P_{11} = \frac{4P}{ab} F_2^2 \qquad \cdots (4.4.5)$$

where F_2 is given by Eq.(4.2.5)

Therefore, the fundamental mode response for the plate is obtained as

$$W(x,y) = \frac{4Pa^2 e F_2^2}{i\eta_{11} B\lambda_{11}}\left[\cos \gamma_1\left(\frac{x}{a} - \frac{1}{2}\right) + \frac{\sin(0.5\gamma_1)}{\sinh(0.5\gamma_1)} \cosh\gamma_1\left(\frac{x}{a} - \frac{1}{2}\right)\right] \cdot$$

$$\cdot \left[\cos\gamma_1\left(\frac{y}{b} - \frac{1}{2}\right) + \frac{\sin(0.5\gamma_1)}{\sinh(0.5\gamma_1)} \cdot \cosh\gamma_1\left(\frac{y}{b} - \frac{1}{2}\right)\right]$$

$$\cdots (4.4.6)$$

Having obtained the resonant response, the loss factor for the fundamental mode is obtained as indicated before.

In all the above cases the values of γ_1 and γ_2 are to be used. These are known from literature [30] as

$$0.5\gamma_1 = 4.7300$$
$$0.5\gamma_2 = 7.8532$$

Thus the fundamental mode loss factors for different sets of boundary conditions and for different plate aspect ratios are computed and effect of inturn clamping of the edges on fundamental mode loss factor studied.

CHAPTER 5

ANALYSIS OF VARIABLE THICKNESS PLATES

The equation of motion of a simply supported rectangular plate having a thickness variation in X-direction has been given in Eq.(2.6.3). When the plate vibrates in one of its resonant mode the approximate one term and two term solutions can be obtained with the help of Galerkin's Method [30] and the fundamental mode responses are given by Eqs.(2.6.11) and (2.6.12) wherein the Galerkin's coefficients A_{11}, A'_{11} and A'_{21} are to be evaluated. After determining the response, the modal damping can then be obtained. The following two cases of variation in thicknesses are considered.

1. Linear variation in thickness, and
2. Parabolic variation in thickness.

5.1 FUNDAMENTAL MODE RESPONSE FOR THE PLATE WITH LINEAR THICKNESS VARIATION

The approximate expression for the response is obtained by considering one term or two terms in the Galerkin solution. Both of these will now be discussed.

5.1.1 One Term Solution

Substituting Eqs.(2.6.4), (2.6.7), (2.6.9),(2.6.10) and (2.6.11) in Eq.(2.6.3) and performing the necessary

differentiations one obtains

$$(1+i\eta_{11})\left[B_o\left[G(x)\right]^3\pi^4 A_{11}\sin(\tfrac{\pi x}{a})\sin(\tfrac{\pi y}{b})\{\tfrac{1}{a^2}+\tfrac{1}{b^2}\}^2\right.$$

$$-\frac{6\pi^3}{a}A_{11}B_o\left[G(x)\right]^2 G'(x)\{\tfrac{1}{a^2}+\tfrac{1}{b^2}\}\cdot$$

$$\cdot\cos(\tfrac{\pi x}{a})\sin(\tfrac{\pi y}{b})-3\pi^2 A_{11}\sin(\tfrac{\pi x}{a})\sin(\tfrac{\pi y}{b})B_o\cdot$$

$$\left.\cdot(\tfrac{1}{a^2}+\tfrac{\nu}{b^2})\{2G(x)(G'(x))^2+(G(x))^2 G''(x)\}\right]$$

$$-\rho h_o\, G(x)\,\omega_{11}^2 A_{11}\sin(\tfrac{\pi x}{a})\sin(\tfrac{\pi y}{b})$$

$$-\frac{4P}{ab}\sin(\tfrac{\pi x}{a})\sin(\tfrac{\pi y}{b}) \qquad = L(W) \qquad \dots (5.1.1.1)$$

where prime in $G(x)$ represents differentiation with respect to x.

Hence, onwards, the suffixes in η shall be dropped and it would be considered to represent the fundamental mode value of the loss factor.

Now, the linear thickness variation is given by Eq.(2.6.5) such that

$$G(x) = 1+\delta(\tfrac{x}{a}),$$
$$G'(x) = \tfrac{\delta}{a},$$
$$G''(x) = 0.$$

The application of Galerkin's method leads to the solution of the following integral equation

$$\int_0^b \int_0^a L(W)\,\sin(\tfrac{\pi x}{a})\sin(\tfrac{\pi y}{b})\,dx\,dy = 0 \qquad \dots (5.1.1.2)$$

The coefficient A_{11} of Eq.(2.6.11) is then obtained from the above equation.

Substituting Eq.(5.1.1.1) in Eq.(5.1.1.2) and solving the resulting integral expression, one obtains

$$A_{11}(1+i\eta) \; B_0\left[\pi^4(\tfrac{1}{a^2} + \tfrac{1}{b^2})^2 \; I_1\{I_2 + \tfrac{3\delta}{a} \; I_3 + \tfrac{3\delta^2}{a^2} \; I_4\right.$$

$$+ \tfrac{\delta^3}{a^3} \; I_5\} - \tfrac{6\pi^3}{a}\cdot\tfrac{\delta}{a}\cdot(\tfrac{1}{a^2} + \tfrac{1}{b^2})I_1\{I_6 +$$

$$+ \tfrac{2\delta}{a} \; I_7 + \tfrac{\delta^2}{a^2} \; I_8 \} - 3\pi^2(\tfrac{1}{a^2} + \tfrac{\nu}{b^2}) \cdot$$

$$\left.\cdot\{ \tfrac{2\delta^2}{a^2}\cdot I_1(I_2 + \tfrac{\delta}{a} \; I_3)\}\right]$$

$$-\rho h_0\omega_{11}^2 A_{11} \; I_1(I_2 + \tfrac{\delta}{a} \; I_3) - \tfrac{4P}{ab} \; I_1 I_2 \; = 0 \qquad \cdots (5.1.1.3)$$

where the integrals I's are given in Appendix 2.

After substituting the values of the integrals and simplifying, one gets the coefficient A_{11} as

$$A_{11} = \frac{P}{(1+i\eta)B_0 C_1 - \rho h_0 \omega_{11}^2 C_2} \qquad \cdots (5.1.1.4)$$

where,

$$C_1 = \left[\frac{\pi^4}{4a^2 e}(1+e^2)^2\{1+1.5\delta + \delta^2(1- \tfrac{1.5}{\pi^2}) + \tfrac{\delta^3}{4}(1- \tfrac{3}{\pi^2})\}\right.$$

$$\left.+1.5 \; \tfrac{\pi^2 e}{a^2}(1-\nu)\delta^2(1+0.5\delta)\right] \qquad \cdots (5.1.1.5)$$

and

$$C_2 = \frac{a^2}{4e}(1+0.5\delta) \qquad \cdots (5.1.1.6)$$

Substitution of Eq.(5.1.1.4) in Eq.(2.6.11) leads to a complex response expression. However, it is known from the resonant response behaviour, that, the phase of the response under resonance condition has to be one of 90°-lag with the excitation(as in Eq.(2.1.16)). Therefore, equating the real part of the denominator of the coefficient A_{11} to zero in order to bring the phase of the resonant response in conformity with known behaviour, one gets the frequency equation as

$$\lambda_{11} = C_1 a^4/C_2$$

where, $\quad \lambda_{11} = \rho h_o a^4 \omega_{11}^2/B_o$

$$\cdots \text{(5.1.1.7)}$$

and response equation as

$$W = \frac{P \ \sin(\frac{\pi x}{a}) \ \sin(\frac{\pi y}{b})}{i\eta \ B_o C_1}$$

$$\cdots \text{(5.1.1.8)}$$

The term $1/i$ can be dropped once again as was done in constant thickness plate analysis, since it indicates the phase only. Eq.(5.1.1.7) gives the one term approximation to the fundamental mode frequency parameter λ_{11}.

5.1.2 Two Term Solution

Substituting Eqs.(2.6.4), (2.6.7), (2.6.9), (2.6.10) and (2.6.12) in Eq.(2.6.3) and performing the necessary differentiations one obtains

$$(1+i\eta) \left[B_0 \left[G(x) \right]^3 \pi^4 \left\{ \left(\frac{1}{a^2} + \frac{1}{b^2} \right)^2 A'_{11} \sin\left(\frac{\pi x}{a}\right) + \left(\frac{2^2}{a^2} + \frac{1}{b^2} \right)^2 A'_{21} \cdot \right. \right.$$

$$\left. \cdot \sin\left(\frac{2\pi x}{a}\right) \right\} \sin\left(\frac{\pi y}{b}\right) - 6 B_0 \left[G(x) \right]^2 G'(x) \frac{\pi^3}{a} \left\{ \left(\frac{1}{a^2} + \frac{1}{b^2} \right) \cdot \right.$$

$$\left. \cdot A'_{11} \cos\left(\frac{\pi x}{a}\right) + \left(\frac{2^2}{a^2} + \frac{1}{b^2} \right) 2 A'_{21} \cdot \cos\left(\frac{2\pi x}{a}\right) \right\} \sin\left(\frac{\pi y}{b}\right)$$

$$- 3 B_0 \pi^2 \left\{ 2 G(x) (G'(x))^2 + (G(x))^2 G''(x) \right\} \cdot \sin\left(\frac{\pi y}{b}\right)$$

$$\cdot \left\{ \left(\frac{1}{a^2} + \frac{\nu}{b^2} \right) A'_{11} \sin\left(\frac{\pi x}{a}\right) + \left(\frac{2^2}{a^2} + \frac{\nu}{b^2} \right) A'_{21} \cdot \sin\left(\frac{2\pi x}{a}\right) \right\} \right]$$

$$- \rho h_0 G(x) \omega_{11}^2 \left\{ A'_{11} \sin\left(\frac{\pi x}{a}\right) + A'_{21} \sin\left(\frac{2\pi x}{a}\right) \right\} \sin\left(\frac{\pi y}{b}\right)$$

$$- \frac{4P}{ab} \sin\left(\frac{\pi x}{a}\right) \sin\left(\frac{\pi y}{b}\right) = L(W) \qquad \qquad \ldots (5.1.2.1)$$

Galerkin's method is applied for obtaining the coefficients A'_{11} and A'_{21} and the following two integral equations are to be solved.

$$\int_0^b \int_0^a L(W) \sin\left(\frac{\pi x}{a}\right) \sin\left(\frac{\pi y}{b}\right) dx \, dy = 0 \qquad \ldots (5.1.2.2)$$

$$\int_0^b \int_0^a L(W) \sin\left(\frac{2\pi x}{a}\right) \sin\left(\frac{\pi y}{b}\right) dx \, dy = 0 \qquad \ldots (5.1.2.3)$$

where $L(W)$ is given by Eq.(5.1.2.1).

Solving these integral expressions one obtains

$$B_0 (1+i\eta) \left[\pi^4 \cdot I_1 \left\{ \left(\frac{1}{a^2} + \frac{1}{b^2} \right)^2 A'_{11} \left(I_2 + \frac{3\delta}{a} I_3 + \frac{3\delta^2}{a^2} I_4 + \frac{\delta^3}{a^3} I_5 \right) \right. \right.$$

$$\left. + \left(\frac{2^2}{a^2} + \frac{1}{b^2} \right)^2 A'_{21} \left(I_9 + \frac{3\delta}{a} I_{10} + \frac{3\delta^2}{a^2} I_{11} + \frac{\delta^3}{a^3} I_{12} \right) \right\}$$

$$- 6 \frac{\pi^3}{a} \frac{\delta}{a} I_1 \left\{ \left(\frac{1}{a^2} + \frac{1}{b^2} \right) A'_{11} \left(I_6 + \frac{2\delta}{a} I_7 + \frac{\delta^2}{a^2} I_8 \right) \right.$$

$$+(\tfrac{2^2}{a^2} + \tfrac{1}{b^2})2.A'_{21}(I_{13} + \tfrac{2\delta}{a} I_{14} + \tfrac{\delta^2}{a^2} I_{15})\}$$

$$-3\pi^2 2 \tfrac{\delta^2}{a^2} I_1\{(\tfrac{1}{a^2} + \tfrac{\nu}{b^2})A'_{11}(I_2 + \tfrac{\delta}{a}I_3) +$$

$$+(\tfrac{2^2}{a^2} + \tfrac{\nu}{b^2})A'_{21}(I_9 + \tfrac{\delta}{a} I_{10})\}\Big]$$

$$-\rho h_0\omega^2_{11}I_1\{(I_2 + \tfrac{\delta}{a}I_3) A'_{11} + (I_9 + \tfrac{\delta}{a}I_{10})A'_{21}\}$$

$$- \tfrac{4P}{ab} I_1 I_2 \;= 0$$

$$\left.\right\} \;\ldots(5.1.2.4)$$

and,

$$B_0(1+i\eta)\Big[\pi^4 I_1\{(\tfrac{1}{a^2} + \tfrac{1}{b^2})^2 A'_{11}(I_9 + \tfrac{3\delta}{a}I_{10} + \tfrac{3\delta^2}{a^2}I_{11} + \tfrac{\delta^3}{a^3}I_{12})$$

$$+(\tfrac{2^2}{a^2} + \tfrac{1}{b^2})^2 A'_{21}(I_{16} + \tfrac{3\delta}{a} I_{17} + \tfrac{3\delta^2}{a^2}I_{18} + \tfrac{\delta^3}{a^3}\cdot I_{19})\}$$

$$-6\tfrac{\delta}{a} \tfrac{\pi^3}{a} I_1\{(\tfrac{1}{a^2} + \tfrac{1}{b^2})A'_{11}(I_{20} + \tfrac{2\delta}{a}I_{21} + \tfrac{\delta^2}{a^2} I_{22})$$

$$+2(\tfrac{2^2}{a^2} + \tfrac{1}{b^2})A'_{21}(I_{23} + \tfrac{2\delta}{a}I_{24} + \tfrac{\delta^2}{a^2}I_{25})\} -3\pi^2 2 \tfrac{\delta^2}{a^2} I_1.$$

$$\{(\tfrac{1}{a^2} + \tfrac{\nu}{b^2})A'_{11}(I_9 + \tfrac{\delta}{a}I_{10}) + (\tfrac{2^2}{a^2} + \tfrac{\nu}{b^2})A'_{21} (I_{16} + \tfrac{\delta}{a} I_{17})\}\Big]$$

$$-\rho h_0\omega^2_{11} I_1\{(I_9 + \tfrac{\delta}{a} I_{10})A'_{11} + (I_{16} + \tfrac{\delta}{a} I_{17})A'_{21}\}$$

$$- \tfrac{4P}{ab} I_1 I_9 = 0$$

$$\ldots (5.1.2.5)$$

where the integrals I's are given in Appendix 2.

Substitution of these integrals into the above equations and simplification leads to the following two simultaneous equations:

$$A'_{11}\Big[F_1 + i\eta B_1\Big] + A'_{21}\Big[F_4 + i\eta B_2\Big] = \tfrac{P}{B_0} \qquad \ldots (5.1.2.6)$$

and,

$$A'_{11}\left[F_3+i\eta A_1\right]+A'_{21}\left[F_2+i\eta A_2\right] = 0 \qquad \qquad \text{... (5.1.2.7)}$$

where,

$$\left.\begin{array}{l} F_1 = (B_1+G_6), \quad F_2 = (A_2+H_6), \quad F_3=(A_1+H_8), \\ F_4 = (B_2+G_8) \\ A_1 = (H_1+H_3+H_7), \quad A_2 = (H_2+H_4+H_5) \\ B_1 = (G_1+G_3+G_5), \quad B_2 = (G_2+G_4+G_7) \end{array}\right\} \quad \text{... (5.1.2.8)}$$

Here, G_1 to G_8 and H_1 to H_8 are the taper coefficients for linear thickness variation and are given in Appendix 3.

Solving simultaneously, the Eqs.(5.1.2.6) and(5.1.2.7) one obtains,

$$A'_{11} = \frac{P/B_0\left[F_2+i\eta A_2\right]}{\left[F_5+i\eta F_6\right]} \qquad \qquad \text{... (5.1.2.9)}$$

and,

$$A'_{21} = \frac{-P/B_0\left[F_3+i\eta A_1\right]}{\left[F_5+i\eta F_6\right]} \qquad \qquad \text{... (5.1.2.10)}$$

where,

$$F_5 = (F_1F_2-F_3F_4)-\eta^2(B_1A_2-A_1B_2) \qquad \text{... (5.1.2.11)}$$
$$F_6 = (F_1A_2+B_1F_2)-(F_3B_2+A_1F_4) \qquad \text{... (5.1.2.12)}$$

It was found that A_2 and F_2 are of same order since H_6 is usually small.Therefore, for low damping, the imaginary

term in the numerator of A'_{11} would contribute a very small phase and hence can be dropped. Similarly, the imaginary term in the numerator of A'_{21} can also be dropped. Now, in order to bring the phase of resonant response in conformity with known behaviour, one has to equate the real part of the denominator of A'_{11} and A'_{21} i.e. F_5 to zero. This would bring the phase of the resonant response to 90°-lag with the excitation. Therefore, one obtains the frequency equation as

$$F_5 = 0$$

or,
$$F_1 F_2 - F_3 F_4 = 0 \text{ after neglecting } \eta^2 \text{ term}$$

which is very small.

This leads to a quadratic equation in terms of the frequency parameter λ_{11}, as

$$\lambda_{11}^2 \left[G'_6 H'_6 - H'_8 G'_8 \right] + \lambda_{11} \left[(G'_6 A_2 + H'_6 B_1) - (H'_8 B_2 + G'_8 A_1) \right]$$
$$+ (B_1 A_2 - A_1 B_2) = 0 \qquad \ldots (5.1.2.13)$$

Lower root of this equation is the two term approximation to the fundamental frequency parameter λ_{11}.

The Galerkin's coefficients reduce to

$$A'_{11} = \frac{P}{i\eta B_0} \times \frac{F_2}{F_6}$$

and
$$A'_{21} = -\frac{P}{i\eta B_0} \times \frac{F_3}{F_6}$$

$$\left. \right\} \qquad \ldots (5.1.2.14)$$

Thus, the two term response Eq.(2.6.12) becomes

$$W' = \frac{P}{i\eta B_0 F_6} \left[F_2 \sin(\frac{\pi x}{a}) - F_3 \sin(\frac{2\pi x}{a}) \right] \sin(\frac{\pi y}{b}) \qquad \ldots (5.1.2.15)$$

The phase term $1/i$ can once again be dropped hence on wards.

5.2 FUNDAMENTAL MODE RESPONSE FOR THE PLATE WITH PARABOLIC THICKNESS VARIATION

The approximate response expression with one term and two terms in the Galerkin's solution are obtained below.

5.2.1 One Term Solution

The parabolic thickness variation is given by Eq.(2.6.6) such that

$$G(x) = 1-\mu \left(\frac{x}{a}\right)^2,$$

$$G'(x) = -\frac{2\mu x}{a^2},$$

and,

$$G''(x) = -\frac{2\mu}{a^2}$$

Substituting Eq.(5.1.1.1) in Eq.(5.1.1.2) and using the above expressions for $G(x)$, $G'(x)$ and $G''(x)$ one obtains after solving the resulting expression,

$$
\begin{aligned}
A_{11}(1+i\eta)B_0 &\left[\pi^4 \left(\frac{1}{a^2} + \frac{1}{b^2}\right)^2 I_1 \left\{ I_2 - \frac{3\mu}{a^2} I_4 + \frac{3\mu^2}{a^4} I_{26} - \frac{\mu^3}{a^6} I_{27} \right\} \right. \\
&- \frac{6\pi^3}{a}\left(\frac{1}{a^2} + \frac{1}{b^2}\right)\left(-\frac{2\mu}{a^2}\right)I_1 \left\{ I_7 - \frac{2\mu}{a^2} I_{28} + \frac{\mu^2}{a^4} I_{29} \right\} - 3\pi^2 \left(\frac{1}{a^2} + \frac{\nu}{b^2}\right) \cdot \\
&\left. \cdot I_1 \left\{ 2\left(-\frac{2\mu}{a^2}\right)^2 \left(I_4 - \frac{\mu}{a^2} I_{26}\right) - \frac{2\mu}{a^2}\left(I_2 - \frac{2\mu}{a^2} I_4 + \frac{\mu^2}{a^4} I_{26}\right)\right\} \right] \\
&- \rho h_0 \omega_{11}^2 A_{11} I_1 \left\{ I_2 - \frac{\mu}{a^2} I_4 \right\} - \frac{4P}{ab} I_1 I_2 = 0 \quad \dots (5.2.1.1)
\end{aligned}
$$

where the integrals I's are given in Appendix 2.

After substituting the values of the integrals and simplifying, one gets the coefficient A_{11} as

$$A_{11} = \frac{P}{(1+i\eta)B_o C_1 - \rho h_o \omega_{11}^2 C_2}$$

which is same as Eq.(5.1.1.4), and wherein

$$C_1 = \frac{\pi^4}{4a^2 e}(1+e^2)^2 \left\{ 1-\mu(1-\frac{1.5}{\pi^2}) + \frac{3\mu^2}{5}(1-\frac{5}{\pi^2} + \frac{7.5}{\pi^4}) \right.$$

$$- \frac{\mu^3}{7}(1-\frac{10.5}{\pi^3} + \frac{52.5}{\pi^4} - \frac{78.75}{\pi^6}) \}$$

$$- \frac{1.5\pi^2 e}{a^2}(1-\nu)\mu \left\{ 1-2\mu(1-\frac{1.5}{\pi^2}) + \mu^2(1-\frac{5}{\pi^2} + \frac{7.5}{\pi^4}) \right\} \quad \ldots (5.2.1.2)$$

$$C_2 = \frac{a^2}{4e}\left[1- \frac{\mu}{3}(1-\frac{1.5}{\pi^2}) \right] \quad \ldots (5.2.1.3)$$

With the help of similar arguments as put forward in the previous section, one observes, that, Eqs.(5.1.1.7) and (5.1.1.8) for the frequency and response hold good in this case as well.

5.2.2 Two Term Solution

Substituting Eq.(5.1.2.1) into Eq.(5.1.2.2) and solving the resulting integral expression, after making use of $G(x)$, $G'(x)$ and $G''(x)$ for parabolic thickness variation, one gets

$$(1+i\eta)B_o \left[\pi^4 I_1 \left\{ A_{11}'(\frac{1}{a^2} + \frac{1}{b^2})^2 (I_2 - \frac{3\mu}{a^2}I_4 + \frac{3\mu^2}{a^4}I_{26} - \frac{\mu^3}{a^6}I_{27}) \right. \right.$$

$$+A_{21}'(\frac{2^2}{a^2} + \frac{1}{b^2})^2 (I_9 - \frac{3\mu}{a^2}I_{11} + \frac{3\mu^2}{a^4}I_{30} - \frac{\mu^3}{a^6}I_{31}) \}$$

$$+ \frac{6\pi^3}{a}(\frac{2\mu}{a^2})I_1 \left\{ A_{11}'(\frac{1}{a^2} + \frac{1}{b^2}) (I_7 - \frac{2\mu}{a^2}I_{28} + \frac{\mu^2}{a^4}I_{29}) \right.$$

$$+A'_{21}(2)(\tfrac{2^2}{a^2} + \tfrac{1}{b^2})(I_{14} - \tfrac{2\mu}{a^2} I_{32} + \tfrac{\mu^2}{a^4} I_{33})\}$$

$$-3\pi^2(2)\tfrac{4\mu^2}{a^4} I_1 \{A'_{11}(\tfrac{1}{a^2} + \tfrac{\nu}{b^2})(I_4 - \tfrac{\mu}{a^2} I_{26})$$

$$+(\tfrac{2^2}{a^2} + \tfrac{\nu}{b^2})A'_{21}(I_{11} - \tfrac{\mu}{a^2} I_{30})\}$$

$$+3\pi^2(\tfrac{2\mu}{a^2})I_1\{A'_{11}(\tfrac{1}{a^2} + \tfrac{\nu}{b^2})(I_2 - \tfrac{2\mu}{a^2} I_4 + \tfrac{\mu^2}{a^4} I_{26})$$

$$+A'_{21}(\tfrac{2^2}{a^2} + \tfrac{\nu}{b^2})(I_9 - \tfrac{2\mu}{a^2} I_{11} + \tfrac{\mu^2}{a^4} I_{30})\}]$$

$$-\rho h_o \omega_{11}^2 I_1 \left[A'_{11}(I_2 - \tfrac{\mu}{a^2} I_4) + A'_{21}(I_9 - \tfrac{\mu}{a^2} I_{11})\right]$$
$$-\tfrac{4P}{ab} I_1 I_2 = 0 \qquad \ldots \ (5.2.2.1)$$

Substitution of Eq.(5.1.2.1) into Eq.(5.1.2.3) and solution of the resulting integral expression, leads to the following expression

$$(1+i\eta)B_o\left[\pi^4 I_1(\tfrac{1}{a^2} + \tfrac{1}{b^2})^2 A'_{11}(I_9 - \tfrac{3\mu}{a^2} I_{11} + \tfrac{3\mu^2}{a^4} I_{30} - \tfrac{\mu^3}{a^6} I_{31})\right.$$

$$+(\tfrac{2^2}{a^2} + \tfrac{1}{b^2})^2 A'_{21}(I_{16} - \tfrac{3\mu}{a^2} I_{18} + \tfrac{3\mu^2}{a^4} I_{34} - \tfrac{\mu^3}{a^6} I_{35})\}$$

$$+6(\tfrac{2\mu}{a^2}) \tfrac{\pi^3}{a} I_1\{(\tfrac{1}{a^2} + \tfrac{1}{b^2})A'_{11}(I_{21} - \tfrac{2\mu}{a^2} I_{36} + \tfrac{\mu^2}{a^4} I_{37})$$

$$+ 2(\tfrac{2^2}{a^2} + \tfrac{1}{b^2})A'_{21}(I_{24} - \tfrac{2\mu}{a^2} I_{38} + \tfrac{\mu^2}{a^4} I_{39})\}$$

$$-3\pi^2(2)(-\tfrac{2\mu}{a^2})^2 I_1\{A'_{11}(\tfrac{1}{a^2} + \tfrac{\nu}{b^2})(I_{11} - \tfrac{\mu}{a^2} I_{30})$$

$$+A'_{21}(\frac{2^2}{a^2} + \frac{\nu}{b^2})(I_{18} - \frac{\mu}{a^2} I_{34})\}$$

$$+3\pi^2(\frac{2\mu}{a^2})I_1\{A'_{11}(\frac{1}{a^2} + \frac{\nu}{b^2})(I_9 - \frac{2\mu}{a^2} I_{11} + \frac{\mu^2}{a^4} I_{30})$$

$$+(\frac{2^2}{a^2} + \frac{\nu}{b^2})A'_{21}(I_{16} - \frac{2\mu}{a^2} I_{18} + \frac{\mu^2}{a^4} I_{34})\}]$$

$$-\rho h_o \omega^2_{11} I_1 [A'_{11}(I_9 - \frac{\mu}{a^2} I_{11}) + A'_{21}(I_{16} - \frac{\mu}{a^2} I_{18})]$$

$$-\frac{4P}{ab} I_1 I_9 = 0 \qquad\qquad \ldots (5.2.2.2)$$

where, the integrals I's are given in Appendix 2.

Substitution of these integrals into Eqs.(5.2.2.1) and (5.2.2.2) and simplification leads to the simultaneous equations of the type (5.1.2.6) and (5.1.2.7). It would be noted that Eq.(5.1.2.8) to Eq.(5.1.2.15) hold good in this case as well, where the taper coefficients G_1 to G_8 and H_1 to H_8 are given in Appendix 4.

5.3 LOSS FACTOR EVALUATION

The one term solution for the response of the plate is given by Eq.(5.1.1.8) as

$$\eta \; W = \frac{P}{B_o C_1} \sin(\frac{\pi x}{a}) \; \sin(\frac{\pi y}{b}) \qquad \ldots (5.3.1)$$

where the coefficient C_1 for linear thickness variation is given by Eq.(5.1.1.5) and for parabolic thickness variation by Eq.(5.2.1.2). Now making use of Eqs.(2.1.17) and putting

$$Z = \frac{h}{16} = \frac{h_o G(x)}{16}$$

One gets the stress expressions as

$$\eta\sigma_x = \frac{0.75\pi^2 P\, G(x)}{a^2 h_0^2 C_1}(1+\nu e^2)\ \sin(\tfrac{\pi x}{a})\sin(\tfrac{\pi y}{b})$$

$$\eta\sigma_y = \frac{0.75\pi^2 P\, G(x)}{a^2 h_0^2 C_1}(\nu+e^2)\sin(\tfrac{\pi x}{a})\ \sin(\tfrac{\pi y}{b})$$

$$\eta\tau_{xy} = \frac{0.75\pi^2 P G(x)}{a^2 h_0^2 C_1}(1-\nu)\ e\ \cos(\tfrac{\pi x}{a})\ \cos(\tfrac{\pi y}{b})\qquad \dots (5.3.2)$$

The stress distribution can be obtained by making use of Eqs.(5.3.2), (2.1.19) and (2.2.4).

As regards the element size, the following points of differences are to be noted, rest of the considerations remaining same.

(1) In the case of constant thickness plates the element size dv remains same at all the points (x,y) and therefore it does not appear in Eq.(2.3.3). For the case of variable thickness plate, the element size will depend on its location.

Therefore, Eq.(2.3.3) modifies to

$$\eta = (\tfrac{JE}{\pi})^{1/(N-1)}\left[\frac{\sum (\eta\sigma_e)^N\ dv}{\sum (\eta\sigma_e)^2\ dv}\right]^{\frac{1}{(N-1)}}\qquad \dots (5.3.3)$$

(2) Since the thickness variation is in X-direction, there is no symmetry of modal wave form and hence of stress patterns about the line X = a/2. Therefore, the stress distribution is to be considered for half the plate size from x = 0 to x = a and from y = 0 to y = $\frac{b}{2}$.

(3) Quite a bit of economy is obtained in computer programme formulation for the determination of stress distribution from Eq.(5.3.2) by considering the periodicity of the trigonometric functions and taking due care of the. $G(x)$ term.

The two term solution for the response is given by Eq.(5.1.2.15) as

$$\eta W' = \frac{P}{B_o r_6}\left[F_2 \sin(\frac{\pi x}{a}) - F_3 \sin(\frac{2\pi x}{a})\right] \sin(\frac{\pi y}{b}) \quad \ldots \ (5.3.4)$$

The loss factor once again is computed by following the steps as indicated before.

5.4 RELATIONSHIP BETWEEN THE LOSS FACTORS OF CONSTANT AND VARIABLE THICKNESS

One observes from Eqs.(5.3.2), (2.1.19) and (2.2.4), that, σ_{am} the maximum value of stress σ_e , would occur when $Z = \frac{h}{2}$ and $\frac{x}{a} = \frac{y}{b} = \frac{1}{2}$ and would be given by

$$\eta \ \sigma_{am} = \frac{6P\pi^2 [G(x)]_{x=a/2} \cdot \{(1+\nu e^2) \text{ or } (\nu + e^2)\}}{h_o^2 a^2 C_1} \cdot (1+\xi)$$

$$\ldots \ (5.4.1)$$

Neglecting the variation in the ratio α/β for uniform thickness and variable thickness plates and observing that ξ would be same for both the plates, one obtains through Eqs.(5.4.1), (2.3.1) and (2.3.5), the following approximate equation

$$\left[\frac{\eta_V}{\eta_c}\right] = \left[\epsilon\right]^{\frac{N-2}{N-1}} \qquad \qquad \dots (5.4.2)$$

where,

$$\epsilon = \left[G(x)\right]_{x=a/2} \cdot \left[\frac{C_{l_c}}{C_{l_v}}\right]$$

Further, one gets

$$\left[G(x)\right]_{x=a/2} = (1 + \frac{\delta}{2}) \quad \text{for linear thickness variation}$$

$$= (1 - \frac{\mu}{4}) \quad \text{for parabolic thickness variation}$$

$$C_{l_c} = \frac{\pi^4}{4a^2e}(1 + e^2)^2$$

and C_{l_V} is given by Eq.(5.1.1.5) or by Eq.(5.2.1.2).

Thus, one can estimate the loss factor for a variable thickness plate with the help of the approximate relationship given in Eq.(5.4.2).

CHAPTER-6

RADIATION EFFICIENCY AND SOUND POWER
RADIATED FOR COMPLEX MODE EXCITATION

The far-field acoustic pressure radiated by a
baffled plate can be obtained from Rayleigh's integral
and is given by Eq.(2.7.14). The far-field acoustic
intensity I is obtained as

$$I = \frac{|p_\omega|^2}{\rho_o c} \qquad \qquad \dots (6.1)$$

For a single odd-odd mode, it becomes [76],

$$I = 2\rho_o c \left[\frac{V_{mn} k \; ab}{\pi^3 R \; m \; n} \right]^2 \left\{ \frac{\cos(\frac{\alpha_o}{2}) \; \cos(\frac{\beta_o}{2})}{\{(\frac{\alpha_o}{m\pi})^2 - 1\}\{(\frac{\beta_o}{n\pi})^2 - 1\}} \right\}^2 \qquad \dots (6.2)$$

Also, the average acoustic power radiated from one side
of the panel is given by

$$\Pi = \int_o^{2\pi} \int_o^{\pi/2} I \; R^2 \sin\theta \; d\theta \; d\emptyset \qquad \dots (6.3)$$

Substituting Eqs.(6.2) in (6.3) and using Eqs.(2.7.7) and
(2.7.13) one gets [76],

$$S_{mn} = \frac{64 \; k^2 ab}{\pi^6 m^2 n^2} \int_o^{\pi/2} \int_o^{\pi/2} \left[\frac{\cos(\frac{\alpha_o}{2}) \; \cos(\frac{\beta_o}{2})}{\{(\frac{\alpha_o}{m\pi})^2 - 1\}\{(\frac{\beta_o}{n\pi})^2 - 1\}} \right]^2 \sin\theta \; d\theta \; d\emptyset \qquad \dots (6.4)$$

It would be seen from the above equation that, the velocity
term does not appear in radiation efficiency expression for

-77-

a single mode. However, when complex mode excitation is considered, the velocity terms do appear in the expression for S_{av} and hence modal velocity coefficients for a type of loading are of importance.

Substituting Eq.(2.7.8) into Eq.(2.7.14) one gets the sound power radiated under complex resonance excitation condition, as

$$\Pi = \frac{8\rho_o c k^2 a^2 b^2}{\pi^6} \int_o^{\pi/2} \int_o^{\pi/2} \cos^2(\frac{\alpha_o}{2}) \cos^2(\frac{\beta_o}{2}) \left[\Sigma \Sigma \frac{V_{mn}}{mn \left[(\frac{\alpha_o}{m\pi})^2 - 1 \right] \left[(\frac{\beta_o}{n\pi})^2 - 1 \right]} \right]^2 \sin\theta \, d\theta \, d\phi \quad \ldots (6.5)$$

From Eqs.(2.7.13) and (6.5) one gets

$$S_{av} = \frac{64 k^2 ab}{\pi^6} \int_o^{\pi/2} \int_o^{\pi/2} \frac{\cos^2(\frac{\alpha_o}{2}) \cos^2(\frac{\beta_o}{2})}{\Sigma \Sigma V_{mn}^2} \left[\Sigma \Sigma \frac{V_{mn}}{mn \left[(\frac{\alpha_o}{m\pi})^2 - 1 \right] \left[(\frac{\beta_o}{n\pi})^2 - 1 \right]} \right]^2 \sin\theta \, d\theta \, d\phi \quad \ldots (6.6)$$

where the summation in the above two equations include all the resonance modes at a particular exciting frequency. When the radiation efficiency and sound power radiated under a number of non-resonant modes are to be evaluated then V_{mn} in the above expressions is to be replaced by $|V'_{mn}|$ which is given by Eq.(2.7.4).

A careful look into the bracket squared part of
the integral of Eq.(6.6) would indicate that there are two
types of terms present in the expansion. The first type are
the 'single' terms like

$$\frac{V_{mn}^2}{m^2 n^2 \left[\left(\frac{\alpha_o}{m\pi}\right)^2 - 1\right]^2 \left[\left(\frac{\beta_o}{n\pi}\right)^2 - 1\right]^2} \quad ,$$

and the second type are the 'product' terms like

$$\frac{2 V_{m_1 n_1} V_{m_2 n_2}}{m_1 n_1 m_2 n_2 \left[\left(\frac{\alpha_o}{m_1\pi}\right)^2 - 1\right] \left[\left(\frac{\beta_o}{n_1\pi}\right)^2 - 1\right] \left[\left(\frac{\alpha_o}{m_2\pi}\right)^2 - 1\right] \left[\left(\frac{\beta_o}{n_2\pi}\right)^2 - 1\right]}$$

where (m_1,n_1) and (m_2,n_2) are the two modes which are
superimposed.

When the effect of superposition of K number of
modes is to be studied, then, there would be K number of
'single' terms and K_{c_2} number of 'product' terms in the
expansion. The concept of 'single'and 'product' terms has
been incorporated only to facilitate the programme formulat-
ion.

For the case when the superposition of a non-resonant
and a resonant mode is to be studied, it would be seen that
the integral of Eq.(6.6) would consist of only 'single' terms.
This is because of the fact, that, under such situations,
it is the pressure squared or sound intensity which is to

be added up instead of addition of sound pressures. However, it can be verified – as shown below – that under such conditions the radiation efficiency and the sound power radiated would be equal to the corresponding values for the resonant mode, due to the fact that the velocity term for the resonant mode is very much larger than the corresponding non-resonant mode value.

Let, (m_1, n_1) be an odd-odd resonant mode and (m_2, n_2) be an odd-odd non-resonant mode. The super-position of these two modes would give the resultant far-field acoustic pressure to be

$$p^2 = p_1^2 + p_2^2$$

From Eq.(6.2) for small values of α_o and β_o, one gets,

$$p^2 = \left\{-ik\rho_o c \; \frac{e^{ikR}}{2\pi R} \; \frac{ab}{\pi^2}(-2e^{-i\alpha_o/2}.\cos(\frac{\alpha_o}{2}))(-2e^{-i\beta_o/2}.\right.$$

$$\left.\cos(\frac{\beta_o}{2})\right\}^2 \left[\frac{V_{m_1 n_1}^2}{m_1^2 n_1^2 \{(\frac{\alpha_o}{m_1 \pi})^2 -1\}^2 \{(\frac{\beta_o}{n_1 \pi})^2 -1\}^2} + \right.$$

$$\left. \frac{V_{m_2 n_2}^2}{m_2^2 n_2^2 \{(\frac{\alpha_o}{m_2 \pi})^2 -1\}^2 \{(\frac{\beta_o}{n_2 \pi})^2 -1\}^2} \right] \qquad \dots (6.7)$$

With the help of Eq.(6.5) one gets, the sound power radiated as

$$\Pi = \int_0^{\pi/2} \int_0^{\pi/2} \frac{8\rho_o c k^2 a^2 b^2}{\pi^6} \cos^2\left(\frac{\alpha_o}{2}\right) \cos^2\left(\frac{\beta_o}{2}\right)$$

$$\cdot \left[\frac{V_{m_1 n_1}^2}{m_1^2 n_1^2 \left\{ \left(\frac{\alpha_o}{m_1 \pi}\right)^2 - 1 \right\}^2 \left\{ \left(\frac{\beta_o}{n_1 \pi}\right)^2 - 1 \right\}^2} \right.$$

$$\left. + \frac{V_{m_2 n_2}^2}{m_2^2 n_2^2 \left\{ \left(\frac{\alpha_o}{m_2 \pi}\right)^2 - 1 \right\}^2 \left\{ \left(\frac{\beta_o}{n_2 \pi}\right)^2 - 1 \right\}^2} \right] \sin\theta \, d\theta \, d\phi \qquad \dots (6.8)$$

Using Eq.(2.7.13) one obtains, from the above equation,

$$S = S_{m_1 n_1} \cdot \frac{V_{m_1 n_1}^2}{\sum V_{mn}^2} + S_{m_2 n_2} \cdot \frac{V_{m_2 n_2}^2}{\sum V_{mn}^2} \qquad \dots (6.9)$$

where, $\sum V_{mn}^2 = (V_{m_1 n_1}^2 + V_{m_2 n_2}^2)$

Since, $V_{m_1 n_1}^2 \gg V_{m_2 n_2}^2$, one can see, that

$$\sum V_{mn}^2 \simeq V_{m_1 n_1}^2$$

$$\frac{V_{m_2 n_2}^2}{\sum V_{mn}^2} \simeq 0$$

$$\frac{V_{m_1 n_1}^2}{\sum V_{mn}^2} \simeq 1.0 \; .$$

Therefore, Eq.(6.9) reduces to

$$S = S_{m_1 n_1} \qquad \dots (6.10)$$

With the similar arguments for the case of sound power radiated which is proportional to $[S_{av} \cdot \langle |V_\omega|^2 \rangle]$ one sees that

$$\Pi \simeq (\Pi)_{m_1 n_1} \qquad \qquad \dots (6.11)$$

Although above approximations have been derived for odd-odd modes, but, these are found to hold good for any mode.

The integrals of Eq.(6.6) are integrated by means of two-dimensional Gauss type quadrature formula [62].

Thus, the radiation efficiency (from Eq.(6.6)) and the sound power radiated (from Eq.(2.7.13)) from a rectangular plate, simply supported in an infinite baffle, and, excited by a central point force, are evaluated and effect of superposition of any number of resonant and non-resonant modes on these two quantities studied. Having obtained these, the effect of excitation frequency on these two quantities is also studied.

CHAPTER -7

RESULTS, DISCUSSIONS AND CONCLUSIONS

7.1 RESULTS AND DISCUSSIONS

For the purpose of analysis a rectangular plate of SAE 1020 steel of following dimension was considered:

$$a = 59.06''(1.5m); \quad e = 2.0; \quad \nu = 0.3; \quad h = 0.09842''$$
$$(0.0025m)$$

$$E = 30.0 \times 10^6 \text{ psi}; \quad \rho = 460 \text{ lbs/cft.} (7.6 \times 10^3 \text{ kg/m}^3)$$
$$(20.682 \times 10^{10} \text{ N/m}^2)$$

The damping constants J and N as obtained from Ref. [37] were chosen as,

$$J = 2.626 \times 10^{-13}; \quad N = 2.286$$

A central point harmonic force of amplitude $P = 0.2248$ lb (1 Newton) was assumed to act on the plate.

The modal damping for the above reference plate has been classified as η_{mn}^{x} in the text.

7.1.1 The Upper and Lower Bounds for Fundamental Mode Damping

The ratio of loss factors dependent on dilatational energy dissipation (E .(2.2.4)) to that dependent on distortional energy dissipation (Eq.(2.2.3)) were computed for different values of aspect- ratios and damping indices. These computations were done for both the constant force and constant maximum amplitude excitations. Figure 7.1 gives the variation of this ratio with the aspect ratio of the plate,

whereas, the variation with respect to the damping index
is indicated in Fig.7.2.

It is seen from these plots that the ratio of
upper and lower bounds for the fundamental mode loss
factors is maximum for the square plate and decreases with
the increase of aspect ratio. This practically becomes
constant for the values of aspect ratios beyond 5.0

For the case of constant force excitation the ratio
of loss factors decreases with the increase of damping
index and becomes constant as N increases beyond 3.0. But,
for the case of constant maximum amplitude excitations this
ratio increases with the increase of damping index. This is
in conformity to the behaviour shown by uniform uniaxial
stress case where this ratio is 2^N.

It is known that both the dilatational and distort-
ional effects should be taken into consideration for
calculating the modal damping. This requires an experi-
mental determination of the factor Γ in expression (2.2.2).
It is noted that an approximate estimate of the fundamental
mode loss factor can be obtained for the case of constant
force excitation particularly so, for large aspect ratio
plates and for large indices, by making use of either of
the Eqs. (2.2.3) or (2.2.4). This is based on the concept
that actual damping would be a value in between the two
bounded values as observed by Whittier. The large value of

this ratio obtained for the constant maximum amplitude excitation compares favourably with the ratio of 7 as obtained by Whittier for circular plates.

7.1.2 Modal Damping Under Constant Force Excitation

The normalized damping energy integrals α and normalized strain energy integrals β were computed for various resonant modes by obtaining the stress distribution throughout the plate volume and writing a polynomial of the form

$$\left(\frac{V}{V_p}\right) = a_1\left(\frac{\sigma_e}{\sigma_{am}}\right)^4 + a_2\left(\frac{\sigma_e}{\sigma_{am}}\right)^3 + a_3\left(\frac{\sigma_e}{\sigma_{am}}\right)^2 + a_4\left(\frac{\sigma_e}{\sigma_{am}}\right) + a_5$$

and

$$\left(\frac{V}{V_p}\right) = a_1'\left(\frac{\sigma_{eT}}{\sigma_{eTm}}\right)^4 + a_2'\left(\frac{\sigma_{eT}}{\sigma_{eTm}}\right)^3 + a_3'\left(\frac{\sigma_{eT}}{\sigma_{eTm}}\right)^2 + a_4'\left(\frac{\sigma_{eT}}{\sigma_{eTm}}\right) + a_5'$$

The coefficients a_1 to a_5 and a_1' to a_5' were obtained through curve fitting and the integrals could then be simplified to

$$\alpha = \frac{4a_1}{N+4} + \frac{3a_2}{N+3} + \frac{2a_3}{N+2} + \frac{a_4}{N+1} \; ,$$

$$\beta = \frac{2a_1'}{3} + \frac{3a_2'}{5} + \frac{a_3'}{2} + \frac{a_4'}{3}$$

Table 7.1 indicates the modal (β/α) values along with the nodal aspect ratios. It is seen that there is a negligible variation in β/α from mode to mode. This therefore justifies the assumption made in the derivation of the simplified expression for the loss factor given in Eq.(3.1.7).

The modal loss factors for number of resonant modes were computed with the help of Eq.(2.3.3). These were checked with the evaluations made with Eq.(2.3.5). These

are also indicated in Table 7.1 and the values are found to match well.

The simplified relationship (3.1.7) which has been obtained in the present work, was also verified. This equation correlates the higher mode damping with the fundamental mode value. The factor K, as given in Eq.(3.1.1) were evaluated. Table 7.2, gives the values of this factor K for certain resonant modes and also compares the loss factor values as obtained from Eq.(3.1.7) with the computed values. It is seen that the approximate expression gives the modal damping within 3% of the actual value. Therefore, use of this relationship would obviate the need of repeating cumbersome computations every time for estimating the modal damping for higher modes.

Figure 7.3 gives the plot of modal damping under constant force excitation. It is observed that the modal damping decreases with the increase of modal frequency. Now, if the magnitude of the constant force changes then the effect of this change on the damping of a mode can be obtained with the help of Eq.(3.1.9). Figure 7.4 shows the effect of load ratio k_1 on the damping of any mode. This is a straight line with a slope of $(\frac{N-2}{N-1})$ and indicates an increase in damping with the increase in force. The effect of change in force on the damping from mode to mode is also shown in Fig.7.3 where the parallel shift i_1 has been obtained from Fig.7.4.

7.1.3 Modal Damping under Constant Amplitude Excitation

The factor K_0 as given by Eq.(3.2.3) was evaluated for number of resonant modes. Table 7.3 gives the value of this factor for several modes and compares the computed loss factor values with the values obtained from the simplified expression (3.2.4). This equation correlates the higher mode damping with the fundamental mode value. This is subject to the condition that in each case excitation force is adjusted such that the maximum amplitude of vibration is brought equal to the fundamental mode value corresponding to the force P. It is seen that the simplified equation gives a sufficiently accurate result.

Figure 7.3 also shows the modal damping vs. modal frequency under constant maximum amplitude excitation. The damping increases with the increase of modal frequency in such case. Eq.(3.2.6) for a mode is plotted in Fig.7.4 and is a straight line with a slope of (N-2). This gives the effect of amplitude ratio on the modal damping. It is seen that for the same ratio of increase in constant amplitude excitation and constant force excitation ($k_1 = k_2, > 1.0$), the increase in loss factor for a mode is larger in the former case. Figure 7.3 also indicates the effect of amplitude ratio on the damping from mode to mode, the parallel shift i_2 having been obtained from Fig.7.4.

7.1.4 Loss Factor under Complex Resonance Condition

Loss factors for the plate when it is vibrating under complex resonance condition, were evaluated by performing the modal superposition and using Eq.(2.5.2). The loss factors under such complex resonance condition were also computed from the simplified expression (3.3.5) which has been obtained in the present work.

The loss factor computations for certain complex resonance modes and for three values of damping index N are shown in Table 7.4. It is noted that the approximate relationship gives a satisfactory value for two cases of complex modes but the error is rather large in the other two cases. This is probably due to unfavourable combinations of nodal aspect ratios of the constituent resonant modes. It is further seen that the errors are quite large when N increases. A possible cause for this behaviour might be that the approximations incorporated in the derivation of the simplified expression are not holding good to that extent.

It is observed that the total loss factor, in general, is larger than each of the individual values contributing to the complex resonance condition. Therefore, it is imperative to calculate this, rather than using any sort of average value.

Table 7.5 shows the computed values of η_T for certain

complex resonance conditions when the constant force excitation is 2P. These values are compared with η_T values as obtained from Eq.(3.1.9) and it is seen that one can make use of Eq.(3.1.9) to study the effect of force ratio on the total loss factor under complex resonance excitation. It is noted, that, as force increases, damping also increases.

Table 7.6 gives the computed values of the total loss factor and as obtained from Eq.(3.3.5) when a constant amplitude excitation is considered. Similar observation as in Table 7.4 as regards the error is made in this case as well. Table 7.7 indicates the effect of amplitude ratio on the total loss factor and verifies the Eq.(3.2.6). It is seen that the damping under such situation increases as the constant amplitude excitation increases. As a matter of fact the plot of Fig.7.4 which gives the effect of force and amplitude ratio on the modal damping is true for the case of total damping under complex resonance condition as well.

7.1.5 Effect of Aspect Ratio, Thickness, Damping Constants and Eccentric Force on the Fundamental Mode Damping

The ratio (β/α) was calculated for plates of different aspect ratios and thicknesses and is shown in Table 7.8. A negligible variation was observed in the values of (β/α) thus justifying the approximation made in deriving Eq.(3.4.1). This table also gives the values of

computed η_{11} and as obtained with the help of the
proposed simplified Eq.(3.4.1). The error in such compu-
tation is not large indicating that Eq.(3.4.1) can be
used to study the effect of changes in aspect ratios
and thicknesses on the modal damping. It is also seen
that the loss factor is independent of the absolute
dimensions of the plate and depends only on thickness
and aspect ratio.

Figures 7.5 and 7.6 give the effect of aspect
ratio and thickness on the fundamental mode damping,
respectively, for the constant force and constant maxi-
mum amplitude excitations. The damping is maximum for a
square plate and decreases as the aspect ratio increases
for the constant force excitation. Damping increases with
the increase in aspect ratio for the constant maximum
amplitude excitation. It is further seen that the damp-
ing increases with the increase of thickness for cons-
tant amplitude excitation and decreases with the increase
of thickness for constant force excitation. It would
be noted that the fundamental mode damping has been
evaluated in the above cases, however, the value of the
natural frequency is different in each case.

To study the effect of damping index N on the
modal damping, five different steel materials were
considered [37]. The integral ratio (β/α) was computed
in each case. The loss factors were computed and were

also evaluated from the proposed simplified expression
(3.5.1). These two sets of values are shown to match well
in Table 7.9. It is seen from this table that the damping
increases with index N in the range $N > 2$. Figure 7.7
gives the (β/α) variation with the index N. This ratio
is seen to increase with the damping index.

The effect of the change in location of the point
force was studied by considering various excitation posi-
tions. The Eq.(3.6.1) was verified with the computed values
for odd-odd mode. Values for a few modes and for certain
excitation positions are given in Table 7.10. The loss
factors for additional even-even, even-odd and odd-even
modes which are excited under eccentric point force were
also computed. These were compared with the calculations
done with the help of the proposed Eq.(3.6.2) and were found
to match well as shown for certain modes in Table 7.11. For
the case of complex resonance excitation under eccentric
point force, the computations for the loss factors were
made and checked with the values as obtained from Eq.(3.3.5).
Table 7.12 shows this comparison for a few cases and indicates
that the simplified relation holds good in two cases as
observed in Table 7.4, and 7.6.

It would be observed that the modal loading coeff-
icient is no more a constant and independent of mode numbers
but now depends on the force position and the mode numbers.
Thus, it decreases by a factor $\sin(\frac{m\pi x_1}{a}) \cdot \sin(n\pi y_1/b)$ when

the force is eccentric. Maximum damping is obtained when
the force is central and it decreases gradually according
to a sine law when the force position shifts towards the
edges. Evidently system does not vibrate when the force
acts on edges. The variation in modal damping with respect
to force position is symmetrical throughout in mirror image
formation about the lines $x = \frac{a}{2}$ and $y = \frac{b}{2}$.

7.1.6 Fundamental Mode Damping of Plates with Clamped Edges

The fundamental mode frequency parameters λ_{11} for
different aspect ratios were computed for all the four
cases of clamped and simply supported boundary conditions
(Fig.4.1) with the help of Eqs.(4.1.2), (4.2.2), (4.3.2) and
(4.4.2). These values along with the λ_{11} for all edges
simply supported case (Eq.(2.1.14)) are given in Table 7.13.
The frequency increases with the increase in aspect ratio
for all the cases. It is minimum for all the edges simply
supported case and is maximum for all clamped edge case.

The fundamental mode loss factors were computed for
various cases. The effect of aspect ratio on these is shown
in Fig.7.8. As expected the loss factor values are symmetrical
about the square plate (e = 1.0) for the cases when all
the four edges are either simply supported or clamped.
The latter case provides a larger damping for all the values
of aspect ratios, though the difference is small for low

and high aspect ratios.

The single edge clamped case (Case 1) provides
the largest damping for all values of aspect ratios,
while opposite edges clamped case (Case 2) provides
the minimum damping for all values of aspect ratios
greater than 0.8. For aspect ratios lower than 0.8, the
minimum damping is provided by a plate with all its
edges simply supported. Case 3- a combination of 3 edges
clamped and one edge simply supported gives a damping
which is lower than that of a plate with one edge
clamped and 3 edges simply supported for all aspect
ratios, but, these provide dampings which are larger
than that provided by the other three cases of plate bound-
ary conditions. For low aspect ratios, case 2 which amounts
to two opposite short edges clamped has got damping values
which is greater than that of plates having all edges either
clamped or simply-supported.

Thus, it is observed that the damping of plates
would depend on the boundary conditions of the edges.

Above is the effect which is purely contributed by the change in the boundary conditions of the plate.

7.1.7 Fundamental Mode Loss Factor for Plates of Variable Thickness

The fundamental mode frequency parameter λ_{11} was calculated for linearly varying thickness plate. One term approximation (Eq.(5.1.1.7)) and two term approximation (Eq.(5.1.2.13)) were evaluated for different combinations of aspect ratios 'e' and taper parameters 'δ'. The range of 'e' considered was from 0.25 to 2.0 and for 'δ' was from 0.1 to 0.8. Table 7.14 gives these values and compares them with λ_{mean} of Appl and Byers[1]. It is noted that the two term Galerkin's solution gives a fast convergency to the frequency parameter and the values thus obtained are of sufficient accuracy. The maximum error which occurs at high taper values is below 1% for the cases studied.

The loss factors for the fundamental resonant mode were evaluated for different taper and aspect ratio combinations. Computations were made corresponding to both one term and two-term responses. The loss factors were also computed with the help of the proposed simplified relationship given in Eq.(5.4.2). In each case the normalized ratio (η_v/η_c) was obtained. It was found that this ratio depends on the taper parameter and is evidently independent of the aspect ratio. Its plot with respect to

δ is indicated in Fig.7.9. It is noted that the loss factor for the linearly varying thickness plate decreases with the increase of taper parameter. This is because of the fact that a larger taper parameter corresponds to a larger thickness of an equivalent constant thickness plate (Fig.2.3(a)). This would result in a lower value of damping as is evidenced by Fig.7.6.

Since the two term solution gives a fairly accurate value of the natural frequency, it is inferred that the loss factors calculated at these values of the resonant frequencies would not be far-off from the actual values. It is further observed that the proposed simplified Eq.(5.4.2) gives a loss factor value which is within 5% of the two term approximation. Hence, this could be used for obtaining an estimate of the fundamental mode internal loss factor of the plate.

The frequency parameters for the parabolically varying thickness plate were computed for different combinations of aspect ratios and taper parameters μ.The aspect ratios considered were 0.25, 0.50, 0.75 and 1.00 and the taper parameters were 0.1, 0.3, 0.5 and 0.7. Both the one term and the two term approximations were evaluated. Table 7.15 gives these values and compares them with those obtained by Jain and Soni [27] . It is noted that two term approximation gives frequency parameters of sufficient accuracy for low taper values. The error is rather large

at higher taper values.

The fundamental mode loss factors were also evaluated for different cases and the ratios (η_v/η_c) were obtained. The effect of aspect ratio on this ratio was once again found to be negligible. Figure 7.10 gives the plot of (η_v/η_c) vs. taper parameter μ. It is observed that the loss factor increases with the increase of the taper parameter. This is due to the fact that a larger taper parameter corresponds to a smaller thickness of an equivalent constant thicknesses plate (Fig.2.3(b)). This would result in a higher value of damping as is indicated by Fig.7.6.

It is seen that Eq.(5.4.2) which is obtained in the present work gives loss factor values within a few percent of the two term approximation value for low taper cases.Since the two term frequency parameter for low taper values is reasonably accurate it is inferred that the damping calculated at these resonant frequencies would not be far-off from the actual value.Thus it is concluded that Eq.(5.4.2) would give a fairly good estimate of the fundamental mode damping at low taper values only.

more or less identical to one term approximation

Figures 7.9 and 7.10 also show that the loss factors as obtained with two term solution are greater than those obtained with one term approximation. The reason for this observation is as follows:

A look into tables 7.14 and 7.15 indicates
that for any combination of the aspect ratio and taper
parameter, the two term frequency parameter is greater
than the actual value. Further, one term value is
greater than the corresponding value of the two term
frequency parameter. This observation is expected and
is in conformity with the Rayleigh's concept relating
the mode shape with the natural frequency. Now, a lower
frequency would correspond to a smaller thickness and a
higher frequency to a larger thickness of an equivalent
constant thickness plate. Since thin plate has larger
damping and thick plate has smaller damping (Fig.7.6) it
is easily understood that the two term damping values
would be greater than one term damping values. The acc-
uracy of the computations would obviously depend upon
the error in the frequency parameter i.e. on the fact
that how near to the actual frequency value one is work-
ing.

7.1.8 Radiation Efficiency and Sound Power Radiated under Complex Mode of Vibration

The radiation efficiency for single resonant mode
of vibration were computed with the help of Eq.(6.4). It
was found that 5 point Gauss quadrature for numerical
integration gives results of sufficient accuracy. Values
of radiation efficiencies and sound power radiated for

the corner modes $(k_{mx}^2 \gg k^2;\ k_{ny}^2 \gg k^2)$, X-edge modes
$(k > k_{mx};\ k_{ny}^2 \gg k^2)$ and Y-edge modes $(k > k_{ny};\ k_{mx}^2 \gg k^2)$
occuring upto 2000.0 Hz are given in Tables 7.16, 7.17
and 7.18 respectively. It is seen that edge modes are
better sound radiators than the corner modes, as has
been observed by other workers as well.

For studying the superposition effect of number
of non-resonant modes, the average radiation efficienc-
ies at different excitation frequencies were computed
with the help of Eq.(6.6).The sound power radiated under
such conditions were evaluated from Eq.(2.7.13). These
values are shown in Table 7.19. The number of modes super-
imposed along with the number of modes which are having
natural frequencies less than the exciting frequencies
are also indicated in the table. It is observed that both
the radiation efficiency and sound power radiated increase
with the excitation frequencies for large values of ω_{ex}.

The gradual effect of superposition of non-resonant
modes on the radiation efficiency and the sound power
radiated are shown in Figs.7.11 and 7.12, respectively.
The abscissa for each of these graphs represents the
frequencies below which the contribution of all the vib-
rating modes has been considered. Thus, each point on
these graphs indicates the effect of summation of all the
modal contributions upto and including the mode corres-
ponding to that point. Thus, with the help of these curves,

one could study the effect of summation of each successive mode.

A sort of waviness is observed around $S_{av}=1.0$ in Fig.7.11 upto the mode order where they enter acoustic short circuit (i.e. all modes whose $k_{mn} < k$ at that exicìting frequency). This is observed at higher values of excitation frequencies. Then there is a sudden fall in the value as further modal contributions, till the excitation frequency, are considered. Beyond this only few modes contribute and S_{av} becomes constant.

The radiated sound power (Fig.7.12) increases with the increase in modal contribution, reaching a peak near the excitation frequency. Beyond this peak, it settles down to a constant value. These effects are more pronounced in case of large excitation frequencies.

Skudrzyk[64] and Greene[20] have observed that the sound pressure at any exciting frequency aan be obtained by summing up the contributions of low order modes. Skudrzyk has further observed that modes upto acoustic short circuit contribute. The results of the present analytical analysis for the radiation efficiency and the sound power radiated indicate that not only the modes upto acoustic short circuit but also the modes beyond this region and upto the excitation frequency contribute. When the excitation frequencies are near to the coincidence frequency these observations match with

those of Skudrzyk.

The effect of excitation frequency on the radiation efficiency is shown in Fig.7.13. The frequency variation upto 500.0 Hz only, is shown. The points joined by dashed line indicate the resonant mode values as obtained from Tables 7.16, 7.17 and 7.18. For excitation frequencies not coinciding with any of the natural frequencies, the effect of superposition of large number of non-resonant modes was considered, as was done in Fig.7.11. The final constant value thus obtained from this type of plot was then plotted in Fig.7.13.

A number of computations were made for large number of exciting frequencies. This indicates a variation in radiation efficiency which is highly dependent on excitation frequency. The plot shows a trend which indicates an occurrence of a peak and of a trough in between any two consecutive resonant frequencies. Thus it appears, that, the location of the excitation frequency on the frequency spectrum base with regard to the modal resonant frequencies, plays an important role in sound radiation problem.

Figure 7.14 shows a similar study for the variation of sound power radiated with the excitation frequency upto 500.0 Hz. In this plot also the final constant value

from the plot of the type as given in Fig.7.12 are
plotted. It is observed, that, these are also highly
dependent on the excitation frequencies ahowing a very
low trough in between any two consecutive resonant
large values.

The effect of superposition of two resonant
modes having same natural frequencies are indicated in
Figs.7.15 and 7.16. All the complex resonances occur-
ing upto 4000.0 Hz are indicated. It is observed that
the average radiation efficiency lies in botween the
individual contributions of the corner and the edge
modes, the major share being of the edge mode. The
sound power radiated under complex resonance case is larger
than that radiated by either mode. Therefore, in order
to estimate the sound radiation under such condition,
it would be necessary to evaluate it by resorting to
the modal superposition, since this value is neither
equal to nor is the average of the contributing modal
values.

7.2 CONCLUSIONS

7.2.1 Modal Loss Factor of Simply Supported Rectangular
       Plate of Uniform Thickness

        (i) For the case of constant force excitation, the
            ratio of fundamental mode damping based on
            dissipation dependent on dilatational and

distortional energies, decreases with the increase in both the aspect ratio and the damping index. For the case of constant maximum amplitude excitation, this ratio decreases with the increase of aspect ratio and increases with the increase in N.

(ii)   In the case of constant force excitation, an approximate value of the loss factor of the plate can be estimated with either of the criteria, particularly so for large aspect ratio plates and for large values of damping indices.

(iii)   The variation of integral ratio (β/α) from mode to mode is negligible as shown in Table 7.1.

(iv)   Resonant mode damping under constant force excitation decreases with the increase of modal frequency. If the force increases k_1 times then, the modal damping increases $k_1^{(N-2/N-1)}$ times.

(v)   One can estimate the higher mode order damping from the fundamental mode value with the help of the proposed simplified expression (3.1.7), when a constant force excitation is considered.

(vi)   Resonant mode damping under constant maximum amplitude excitation increases with the increase in modal frequency. If the maximum amplitude increases k_2 times the modal damping increases $k_2^{(N-2)}$ times.

are about 1% in linear case and about 4%.
in parabolic case.

(ii) The loss factor ratio (η_v/η_c) was found to be
independent of aspect ratio but was dependent
on the taper parameter.

(iii) The damping of linearly varying thickness
plate decreases with the increase of taper
parameter δ whereas of the parabolically varying
thickness plate was found to increase with the
taper parameter μ.

(iv) The loss factor for plate of variable thickness
can be estimated from the corresponding value
of the constant thickness plate with the help
of the proposed equation (5.4.2), within a
reasonable accuracy. This equation gives values
within 5% in case of linear thickness variation
for the taper range considered but is useful
for only low taper values in case of parabolic
thickness variation.

7.2.4 Radiation Efficiency and Sound Power Radiated
under Complex Mode of Vibration

(i) The gradual effect of superposition of large
number of non-resonant modes on the radiation
efficiency and sound power radiated were studied
at various excitation frequencies. It is observed

that all the modes upto exciting frequency
contribute towards the sound radiation.
These two quantities. become constant as
further modal contributions beyond the exci-
tation frequency are considered. These
effects are more pronounced at higher excita-
tion frequencies.

(ii) Both radiation efficiency and sound power
radiated are found to be highly dependent
on the excitation frequency. The location of
the excitation frequency on the frequency spec-
trum base with regard to the modal resonant
frequencies, plays an important role in sound
radiation. In between any two consecutive
modal resonant frequencies, the plot of radia-
tion efficiency shows a peak and a trough and
the plot of radiated sound power shows a
low trough.

(iii) The average radiation efficiency under complex
resonance excitation condition lies in between
the individual contributing modal values.
Since this value is neither equal to nor is
the average of the contributing values, it
becomes imperative to resort to the modal
superposition in order to estimate the sound
radiation. The sound power radiated under such

condition is larger than that radiated by
either modes.

Thus, in this work reported here, the dependence
of the modal damping of rectangular plates on the excita-
tion distribution has been quantified. The effects of
various parameters including thickness variation on the
modal loss factors have been quantitatively studied.
Number of simplified practical relationships correlating
the modal loss factors with the fundamental value under
different conditions have been derived. The loss factors
and radiation efficiencies for the plate vibrating under
complex resonance conditions have been obtained. The
radiation efficiencies of the plate vibrating under
complex non-resonance conditions have also been evaluated.
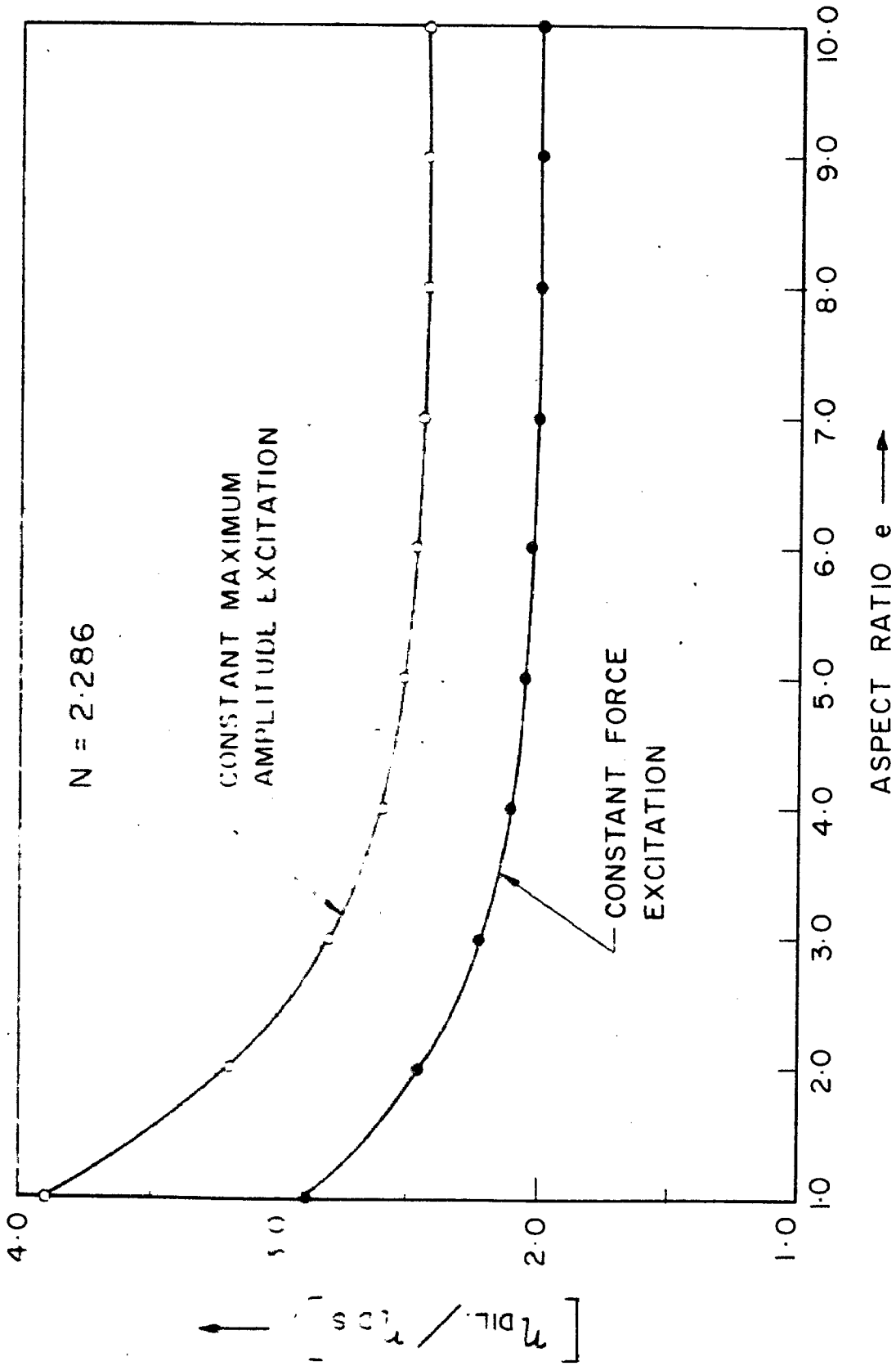
FIG. 7·1 EFFECT OF PLATE ASPECT RATIO ON THE RATIO OF UPPER AND LOWER BOUNDS OF η_{11}
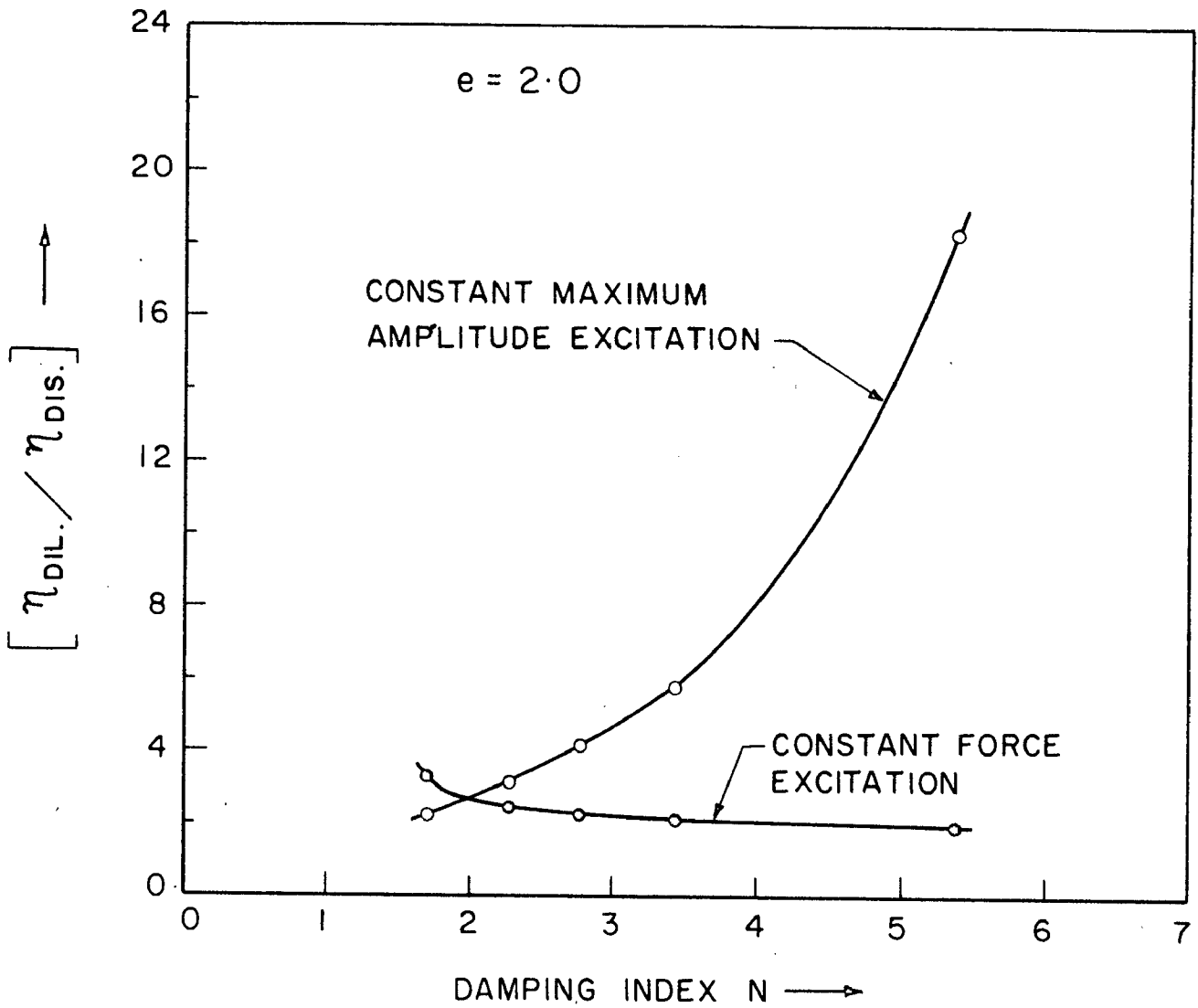
FIG. 7·2 EFFECT OF DAMPING INDEX N ON THE RATIO OF UPPER AND LOWER BOUNDS OF η_{11}
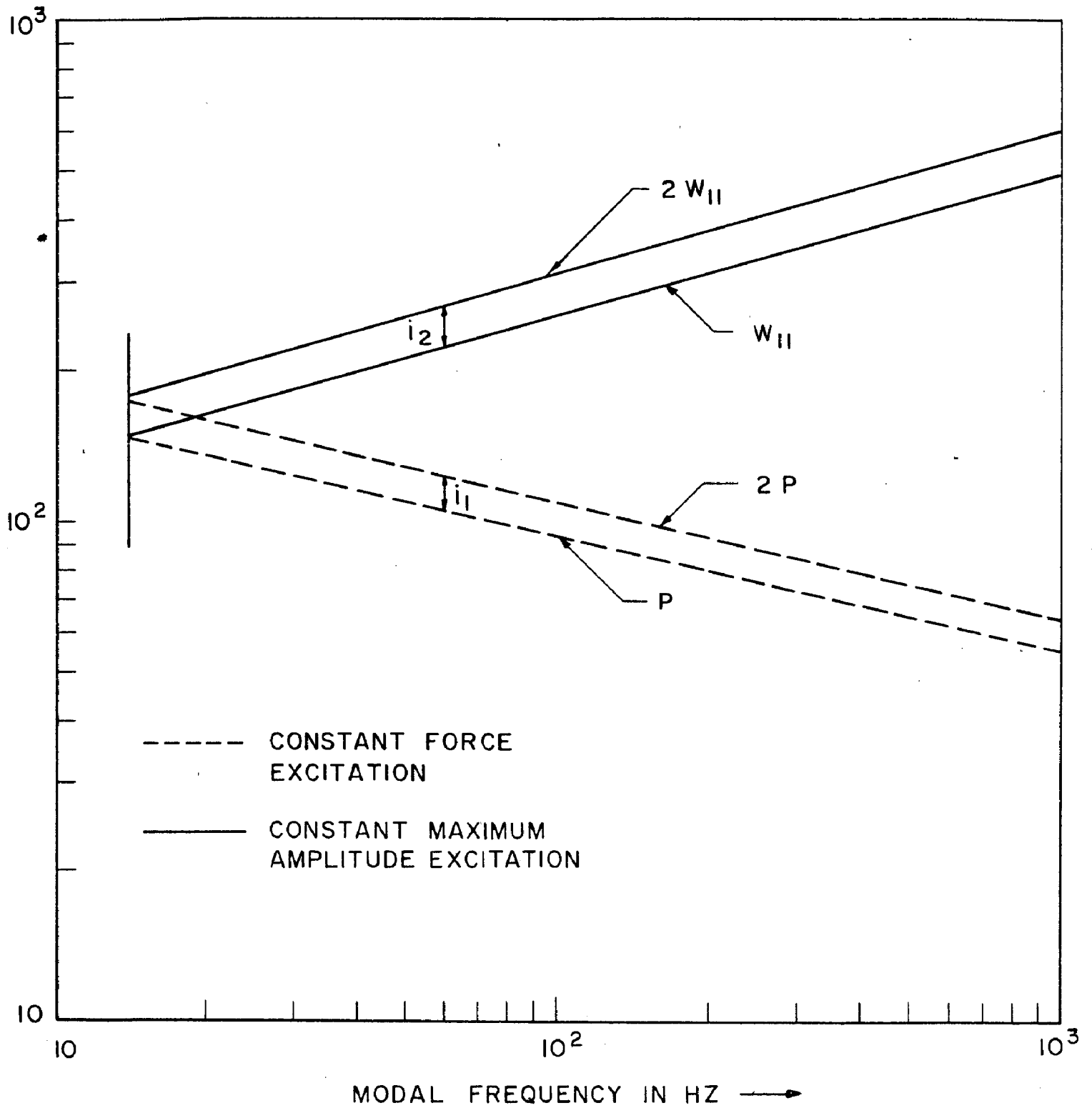
FIG. 7·3 EFFECT OF CONSTANT FORCE AND CONSTANT AMPLITUDE
EXCITATION ON THE MODAL LOSS-FACTORS.
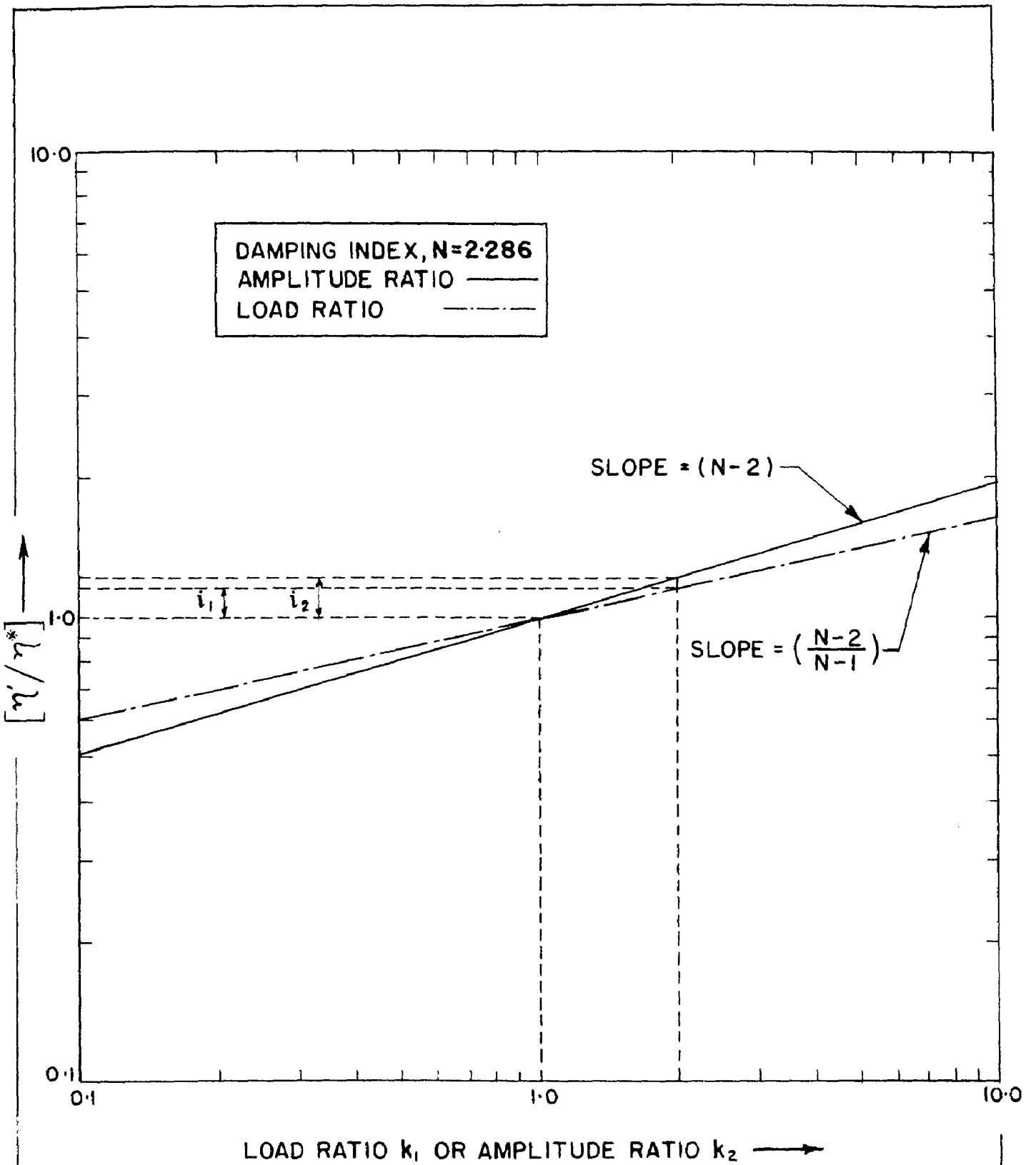
FIG. 7·4 EFFECT OF FORCE AND AMPLITUDE RATIOS ON THE MODAL LOSS FACTOR.
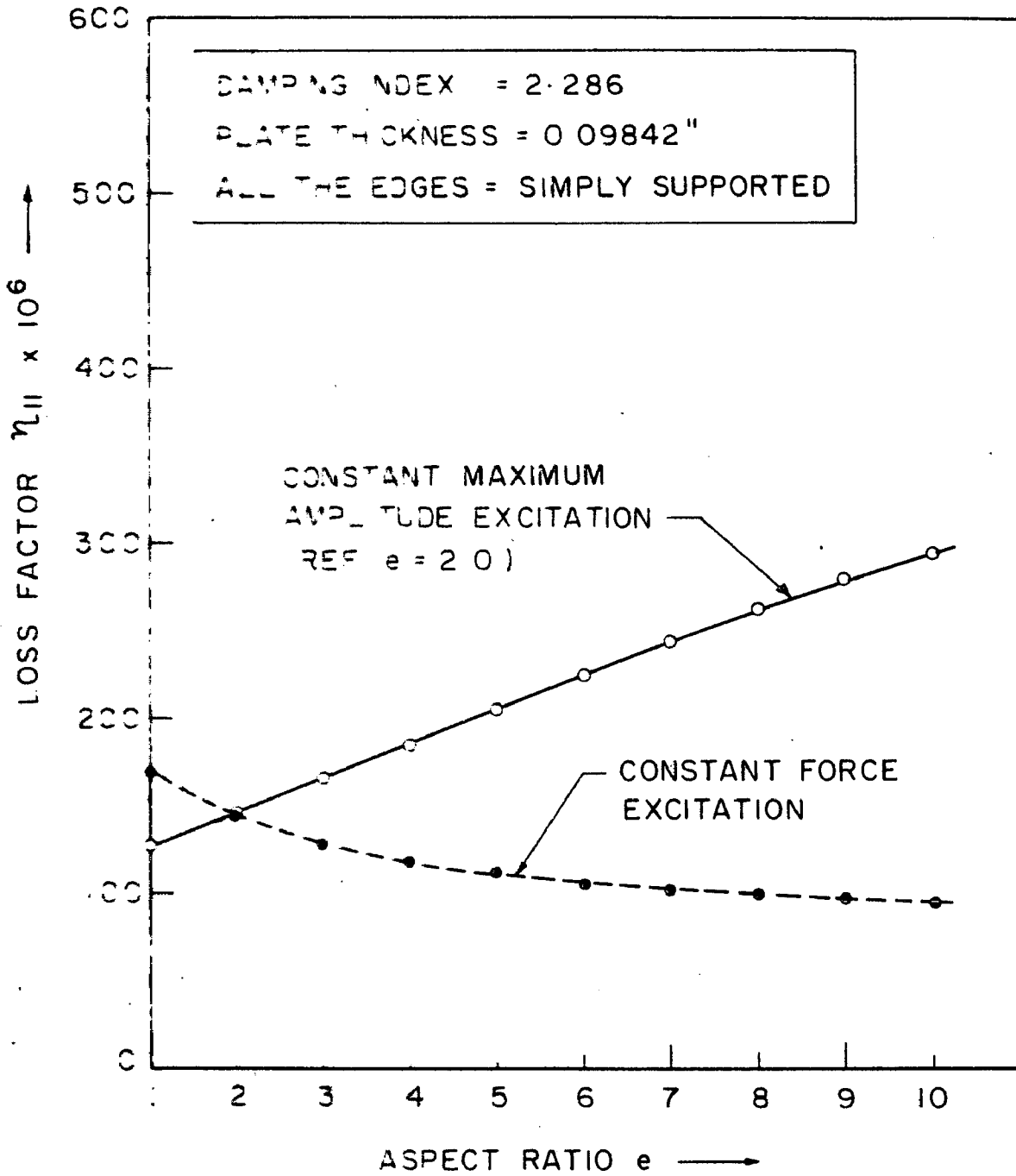
FIG. 7.5 EFFECT OF ASPECT RATIO ON THE FUNDAMENTAL MODE DAMPING.
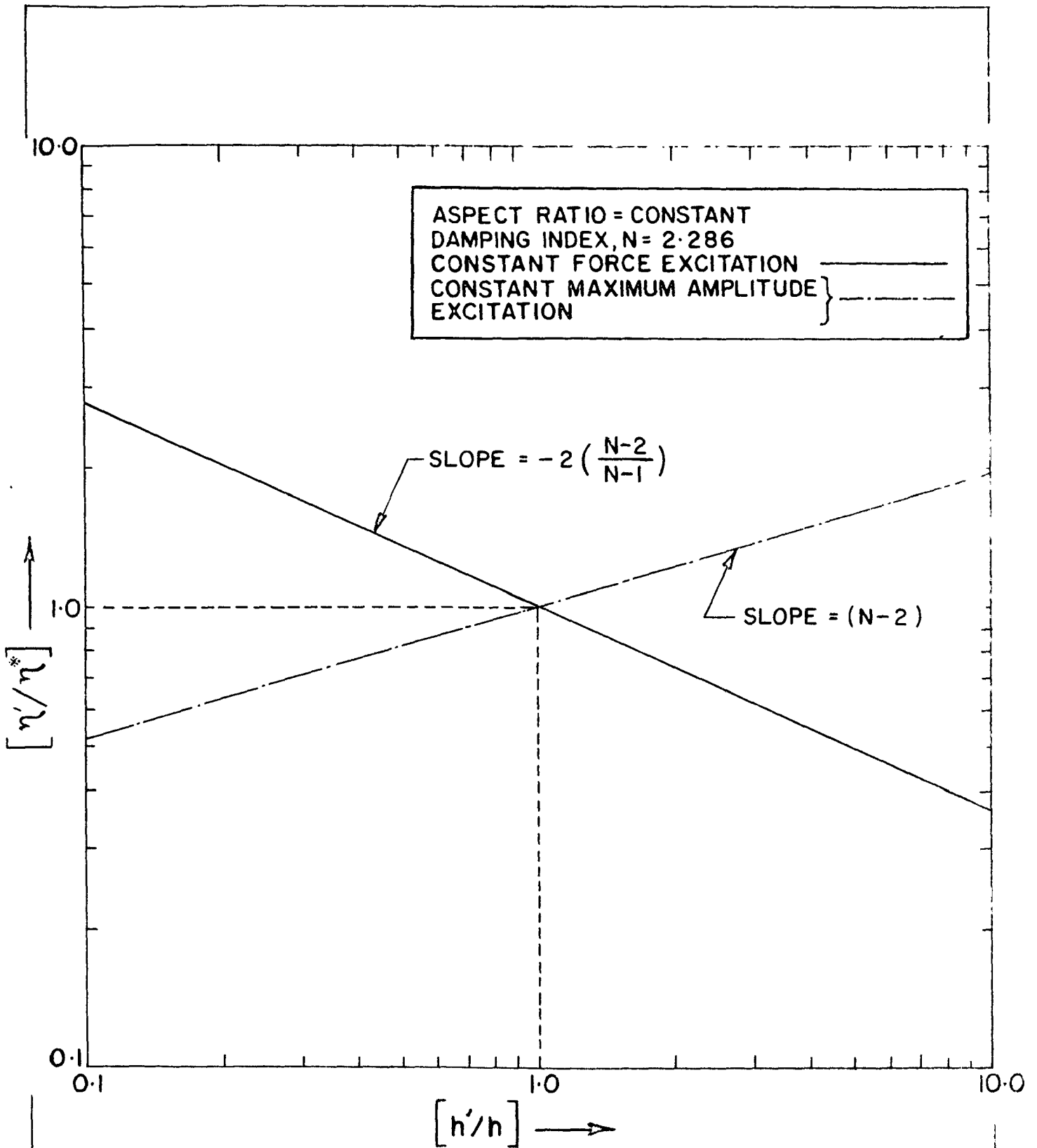
FIG. 7·6 EFFECT OF PLATE THICKNESS ON THE FUNDAMENTAL MODE DAMPING.
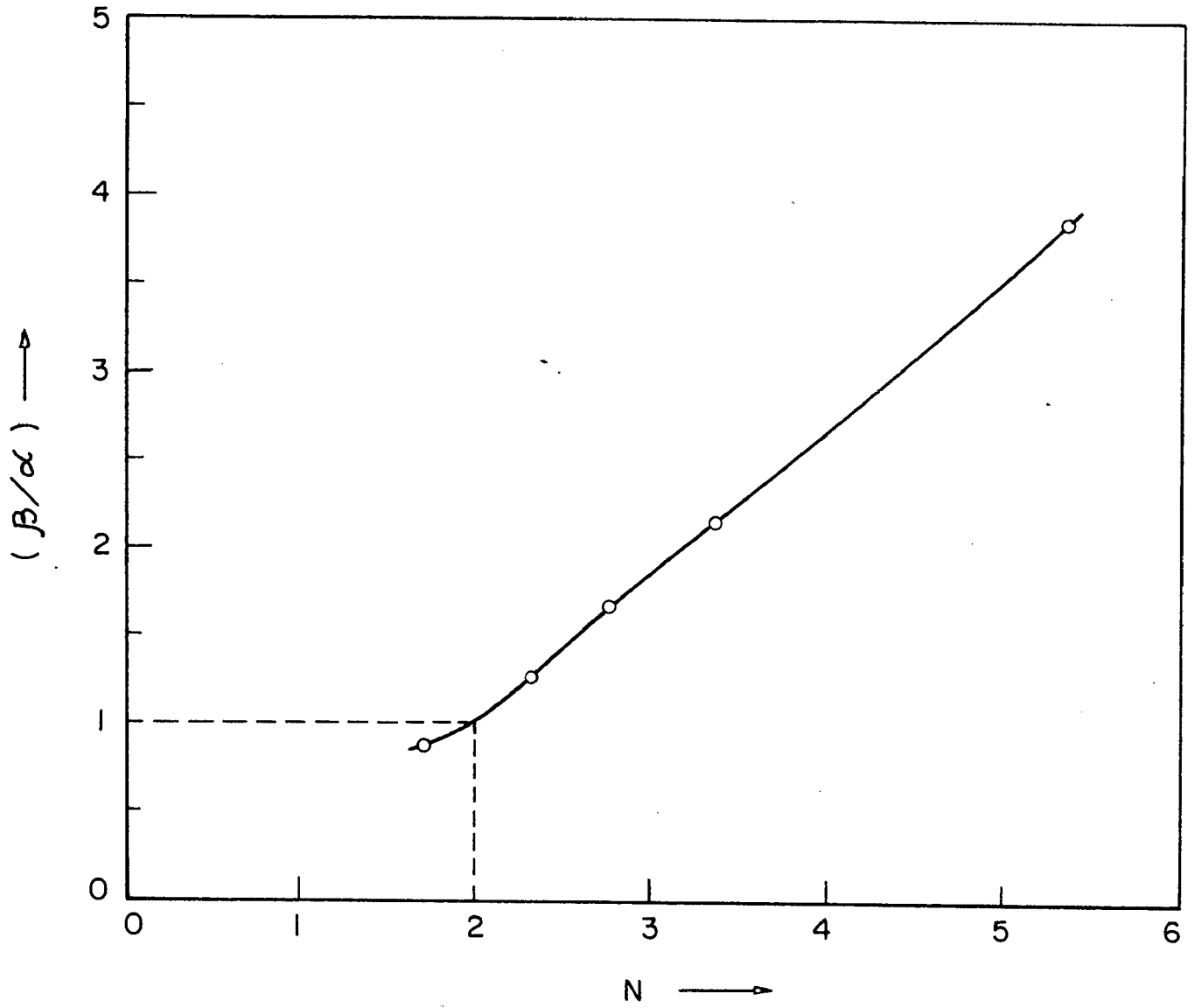
FIG. 7·7 INTEGRAL RATIO vs DAMPING INDEX FOR SIMPLY
SUPPORTED RECTANGULAR PLATE.
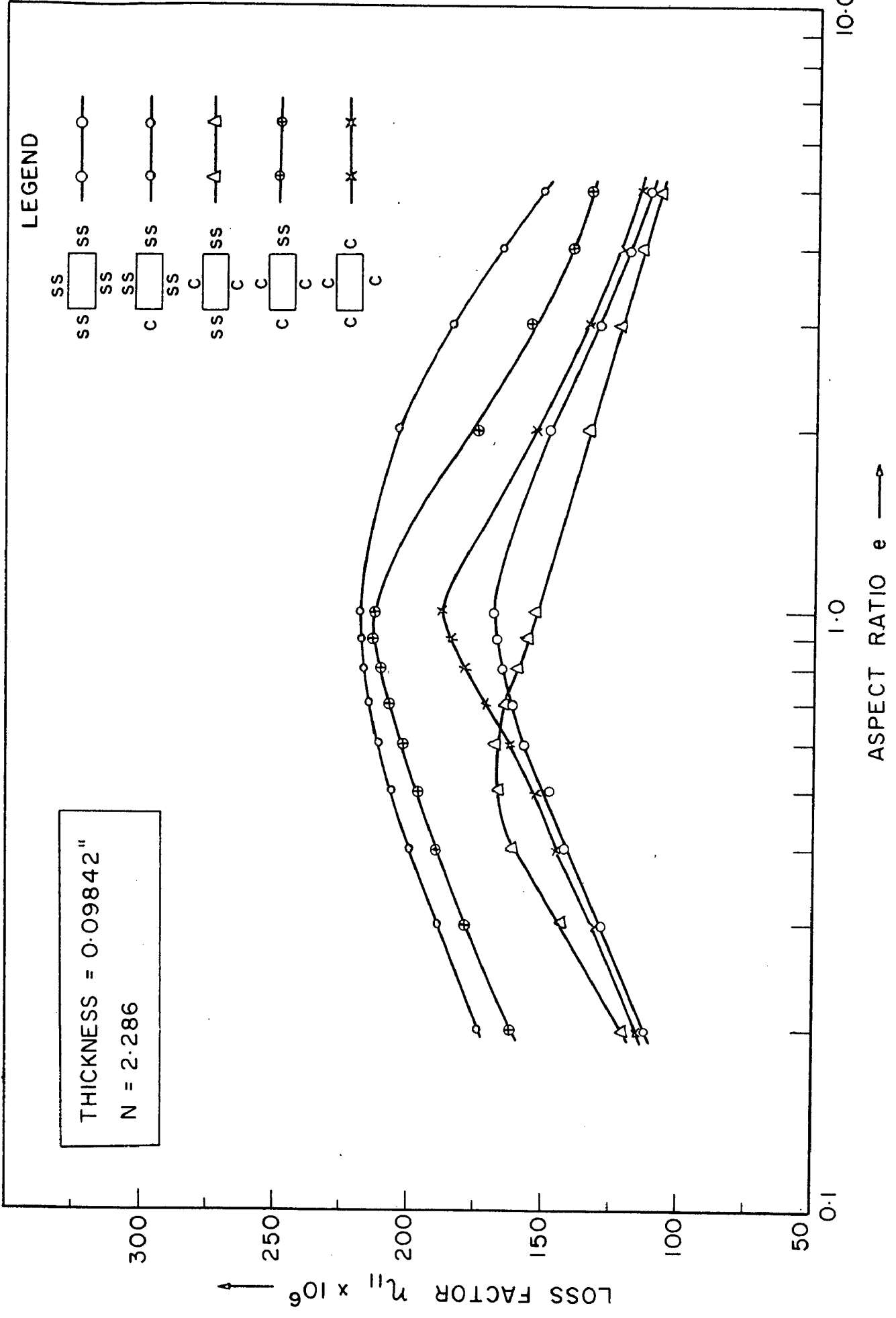
FIG. 7.8 FUNDAMENTAL RESONANT MODE LOSS FACTOR FOR PLATES OF DIFFERENT BOUNDARY CONDITIONS.
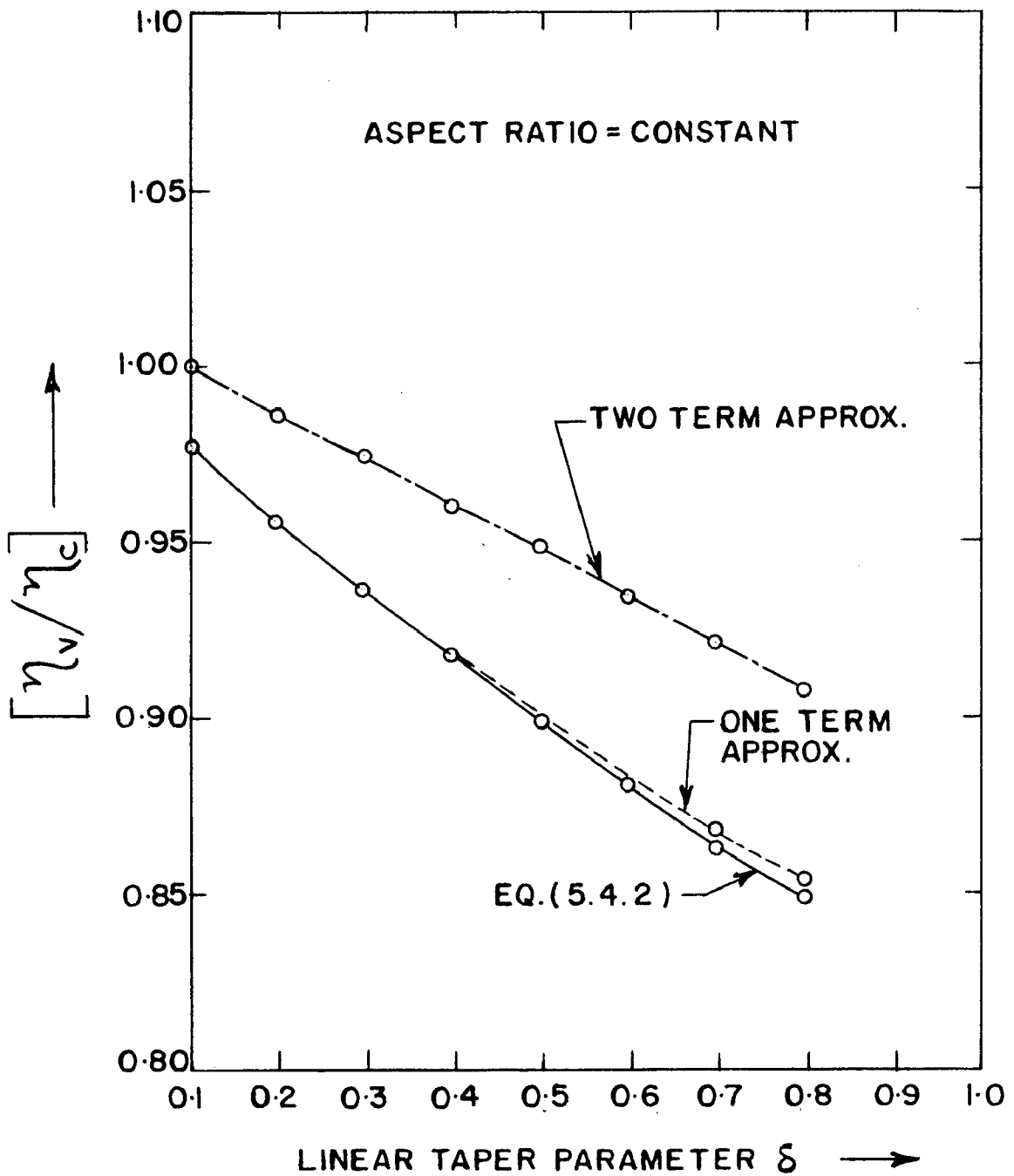
FIG. 7·9 EFFECT OF TAPER ON THE FUNDAMENTAL MODE LOSS FACTOR.
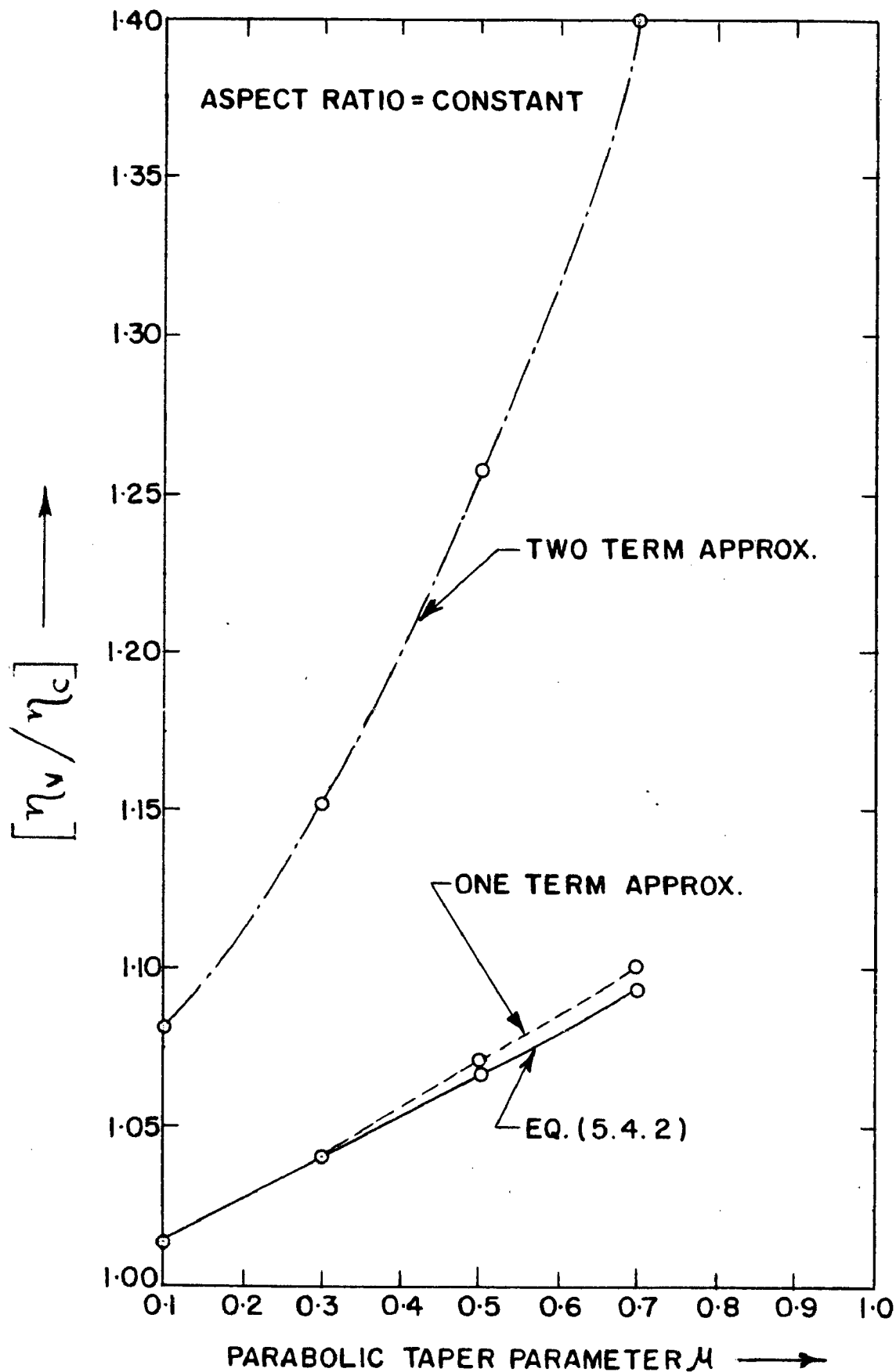
FIG. 7·10 EFFECT OF TAPER ON THE FUNDAMENTAL MODE LOSS FACTOR.
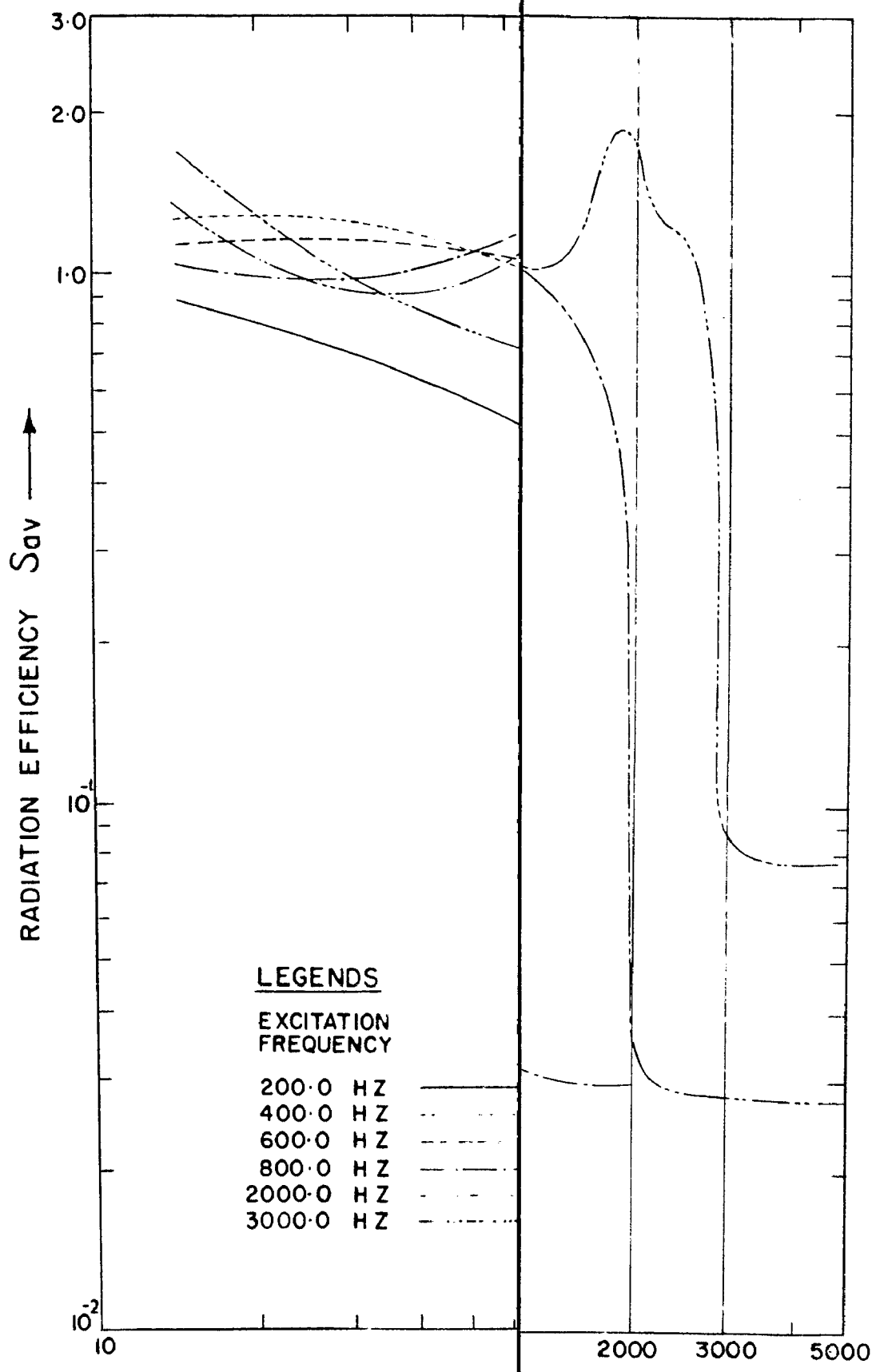
FIG. 7·II EFFECT OF SUPERE RADIATION
EFFICIENCY AT VARIOUS E
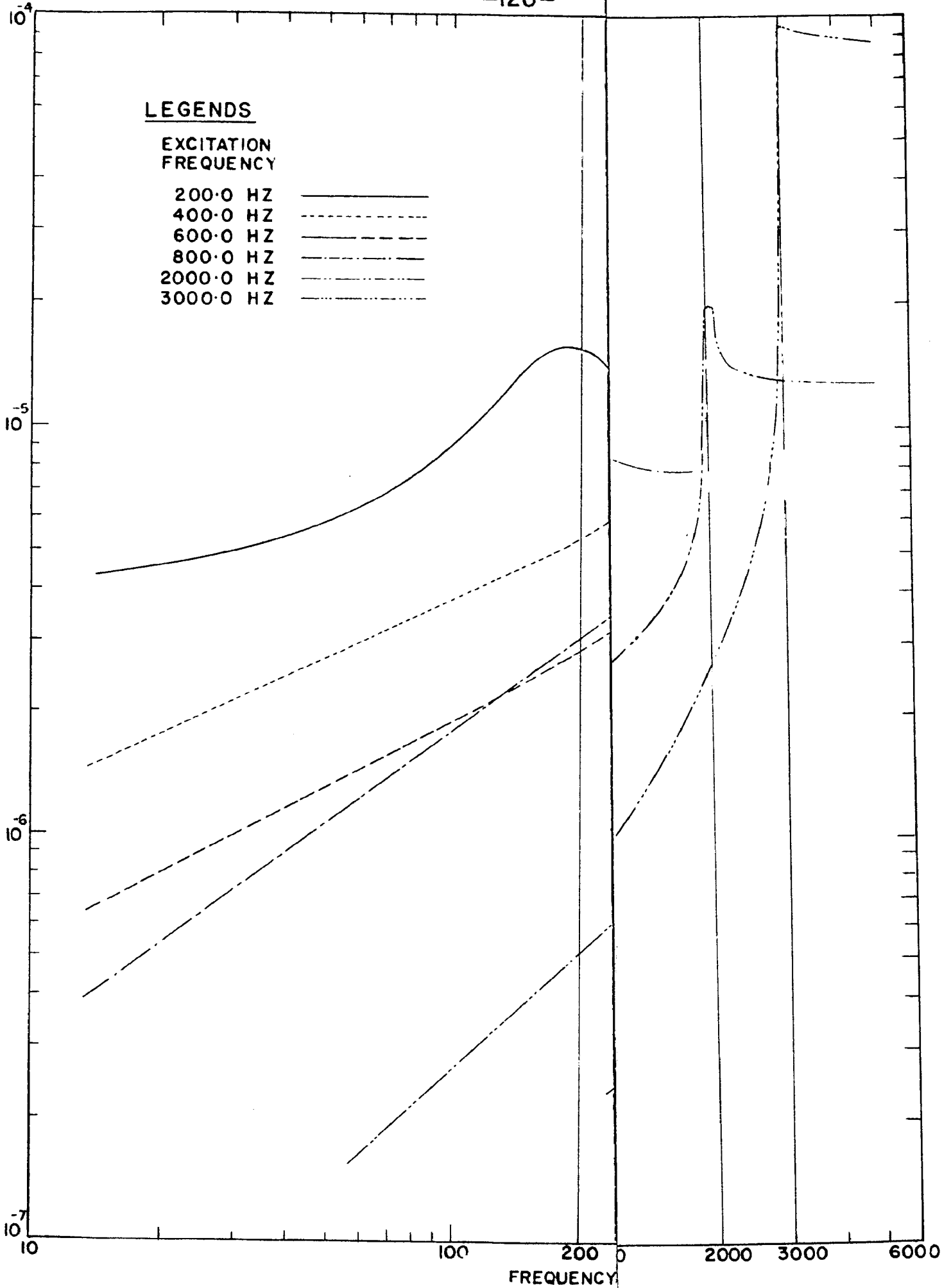
FIG. 7·12 EFFECT OF SUPERPOSITION OF NON-RE̶ HE SOUND POWER
RADIATED AT VARIOUS EXCITATION FREQUEN
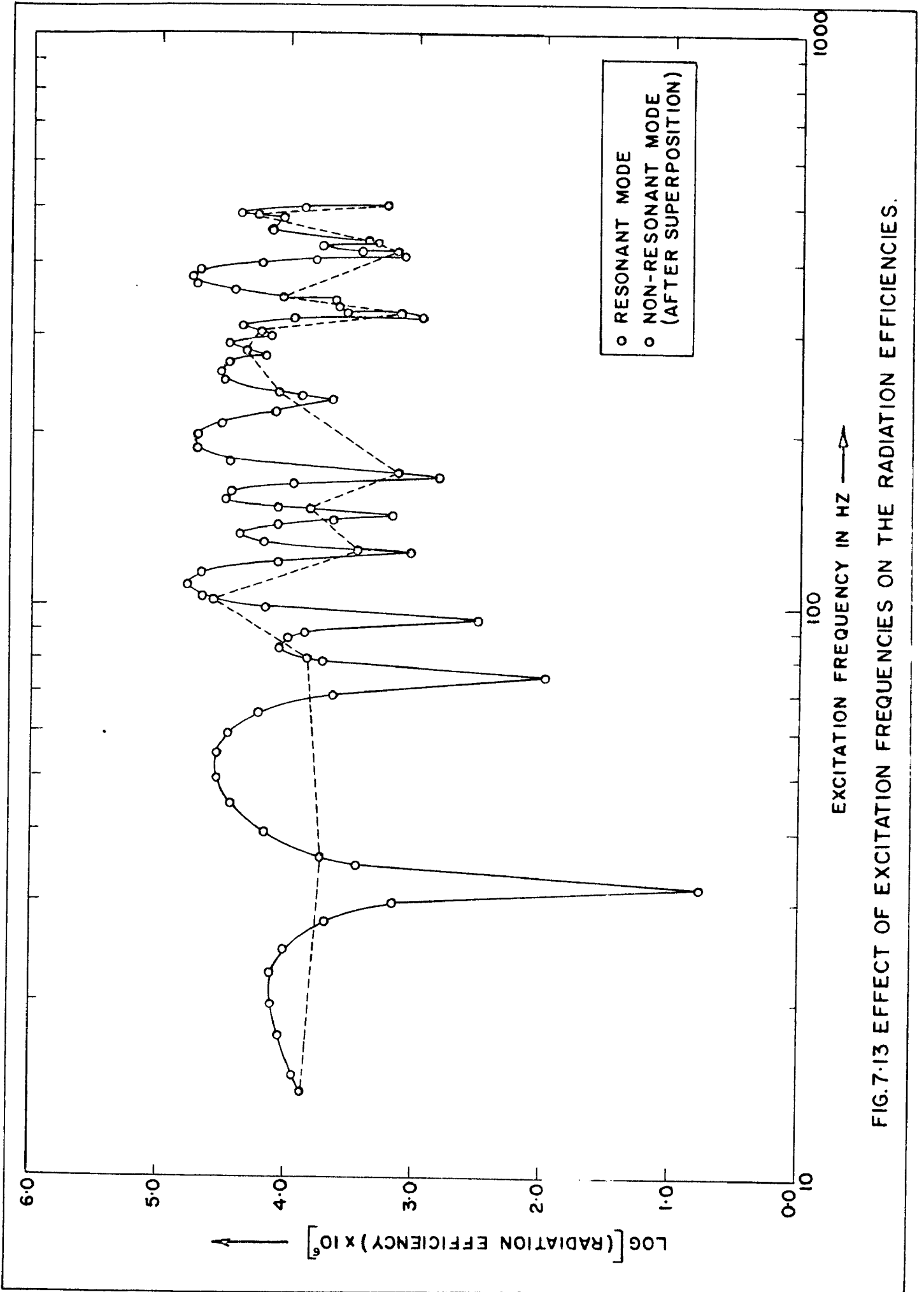
FIG.7.13 EFFECT OF EXCITATION FREQUENCIES ON THE RADIATION EFFICIENCIES.
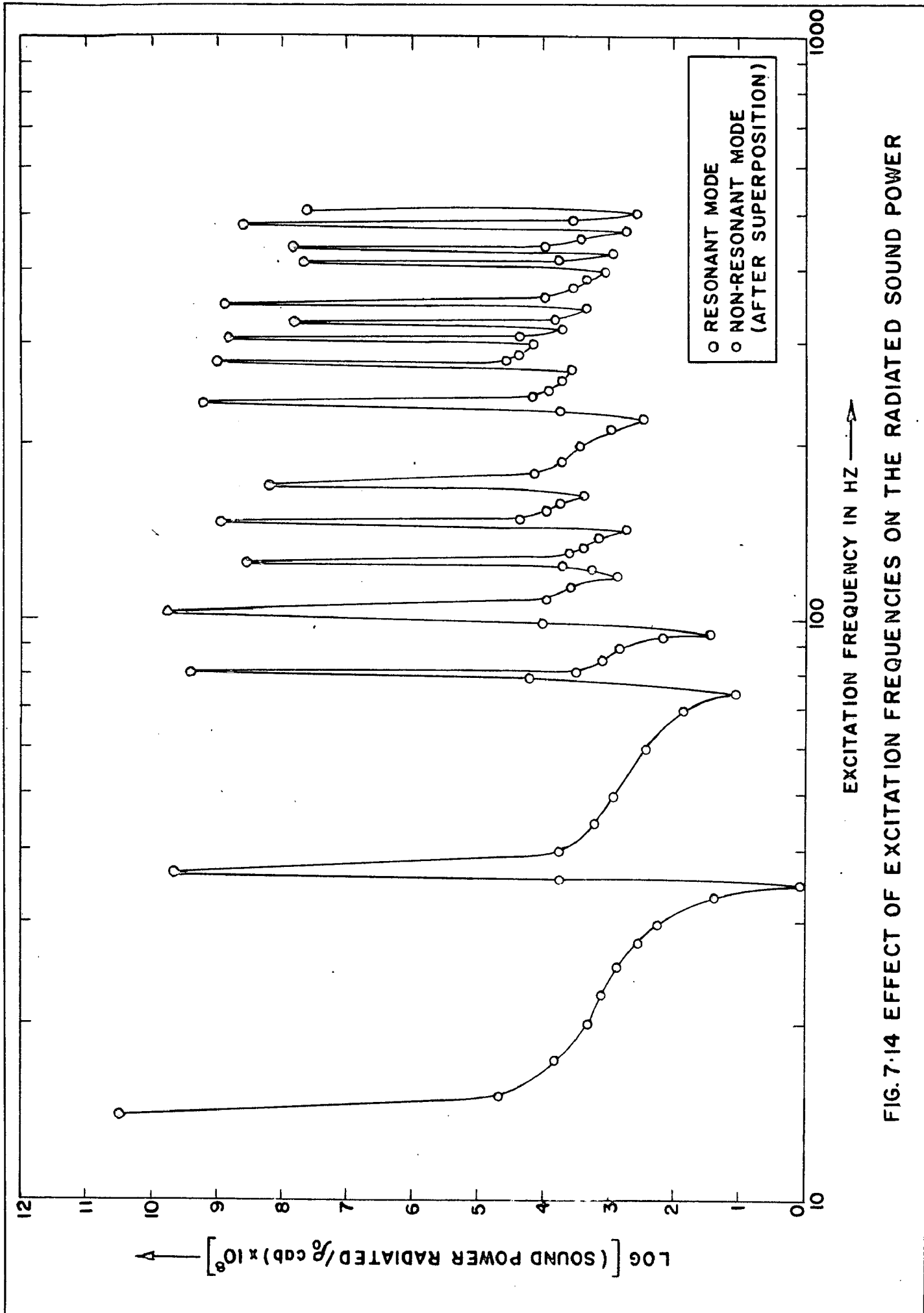
FIG. 7.14 EFFECT OF EXCITATION FREQUENCIES ON THE RADIATED SOUND POWER
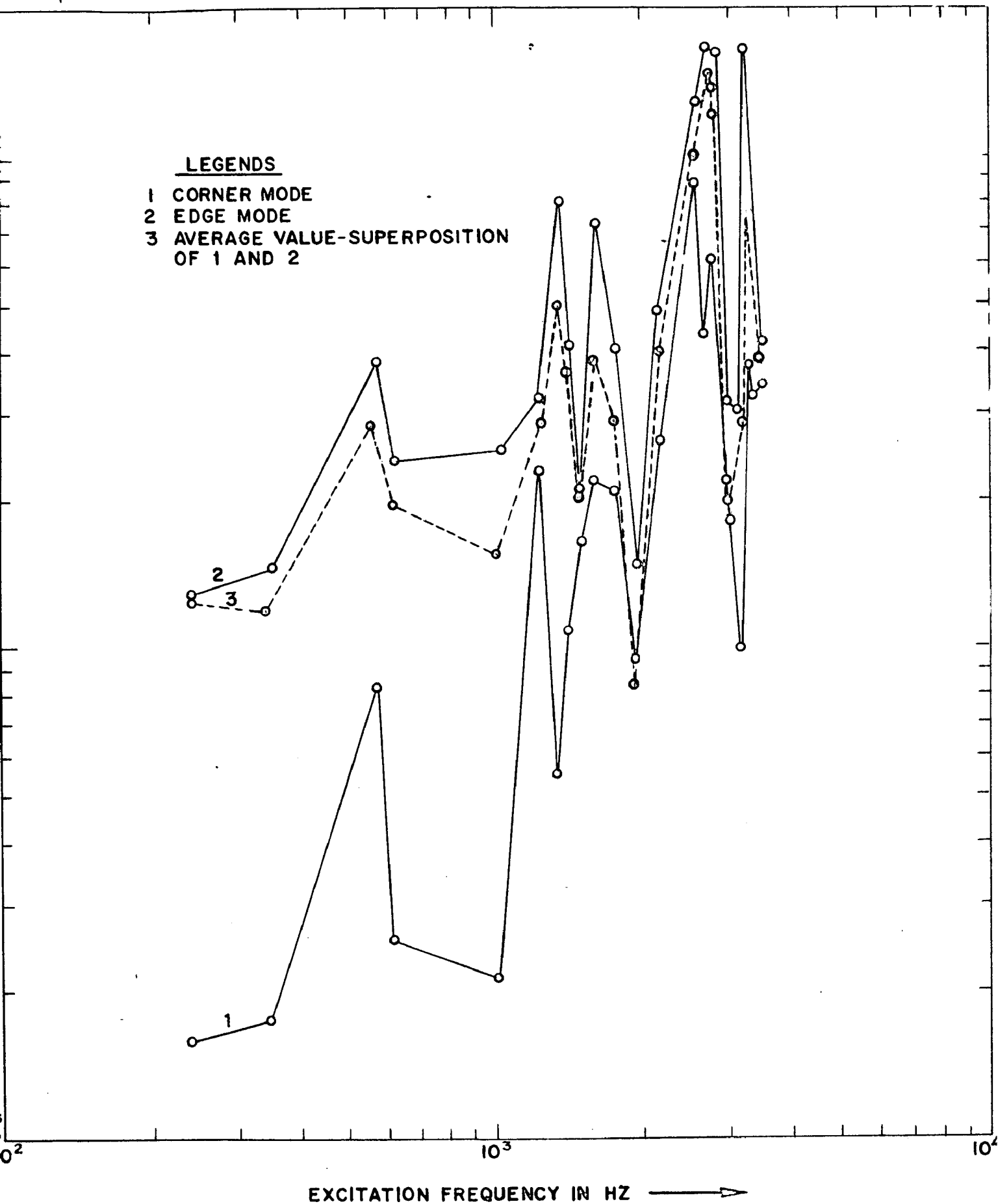
FIG. 7·15 RADIATION EFFICIENCY FOR COMPLEX RESONANT MODES
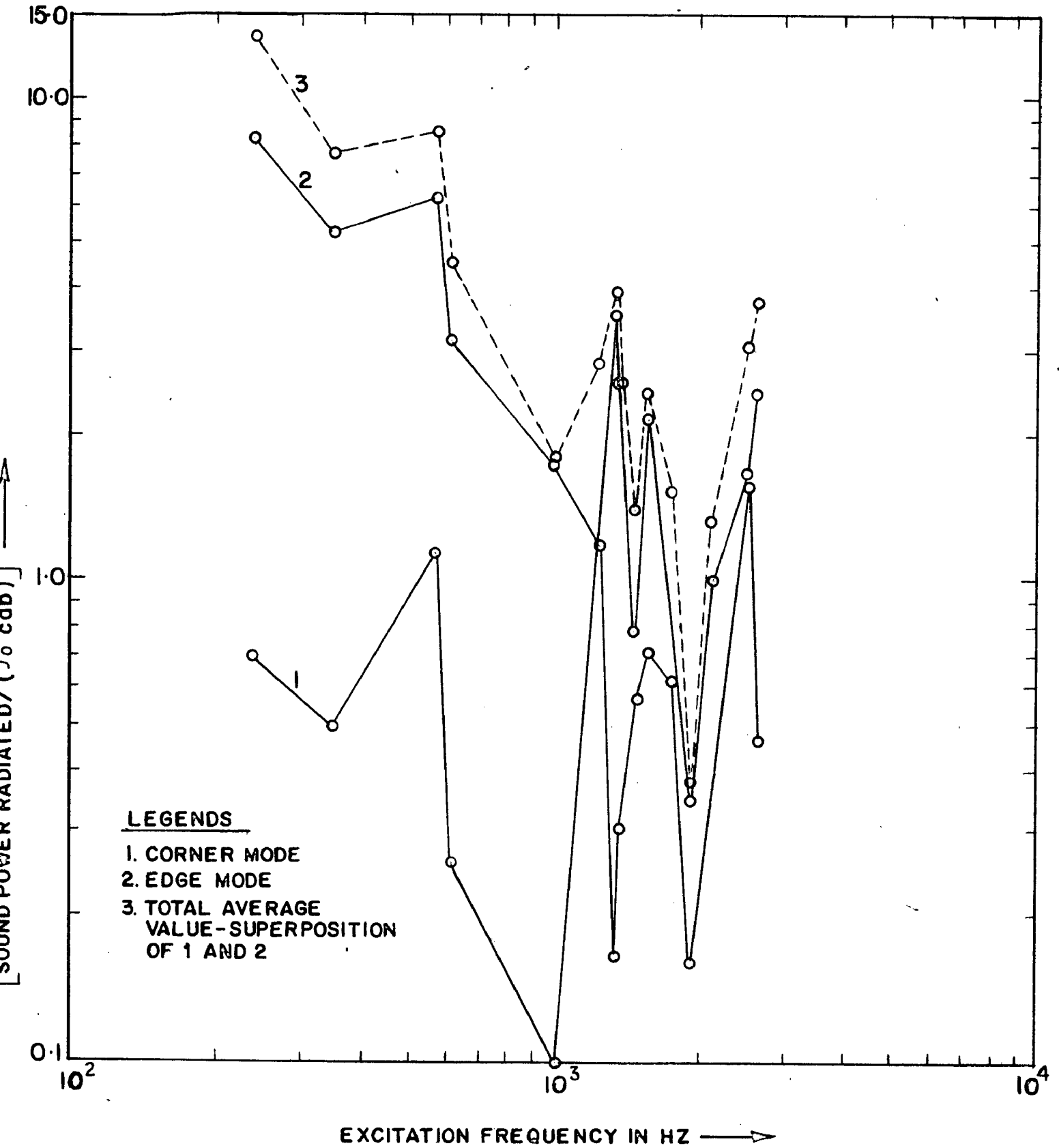
FIG. 7·16 SOUND POWER RADIATED FOR COMPLEX RESONANT MODES

Table 7.1

Modal Variation of (β/α)

$e = 2.0$; $h = 0.09842"$, $P = 0.2248$ lb., $N = 2.286$

S.No	Mode (m,n)	Frequency Hz	Nodal Aspect Ratio (e/m:n)	β/α	$\eta_{mn} \times 10^6$ computed Eq.(2.3.3)	$\eta_{mn} \times 10^6$ Eq.(2.3.5)	Error %
1.	(1,1)	14.0	2.00	1.287	147.1	147.0	-0.07
2.	(3,1)	36.4	0.67	1.292	125.3	124.2	-0.87
3.	(1,3)	103.6	6.00	1.260	84.1	84.6	+0.59
4.	(3,3)	126.0	2.00	1.287	90.2	90.2	Zero
5.	(7,1)	148.4	0.29	1.241	80.2	79.2	-1.20
6.	(7,3)	238.0	0.86	1.261	85.2	87.1	+2.20
7.	(5,5)	350.0	2.00	1.287	71.9	72.4	+0.69
8.	(3,7)	574.0	4.67	1.239	58.1	58.3	+0.30
9.	(5,7)	618.8	2.80	1.281	59.9	59.0	-1.66

Table 7.2

Modal Loss Factors 'K' for Constant Force Excitation

e = 2.0, h = 0.09842", P = 0.2248 lb., N = 2.286

S.No	Mode (m,n)	Frequency Hz	K	$\eta_{mn} \times 10^6$ computed Eq.(2.3.3)	$\eta_{mn} \times 10^6$ Eq.(3.1.7)	Error %
1.	(1,1)	14.0	1.0000	147.1	147.1	Zero
2.	(3,1)	36.4	0.841	125.3	128.6	+2.7
3.	(1,3)	103.6	0.454	84.1	79.7	-5.3
4.	(3,3)	126.0	0.533	90.2	90.2	Zero
5.	(7,1)	148.4	0.438	80.2	77.4	-3.6
6.	(7,3)	238.0	0.524	85.2	89.0	+4.6
7.	(5,5)	350.0	0.398	71.9	71.9	Zero
8.	(3,7)	574.0	0.285	58.1	55.4	-4.6
9.	(7,7)	686.0	0.329	61.9	61.9	Zero
10.	(9,9)	1134.0	0.284	55.4	55.4	Zero

Table 7.3

Modal Loss Factors and Factor 'K$_o$' for constant Amplitude Excitation

$N = 2.286$, $e = 2.0$, $a = 59.06''$, $h = 0.09842''$, $(w_{11})_{max.} = \dfrac{4a^2 e}{B\pi^4}\dfrac{P}{(1+e^2)^2\,\eta_{11}} = 6.7''$

S. No.	Mode (m,n)	Frequency Hz	K$_o$	η_{mn} x 10^6 Computed	η_{mn} x 10^6 Eq.(3.2.4)	Error %
1.	(1,1)	14.0	1.000	147.1	147.1	Zero
2.	(3,1)	36.4	1.452	206.8	213.6	+3.2
3.	(1,3)	103.6	1.425	225.2	210.0	-6.6
4.	(3,3)	126.0	1.875	275.7	275.7	Zero
5.	(7,1)	148.4	1.693	260.3	249.1	-4.3
6.	(7,3)	238.0	2.657	368.3	390.8	+6.1
7.	(5,5)	350.0	2.511	369.3	369.3	Zero
8.	(3,7)	574.0	2.381	372.5	350.1	-6.0
9.	(7,7)	686.0	3.043	447.7	447.7	Zero

Table 7.4

Loss Factor under Complex Resonance Excitation Conditions-
Constant Force Excitation

e = 2.0, P=0.2248 lb, h = 0.09842"

S. No.	Mode (m,n)	Frequency Hz	N = 2.286				N = 2.765			
			η_{mn}x10^6 Eq.2.2.3	η_T x 10^6 Eq.2.5.2	η_T x 10^6 Eq.3.3.5	Error %	η_{mn}x10^6 Eq.2.3.3	η_Tx10^6 Eq.2.5.2	η_Tx10^6 Eq.3.3.5	Error %
1.	(7,3) (9,1)	238.0	85.2 70.8	81.5	93.1	+14.2	115.2 101.9	135.3	181.8	+34.0
2.	(5,5) (11,1)	350.0	71.9 64.4	84.0	82.4	-.9	91.9 85.7	127.9	150.2	+17.4
3.	(3,7) (13,3)	574.0	58.8 63.4	75.5	73.5	-2.6	69.5 73.5	103.6	120.7	+16.5
4.	(5,7) (11,5)	618.8	59.9 69.1	68.3	77.4	+13.3	69.3 76.3	91.4	122.3	+33.8

N = 3.343

S. No.	Mode (m,n)	Frequency Hz	$\eta_{mn} \times 10^6$ Eq.(2.3.3)	$\eta_T \times 10^6$ Eq.(2.5.2)	$\eta_T \times 10^6$ Eq.(3.3.5)	Error %
1.	(7,3) (9,1)	238.0	101.1 93.2	148.8	243.5	+63
2.	(5,5) (11,1)	350.0	77.8 74.4	131.9	192.0	+45.6
3.	(3,7) (13,3)	574.0	56.2 58.2	99.8	144.2	+44.5
4.	(5,7) (11,5)	618.8	54.8 58.5	87.4	142.4	+62.1

-129-

Table 7.5

Effect of Force Ratio on Damping Under Complex Resonance Condition

e = 2.0, h = 0.09842", P = 0.4496 lb, k_1 = 2.0, N=2.286

S.No.	Mode (r,n)	Frequency Hz	n_T x 10^6 Eq.(2.5.2)	n_T x 10^6 Eq.(3.1.9)	Error %
1.	(7,3) (9,1)	238.0	95.0	95.1	+0.1
2.	(5,5) (11,1)	350.0	97.9	98.0	+0.1
3.	(3,7) (13,3)	574.0	87.8	88.1	+0.3
4.	(5,7) (11,5)	618.0	79.2	79.7	+0.6

-130-

Table 7.6

Loss Factor under Complex Resonance Excitation Condition—
Constant Amplitude Excitation

N = 2.286, e = 2.0, h = 0.09842", Maximum Amplitude of each mode $=(w_{11})_{max}=6.7$"

S.No.	Mode (m,n)	Frequency Hz	$\eta_{mn} \times 10^6$ computed	$\eta_T \times 10^6$ Eq.(2.5.2)	$\eta_T \times 10^6$ Eq.(3.3.5)	Error %
1.	(7,3) (9,1)	238.0	368.3 290.4	349.0	388.8	+11.40
2.	(5,5) (11,1)	350.0	369.3 320.3	416.3	415.8	-0.12
3.	(3,7) (13,3)	574.0	372.5 417.4	482.5	476.5	-1.24
4.	(5,7) (11,5)	618.8	404.8 486.2	474.3	531.5	+12.10

Table 7.7

Effect of Amplitude Ratio on the damping under complex Resonance Condition

e = 2.0, k_2 = 2.0, N = 2.286

S. No.	Mode (m,n)	Frequency Hz	$\eta_T \times 10^6$ Eq. (2.5.2)	$\eta_T \times 10^6$ Eq. (3.2.6)	Error %
1.	(7,3) (9,1)	238.0	422.5	425.5	+0.7
2.	(5,5) (11,1)	350.0	505.1	507.6	+0.5
3.	(3,7) (13,3)	574.0	585.1	588.2	+0.5
4.	(5,7) (11,5)	618.8	575.8	578.4	+0.4

Table 7.

Fundamental Mode Loss Factor and Integral Ratio (β/α) for Plates of different aspect ratios and thickness

m = 1.0, n = 1.0, P = 0.2248 lb, N = 2.286

S.No.	h in.	a in.	b in.	e	β/α	$\eta_{11} \times 10^6$ Computed Eq.2.3.3	$\eta_{11} \times 10^6$ Eq.3.4.1	Error %
1.	0.04921	59.06	29.53	2.00	1.287	200.2	200.2	Zero
2.	0.19684	60.00	20.00	3.00	1.280	95.1	96.3	+1.3
3.	0.04921	80.00	40.00	2.00	1.287	200.2	200.2	Zero
4.	0.19684	59.06	29.53	2.00	1.287	108.1	108.1	Zero
5.	0.50000	60.00	20.00	3.00	1.280	62.8	61.1	-2.7
6.	0.50000	59.06	59.06	1.00	1.270	82.0	82.6	+0.7
7.	0.09842	59.06	14.76	4.00	1.263	119.1	114.2	-4.1
8.	0.09842	59.06	59.06	1.00	1.270	169.0	167.2	-1.1

Table 7.9

Effect of Damping Index N on the Fundamental Mode

Loss Factor

$m = 1.0$, $n = 1.0$, $e = 2.0$, $h = 0.09842"$, $P = 0.2248$ lb

material = Steel

S.No	J	N	(β/α)	$\eta_{11} \times 10^6$ Computed	$\eta_{11} \times 10^6$ Eq.(3.5.1)	Error %
1.	3.758×10^{-10}	1.702	0.887	347.8	343.2	-1.3
2.	2.626×10^{-13}	2.286	1.287	147.1	147.1	Zero
3.	5.37×10^{-15}	2.765	1.659	371.0	377.7	+1.8
4.	2.153×10^{-17}	3.343	2.131	492.4	498.2	+1.1
5.	1.224×10^{-26}	5.360	3.854	492.6	503.4	+2.2

Table 7.10

Resonant Mode Loss Factors Under Eccentric
Force - Odd-odd Modes

e = 2.0, P = 0.2248 lb, h = 0.09842", N = 2,286

S. No.	Mode (m,n)	$\frac{x_1}{a}$	$\frac{y_1}{b}$	$\eta_{mn} \times 10^6$ Computed	$\eta_{mn} \times 10^6$ Eq.(3.6.1)	Error %
1.	(1,1)	0.3	0.3	130.4	133.9	+2.6
2.	(1,3)	0.3	0.3	60.2	61.7	+2.4
3.	(7,3)	0.3	0.3	48.6	50.5	+3.9
4.	(5,5)	0.3	0.3	70.1	71.9	+2.5
5.	(5,7)	0.3	0.3	45.5	46.1	+1.3
6.	(1,1)	0.1	0.1	85.7	87.2	+1.7
7.	(1,3)	0.1	0.1	60.2	61.7	+2.4
8.	(7,3)	0.1	0.1	49.5	50.5	+2.0
9.	(5,5)	0.1	0.1	70.5	71.9	+1.9
10.	(5,7)	0.1	0.1	55.9	57.1	+2.1

Table 7.11

Resonant Mode Loss Factors under Eccentric
Force- Additional Even Order Modes

e = 2.0, h = 0.09842", P = 0.2248 lb., N = 2.286

S. No.	Mode (m,n)	$\frac{x_1}{a}$	$\frac{y_1}{b}$	$\eta_{mn} \times 10^6$ computed	$\eta_{mn} \times 10^6$ Eq.(3.6.2)	Error %
1.	(2,4)	0.3	0.3	70.1	68.7	-3.4
2.	(2,5)	0.3	0.3	72.4	69.3	-4.2
3.	(4,2)	0.3	0.3	104.0	106.5	+2.4
4.	(3,4)	0.3	0.3	57.6	56.5	-1.9
5.	(4,6)	0.3	0.3	51.2	52.5	+2.5

Table 7.12

Loss Factor under Complex Resonance Excitation - Eccentric Force

$e = 2.0$, $h = 0.09842"$, $P = 0.2248$ lb, $N = 2.286$

$\frac{x_1}{a} = 0.3$, $\frac{y_1}{b} = 0.3$

S.No	Mode (m,n)	η_{mn} x 10^6 Eq.(3.6.1)	η_T x 10^6 Computed	η_T x 10^6 Eq.(3.3.5)	Error %
1.	(7,3) (9,1)	50.5 64.4	59.1	69.1	+16.8
2.	(5,5) (11,1)	71.9 58.6	78.3	77.9	-0.5
3.	(3,7) (13,3)	34.4 37.6	38.7	39.8	+2.8
4.	(5,7) (11,5)	46.1 65.9	58.1	64.5	+11.0

–137–

Table 7.13

Fundamental Mode Frequency Parameter λ_{11} for
Plates with different Boundary Conditions

S.No.	Plate B.C. ↑ e ↓	All edges simply supported	Case 1	Case 2	Case 3	Case 4
1.	0.2	105.36	247.05	107.94	249.94	514.01
2.	0.3	115.73	259.02	123.35	267.36	532.44
3.	0.4	131.07	276.61	149.14	295.95	562.45
4.	0.5	152.20	300.62	189.51	339.92	608.25
5.	0.6	180.17	332.12	249.88	404.69	675.24
6.	0.7	216.26	372.38	336.85	496.87	770.06
7.	0.8	261.99	422.92	458.25	624.27	900.50
8.	0.9	319.12	485.50	623.10	795.92	1075.60
9.	1.0	389.64	562.11	841.61	1022.04	1305.57
10.	2.0	2435.23	2703.91	9087.08	9387.58	9731.93
11.	3.0	9740.91	10169.90	42872.40	43373.00	43818.70
12.	4.0	28151.20	28804.70	132262.00	133043.00	133630.00
13.	5.0	65848.50	66790.70	319345.00	320486.00	321256.00

TABLE 7.14

Fundamental Mode Frequency Parameter λ_{11} for the plate with linear thickness variation.

S.No.	e	δ	λ_{mean} (Ref.1)	One Term Approx. Eq.(5.1.1.7)	Error %	Two Term Approx. Eq.(5.1.2.13)	Error %
1	0.25	0.1	121.089	121.370	0.232	121.084	-0.0041
		0.2	132.436	133.592	0.873	132.450	0.0107
		0.3	143.968	146.631	1.850	144.075	0.0745
		0.4	155.863	160.488	2.967	155.972	0.0697
		0.5	167.908	175.162	4.326	168.154	0.1468
		0.6	180.194	190.653	5.804	180.640	0.2475
		0.7	192.721	206.961	7.389	193.440	0.3731
		0.8	205.497	224.087	9.046	206.570	0.5219
2	0.50	0.1	167.657	168.053	0.236	167.660	0.0017
		0.2	183.581	185.173	0.867	183.600	0.0103
		0.3	199.972	203.560	1.794	200.037	0.0327
		0.4	217.082	223.213	2.824	216.990	0.0424
		0.5	234.215	244.133	4.235	234.480	0.1132
		0.6	251.944	266.320	5.706	252.528	0.2317
		0.7	270.139	289.773	7.268	271.152	0.3752
		0.8	288.786	314.492	8.901	290.373	0.5495
3	0.75	0.1	262.027	262.655	0.240	262.041	0.0055
		0.2	287.149	289.619	0.860	287.164	0.0054
		0.3	313.157	318.704	1.771	313.212	0.0175
		0.4	340.053	349.911	2.899	340.212	0.0467
		0.5	367.650	383.239	4.240	368.198	0.1492
		0.6	396.066	418.690	5.712	397.207	0.2881
		0.7	425.593	456.261	7.206	427.266	0.3932
		0.8	453.818	495.954	8.805	458.408	0.5682

S. No.	e	δ	λ mean (Ref.1)	One Term Approx. Eq.(5.1.1.7)	Error %	Two Term Approx. Eq.(5.1.2.13)	Error %
7.	1.75	0.1	1770.869	1775.242	0.247	1770.681	-0.0106
		0.2	1937.373	1956.595	0.992	1938.435	0.0548
		0.3	2109.946	2151.677	1.978	2111.149	0.0570
		0.4	2286.354	2360.489	3.242	2289.188	0.1240
		0.5	2466.645	2583.030	4.718	2472.910	0.2540
		0.6	2650.873	2819.299	6.354	2662.666	0.4449
		0.7	2840.969	3069.297	8.037	2858.766	0.6265
		0.8	3042.988	3333.021	9.531	3061.499	0.6083
8.	2.00	0.1	2682.541	2688.860	0.236	2681.581	-0.0358
		0.2	2933.149	2962.777	1.010	2933.842	0.0236
		0.3	3190.419	3256.963	2.086	3192.493	0.0650
		0.4	3452.582	3571.415	3.442	3458.204	0.1628
		0.5	3718.769	3906.134	5.038	3731.636	0.3460
		0.6	3996.104	4261.117	6.632	4013.416	0.4332
		0.7	4275.126	4636.367	8.450	4304.090	0.6775
		0.8	4556.204	5031.883	10.440	4604.152	1.0524

Table 7.15

Fundamental Mode Frequency Parameter λ_{11} for the Plate with Parabolic Thickness Variation

S. No.	e	μ	$\sqrt{\lambda}$ (Ref.27)	One Term Approx. Eq.(5.1.1.7)	Error %.	Two Term Approx. Eq.(5.1.2.13)	Error %.
1.	0.25	0.1	10.1695	10.1845	0.147	10.1706	0.0107
		0.3	9.4763	9.6252	1.571	9.4959	0.2074
		0.5	8.6688	9.1311	5.332	8.7687	1.1519
		0.7	7.6582	8.7093	13.720	8.0081	4.5695
2.	0.50	0.1	11.9398	11.9575	0.148	11.9412	0.0114
		0.3	11.0979	11.2704	1.554	11.1210	0.2080
		0.5	10.1598	10.6883	5.201	10.2750	1.1339
		0.7	9.0415	10.2195	13.020	9.4355	4.3576
3.	0.75	0.1	14.9044	14.9263	0.146	14.9061	0.0113
		0.3	13.8308	14.0430	1.534	13.8593	0.2063
		0.5	12.6725	13.3145	5.060	12.8144	1.1202
		0.7	11.3490	12.7520	12.360	11.8226	4.1727
4.	1.00	0.1	19.0703	19.0984	0.147	19.0724	0.0109
		0.3	17.6886	17.9589	1.528	17.7255	0.2088
		0.5	16.2163	17.0262	4.990	16.3987	1.1248
		0.7	14.5683	16.3145	11.980	15.1670	4.1095

Table 7.16

Radiation Efficiency and Sound Power Radiated for Single Resonant Modes – Corner Mode

$$e = 2.0, \quad k_{mx}^2 \gg k^2, \quad k_{ny}^2 \gg k^2$$

S. No.	Mode (m,n)	Frequency Hz	k^2	k_{mx}^2	k_{ny}^2	$S_{mn} \times 10^3$ Eq. (6.4)	$\dfrac{\Pi}{P_o cab}$
1.	(1,1)	14.0	0.000042	0.002830	0.011318	7.652	329.64
2.	(3,1)	36.4	0.000284	0.025466	0.011318	5.326	46.52
3.	(5,1)	81.2	0.001416	0.070738	0.011318	6.916	25.69
4.	(3,3)	126.0	0.003409	0.025566	0.101863	2.672	3.78
5.	(7,1)	148.4	0.004728	0.138647	0.011313	6.546	8.42
6.	(5,3)	170.8	0.006263	0.070738	0.101863	1.269	1.87
7.	(7,3)	238.0	0.012162	0.138647	0.101863	1.591	1.01
8.	(9,3)	327.6	0.023042	0.229191	0.101863	1.298	0.53
9.	(7,5)	417.2	0.037371	0.138647	0.282952	1.359	0.44
10.	(11,3)	439.6	0.041491	0.342372	0.101863	2.370	0.49
11.	(9,5)	506.8	0.055146	0.229191	0.282972	1.735	0.21
12.	(11,5)	618.8	0.082213	0.342372	0.282952	2.607	0.29
13.	(13,5)	753.2	0.121804	0.478189	0.282952	2.377	0.19
14.	(11,7)	887.6	0.169151	0.342372	0.554586	1.007	0.18

Table 7.17

Radiation Efficiency and Sound Power Radiated for single Resonant
Modes - X - Edge Mode

$$e = 2.0, \quad k > k_{mx}, \quad k_{ny}^2 \gg k^2$$

S. No	Mode (m,n)	Frequency Hz	k	k_{mx}	k_{ny}	$S_{mn} \times 10^2$ Eq.(6.4)	$\dfrac{\Pi}{\rho_o cab}$
1.	(1,5)	282.8	0.131	0.053	0.532	2.043	7.92
2.	(1,7)	551.6	0.256	0.053	0.745	4.626	6.71
3.	(3,7)	574.0	0.266	0.160	0.745	3.817	5.36
4.	(5,7)	618.8	0.287	0.266	0.745	2.389	3.97
5.	(1,9)	910.0	0.422	0.053	0.957	4.007	3.36
6.	(3,9)	932.4	0.432	0.160	0.957	5.478	3.89
7.	(5,9)	977.2	0.453	0.266	0.957	2.722	1.92
8.	(7,9)	1044.4	0.484	0.372	0.957	2.033	1.27
9.	(1,11)	1358.0	0.629	0.053	1.170	7.957	2.99
10.	(3,11)	1380.4	0.640	0.160	1.170	5.761	1.86
11.	(5,11)	1425.2	0.660	0.266	1.170	4.876	1.52
12.	(7,11)	1492.4	0.692	0.372	1.170	1.640	0.59
13.	(1,13)	1892.6	0.878	0.053	1.383	9.407	1.63
14.	(3,13)	1918.0	0.889	0.160	1.383	1.480	0.42
15.	(5,13)	1962.8	0.909	0.266	1.383	10.150	1.71

Table 7.18

Radiation Efficiency and Sound Power Radiated for Single Resonant Modes-Y-Edge Mode

$$e = 2.0, \quad k > k_{ny}, \quad k_{mx}^2 \gg k^2$$

S.No	Mode (m,n)	Frequency Hz	k	k_{mx}	k_{ny}	$S_{mn} \times 10^2$ Eq.(6.4)	$\dfrac{\Pi}{P_o\,cab}$
1.	(9,1)	238.0	0.110	0.479	0.106	1.291	7.20
2.	(11,1)	350.0	0.162	0.585	0.106	1.472	5.30
3.	(13,1)	484.4	0.224	0.692	0.106	1.743	3.57
4.	(15,1)	641.2	0.297	0.798	0.106	1.726	2.21
5.	(17,1)	820.4	0.380	0.904	0.106	1.507	1.55
6.	(17,3)	910.0	0.422	0.904	0.319	1.899	1.70
7.	(19,1)	1022.0	0.474	1.011	0.106	2.524	1.91
8.	(19,3)	1111.6	0.515	1.011	0.319	1.458	0.92
9.	(21,1)	1246.0	0.577	1.117	0.106	2.392	0.98
10.	(19,5)	1290.8	0.598	1.011	0.532	2.364	0.97
11.	(21,3)	1335.6	0.619	1.117	0.319	2.685	1.05
12.	(23,1)	1492.4	0.692	1.223	0.106	2.040	0.71
13.	(21,5)	1514.8	0.702	1.117	0.532	1.524	0.49
14.	(23,3)	1582.0	0.733	1.223	0.319	1.621	0.67
15.	(25,1)	1761.2	0.816	1.330	0.106	2.078	0.59
16.	(25,3)	1850.8	0.858	1.330	0.319	4.076	0.85

Table 7.19

Radiation Efficiency and Sound Power Radiated at various excitation Frequencies-Superposition of number of non-resonant modes.

S. No.	Exciting Frequency ω_{ex} Hz	No. of Modes superimposed	No. of Modes having frequency less than ω_{ex}	S_{av}	Sound Power Radiated $\frac{}{\rho_o cab}$ $\times 10^5$
1.	200.0	30	7	0.0489	0.9178
2.	400.0	30	14	0.0273	0.7314
3.	600.0	30	21	0.0266	1.7630
4.	800.0	60	28	0.0292	0.7689
5.	2000.0	175	70	0.0274	1.2540
6.	2500.0	175	86	0.0614	1.6640
7.	3000.0	175	106	0.0764	8.5350
8.	3500.0	175	123	0.1901	3.6950
9.	4000.0	175	140	0.7674	2457.0000
10.	4700.0	175	163	3.0780	126.5000

APPENDIX 1

MODE SHAPES AND FREQUENCY PARAMETERS OF RECTANGULAR PLATE WITH DIFFERENT BOUNDARY CONDITIONS [38,79]

There are 21 possible combinations of the boundary conditions (clamped-C; simple support-SS; Free-F). For obtaining the mode shapes Warburton used the Rayleigh method with deflection functions as the product of beam functions i.e.

$$W(x,y) = X(x).Y(y) \qquad \qquad \cdots \text{(A.1.1)}$$

where, $X(x)$ and $Y(y)$ are the fundamental mode shapes of beams having the boundary conditions of the plate.

The required sets (as in Chapter 4) of boundary conditions along the edges $x = 0$ and $x = a$ are satisfied by the following mode shapes:

(a) $\quad$ S.S. $\quad \cdots \cdots X(x) = \sin \dfrac{(m-1)\pi x}{a}$, $\quad m = 2,3,4 \cdots$

$\quad$ (x=0, x=a) $\qquad \qquad \qquad \cdots \text{(A.1.2)}$

(b) $\quad$ C $\quad \cdots \cdots X(x) = \cos \gamma_1 (\dfrac{x}{a} - \dfrac{1}{2}) + \dfrac{\sin(\gamma_1/2)}{\sinh(\gamma_1/2)} \cdot$

$\quad$ (x=0, x=a)

$$\cosh \gamma_1 (\dfrac{x}{a} - \dfrac{1}{2})$$

$$m = 2,4,6 \cdots$$

$$\cdots \text{(A.1.3)}$$

$$X(x) = \sin \gamma_2 (\dfrac{x}{a} - \dfrac{1}{2}) - \dfrac{\sin(\gamma_2/2)}{\sinh(\gamma_2/2)} \cdot$$

$$\sinh \gamma_2 (\dfrac{x}{a} - \dfrac{1}{2})$$

$$m = 3,5,7 \cdots$$

$$\cdots \text{(A.1.4)}$$

(c) C   at x = 0,
     S.S. at x = a. ... $X(x) = \sin\gamma_2 \left(\dfrac{x}{2a} - \dfrac{1}{2} \right) - \dfrac{\sin(\gamma_2/2)}{\sinh(\gamma_2/2)}$.

$$.\sinh\gamma_2 \left(\dfrac{x}{2a} - \dfrac{1}{2} \right) \qquad m = 2,3,4....$$

... (A.1.5)

<u>Note:</u> (i) For obtaining function Y(y) replace x by y, a by b, and m by n.

(ii) m, n are number of nodal lines in X- and Y- directions including the boundaries as nodal lines and not the number of half waves which represent modal numbers.

The natural frequency ω_{mn} is obtained from

$$\omega_{mn}^2 = \frac{\pi^4 B}{a^4 \rho h} \left[G_x^4 + G_y^4 \left(\frac{a}{b}\right)^4 + 2\left(\frac{a}{b}\right)^2 \left\{ \nu\, H_x H_y + (1-\nu) J_x J_y \right\} \right]$$

... (A.1.6)

i.e. $\lambda_{mn} = \pi^4 \left[G_x^4 + G_y^4 e^4 + 2e^2 \left\{ \nu\, H_x H_y + (1-\nu) J_x J_y \right\} \right]$

... (A.1.7)

The coefficients G_x, H_x, and J_x for conditions at x = 0 and x = a are given in the following table:

Table A.1.1

B.C. at	m	G_x	H_x	J_x
S.S.^{a} S.S.^{b}	2,3,4..	(m-1)	$(m-1)^2$	$(m-1)^2$
C^a	2	1.506	1.248	1.248
C^b	3,4,5..	(m- 1/2)	$\left(m-\frac{1}{2}\right)^2\left[1-\dfrac{2}{\left(m-\frac{1}{2}\right)\pi}\right]$	$\left(m-\frac{1}{2}\right)^2\left[1-\dfrac{2}{\left(m-\frac{1}{2}\right)\pi}\right]$
C^a S.S.^{b}	2,3,4..	$\left(m-\frac{3}{4}\right)$	$\left(m-\frac{3}{4}\right)^2\left[1-\dfrac{1}{\left(m-\frac{3}{4}\right)\pi}\right]$	$\left(m-\frac{3}{4}\right)^2\left[1-\dfrac{1}{\left(m-\frac{3}{4}\right)\pi}\right]$

$^a \rightarrow x = 0$, $^b \rightarrow x = a$

For obtaining G_y, H_y and J_y replace x by y and m by n.

It is seen that $H_x = J_x$; $H_y = J_y$ when there is no free-edge; hence Eq.(A.1.7) reduces to

$$\lambda_{mn} = \pi^4 \left[G_x^4 + e^4 G_y^4 + 2e^2 \, J_x J_y \right] \qquad \qquad \ldots \text{(A.1.8)}$$

APPENDIX 2

INTEGRALS USED IN THE ANALYSIS OF VARIABLE THICKNESS PLATES

$$I_1 \quad - \int_0^b \sin^2\left(\frac{\pi y}{b}\right) dy \quad = \frac{b}{2}$$

$$I_2 \quad - \int_0^a \sin^2\left(\frac{\pi x}{a}\right) dx \quad = \frac{a}{2}$$

$$I_3 \quad - \int_0^a x \sin^2\left(\frac{\pi x}{a}\right) dx = \frac{a^2}{4}$$

$$I_4 \quad - \int_0^a x^2 \sin^2\left(\frac{\pi x}{a}\right) dx = \frac{a^3}{6}\left[1 - \frac{1.5}{\pi^2}\right]$$

$$I_5 \quad - \int_0^a x^3 \sin^2\left(\frac{\pi x}{a}\right) dx = \frac{a^4}{8}\left[1 - \frac{3}{\pi^2}\right]$$

$$I_6 \quad - \int_0^a \sin\left(\frac{\pi x}{a}\right) \cos\left(\frac{\pi x}{a}\right) dx = 0$$

$$I_7 \quad - \int_0^a x \sin\left(\frac{\pi x}{a}\right) \cos\left(\frac{\pi x}{a}\right) dx = - \frac{a^2}{4\pi}$$

$$I_8 \quad - \int_0^a x^2 \sin\left(\frac{\pi x}{a}\right) \cos\left(\frac{\pi x}{a}\right) dx = - \frac{a^3}{4\pi}$$

$$I_9 \quad - \int_0^a \sin\left(\frac{\pi x}{a}\right) \sin\left(\frac{2\pi x}{a}\right) dx = 0$$

$$I_{10} \quad - \int_0^a x \sin\left(\frac{\pi x}{a}\right) \sin\left(\frac{2\pi x}{a}\right) dx = - \frac{8a^2}{9\pi^2}$$

$$I_{11} \quad - \int_0^a x^2 \sin\left(\frac{\pi x}{a}\right) \sin\left(\frac{2\pi x}{a}\right) dx = - \frac{8a^3}{9\pi^2}$$

$$I_{12} \quad - \int_0^a x^3 \sin\left(\frac{\pi x}{a}\right) \sin\left(\frac{2\pi x}{a}\right) dx = \frac{4a^4}{3\pi^2}\left[\frac{40}{9\pi^2} - 1\right]$$

$$I_{13} - \int_0^a \cos\left(\frac{2\pi x}{a}\right) \sin\left(\frac{\pi x}{a}\right) dx = -\frac{2a}{3\pi}$$

$$I_{14} - \int_0^a x \cos\left(\frac{2\pi x}{a}\right) \sin\left(\frac{\pi x}{a}\right) dx = -\frac{a^2}{3\pi}$$

$$I_{15} - \int_0^a x^2 \cos\left(\frac{2\pi x}{a}\right) \sin\left(\frac{\pi x}{a}\right) dx = \frac{a^3}{3\pi}\left[\frac{52}{9\pi^2} - 1\right]$$

$$I_{16} - \int_0^a \sin^2\left(\frac{2\pi x}{a}\right) dx = \frac{a}{2}$$

$$I_{17} - \int_0^a x \sin^2\left(\frac{2\pi x}{a}\right) dx = \frac{a^2}{4}$$

$$I_{18} - \int_0^a x^2 \sin^2\left(\frac{2\pi x}{a}\right) dx = \frac{a^3}{6}\left[1 - \frac{1.5}{4\pi^2}\right]$$

$$I_{19} - \int_0^a x^3 \sin^2\left(\frac{2\pi x}{a}\right) dx = \frac{a^4}{8}\left[1 - \frac{3}{4\pi^2}\right]$$

$$I_{20} - \int_0^a \cos\left(\frac{\pi x}{a}\right) \sin\left(\frac{2\pi x}{a}\right) dx = \frac{4a}{3\pi}$$

$$I_{21} - \int_0^a x \cos\left(\frac{\pi x}{a}\right) \sin\left(\frac{2\pi x}{a}\right) dx = \frac{2a^2}{3\pi}$$

$$I_{22} - \int_0^a x^2 \cos\left(\frac{\pi x}{a}\right) \sin\left(\frac{2\pi x}{a}\right) dx = \frac{2a^3}{3\pi}\left[1 - \frac{28}{9\pi^2}\right]$$

$$I_{23} - \int_0^a \cos\left(\frac{2\pi x}{a}\right) \sin\left(\frac{2\pi x}{a}\right) dx = 0$$

$$I_{24} - \int_0^a x \cos\left(\frac{2\pi x}{a}\right) \sin\left(\frac{2\pi x}{a}\right) dx = -\frac{a^2}{8\pi}$$

$$I_{25} - \int_0^a x^2 \cos\left(\frac{2\pi x}{a}\right) \sin\left(\frac{2\pi x}{a}\right) dx = -\frac{a^3}{8\pi}$$

$$I_{26} - \int_0^a x^4 \sin^2\left(\frac{\pi x}{a}\right) dx = \frac{a^5}{10}\left[1 - \frac{5}{\pi^2} + \frac{7.5}{\pi^4}\right]$$

$$I_{27} - \int_0^a x^6 \sin^2\left(\frac{\pi x}{a}\right) dx = \frac{a^7}{14}\left[1 - \frac{10.5}{\pi^2} + \frac{52.5}{\pi^4} - \frac{78.75}{\pi^6}\right]$$

$$I_{28} - \int_0^a x^3 \sin\left(\frac{\pi x}{a}\right) \cos\left(\frac{\pi x}{a}\right) dx = -\frac{a^4}{4\pi}\left[1 - \frac{1.5}{\pi^2}\right]$$

$$I_{29} - \int_0^a x^5 \sin\left(\frac{\pi x}{a}\right) \cos\left(\frac{\pi x}{a}\right) dx = -\frac{a^6}{4\pi}\left[1 - \frac{5}{\pi^2} + \frac{7.5}{\pi^4}\right]$$

$$I_{30} - \int_0^a x^4 \sin\left(\frac{\pi x}{a}\right) \sin\left(\frac{2\pi x}{a}\right) dx = -\frac{16a^5}{9\pi^2}\left[1 - \frac{20}{3\pi^2}\right]$$

$$I_{31} - \int_0^a x^6 \sin\left(\frac{\pi x}{a}\right) \sin\left(\frac{2\pi x}{a}\right) dx = -\frac{8a^7}{3\pi^2}\left[1 - \frac{200}{9\pi^2} + \frac{3640}{27\pi^4}\right]$$

$$I_{32} - \int_0^a x^3 \cos\left(\frac{2\pi x}{a}\right) \sin\left(\frac{\pi x}{a}\right) dx = -\frac{a^4}{3\pi}\left[1 - \frac{26}{3\pi^2}\right]$$

$$I_{33} - \int_0^a x^5 \cos\left(\frac{2\pi x}{a}\right) \sin\left(\frac{\pi x}{a}\right) dx = -\frac{a^6}{3\pi}\left[1 - \frac{260}{9\pi^2} + \frac{4840}{27\pi^4}\right]$$

$$I_{34} - \int_0^a x^4 \sin^2\left(\frac{2\pi x}{a}\right) dx = \frac{a^5}{10}\left[1 - \frac{5}{4\pi^2} + \frac{15}{32\pi^4}\right]$$

$$I_{35} - \int_0^a x^6 \sin^2\left(\frac{2\pi x}{a}\right) dx = \frac{a^7}{14}\left[1 - \frac{35}{16\pi^2} + \frac{175}{64\pi^4} - \frac{525}{512\pi^6}\right]$$

$$I_{36} - \int_0^a x^3 \sin\left(\frac{2\pi x}{a}\right) \cos\left(\frac{\pi x}{a}\right) dx = \frac{2a^4}{3\pi}\left[1 - \frac{14}{3\pi^2}\right]$$

$$I_{37} - \int_0^a x^5 \sin\left(\frac{2\pi x}{a}\right) \cos\left(\frac{\pi x}{a}\right) dx = \frac{2a^6}{3\pi}\left[1 - \frac{140}{9\pi^2} + \frac{2440}{27\pi^4}\right]$$

$$I_{38} - \int_0^a x^3 \sin\left(\frac{2\pi x}{a}\right) \cos\left(\frac{2\pi x}{a}\right) dx = -\frac{a^4}{8\pi}\left[1 - \frac{3}{8\pi^2}\right]$$

$$I_{39} - \int_0^a x^5 \sin\left(\frac{2\pi x}{a}\right) \cos\left(\frac{2\pi x}{a}\right) dx = -\frac{a^6}{8\pi}\left[1 - \frac{5}{4\pi^2} + \frac{15}{32\pi^4}\right]$$

APPENDIX 3

TAPER COEFFICIENTS FOR PLATES OF LINEAR THICKNESS VARIATION

$$G_1 = (1 + e^2)^2 \frac{\pi^4}{4a^2 e}\left[1 + 1.5\delta + \delta^2(1 - \frac{1.5}{\pi^2}) + \frac{\delta^3}{4}(1 - \frac{3}{\pi^2})\right]$$

$$G_2 = -(2^2 + e^2)^2 \frac{\pi^2}{4a^2 e} \quad \frac{8\delta}{3}\left[2(1+\delta) + \delta^2(1 - \frac{40}{9\pi^2})\right]$$

$$G_3 = (1+e^2) \frac{\pi^2}{4a^2 e} 6\delta^2 (1 + 0.5\delta)$$

$$G_4 = (2^2 + e^2) \frac{\pi^2}{4a^2 e} \cdot 8\delta\left[2(1+\delta) + \delta^2(1 - \frac{52}{9\pi^2})\right]$$

$$G_5 = -(1 + \nu e^2) \frac{\pi^2}{4a^2 e} 6\delta^2(1 + 0.5\delta)$$

$$G_6 = -\frac{\lambda}{4a^2 e}(1 + 0.5\delta) = \lambda G_6'$$

$$G_7 = (2^2 + e^2 \nu) \frac{1}{4a^2 e} \frac{32}{3} \delta^3$$

$$G_8 = \frac{\lambda}{4a^2 e} \frac{16\delta}{9\pi^2} = \lambda G_8'$$

$$H_1 = -(1+e^2)^2 \frac{\pi^2}{4a^2 e} \frac{8\delta}{3}\left[2(1+\delta) + \delta^2(1 - \frac{40}{9\pi^2})\right]$$

$$H_2 = (2^2 + e^2)^2 \frac{\pi^4}{4a^2 e}\left[1 + 1.5\delta + \delta^2(1 - \frac{1.5}{4\pi^2}) + \frac{\delta^3}{4}(1 - \frac{3}{4\pi^2})\right]$$

$$H_3 = -(1+e^2) \frac{\pi^2}{4a^2 e} 8\delta\left[2(1+\delta) + \delta^2(1 - \frac{28}{9\pi^2})\right]$$

$$H_4 = (2^2 + e^2) \frac{\pi^2}{4a^2 e} 6\delta^2(1 + 0.5\delta)$$

$$H_5 = -(2^2 + \nu \ e^2) \ \frac{\pi^2}{4a^2 e} \ 6\delta^2 (1+0.5\delta)$$

$$H_6 = G_6 = \lambda \ H_6'$$

$$H_7 = (1+\nu \ e^2) \ \frac{1}{4a^2 e} \ \frac{32}{3} \ \delta^3$$

$$H_8 = G_8 = \lambda \ H_8'$$

APPENDIX 4

TAPER COEFFICIENTS FOR PLATES OF PARABOLIC THICKNESS VARIATION

$$G_1 = (1+e^2)^2 \frac{\pi^4}{4a^2 e}\left[1 - \mu\left(1 - \frac{1.5}{\pi^2}\right) + \frac{3\mu^2}{5}\left(1 - \frac{5}{\pi^2} + \frac{7.5}{\pi^4}\right) - \frac{\mu^3}{7}\left(1 - \frac{10.5}{\pi^2} + \frac{52.5}{\pi^4} - \frac{78.75}{\pi^6}\right)\right]$$

$$G_2 = (2^2+e^2)^2 \frac{\pi^2}{4a^2 e}\frac{16\mu}{3}\left[1 - 2\mu\left(1 - \frac{20}{3\pi^2}\right) + \mu^2\left(1 - \frac{200}{9\pi^2} + \frac{3640}{27\,\pi^4}\right)\right]$$

$$G_3 = -(1+e^2)\frac{\pi^2}{4a^2 e}6\mu\left[1 - 2\mu\left(1 - \frac{1.5}{\pi^2}\right) + \mu^2\left(1 - \frac{5}{\pi^2} + \frac{7.5}{\pi^4}\right)\right]$$

$$G_4 = -(2^2+e^2)\frac{\pi^2}{4a^2 e}16\mu\left[1 - 2\mu\left(1 - \frac{26}{3\pi^2}\right) + \mu^2\left(1 - \frac{260}{9\pi^2} + \frac{4840}{27\pi^4}\right)\right]$$

$$G_5 = (1+\nu e^2)\frac{\pi^2}{4a^2 e}6\mu\left[1 - 2\mu\left(1 - \frac{1.5}{\pi^2}\right) + \mu^2\left(1 - \frac{5}{\pi^2} + \frac{7.5}{\pi^4}\right)\right]$$

$$G_6 = -\frac{\lambda}{4a^2 e}\left[1 - \frac{\mu}{3}\left(1 - \frac{1.5}{\pi^2}\right)\right] = \lambda\, G_6'$$

$$G_7 = (2^2+\nu e^2)\frac{1}{4a^2 e}64\mu^2\left[1 - \frac{5\mu}{3}\left(1 - \frac{20}{3\pi^2}\right)\right]$$

$$G_8 = -\frac{\lambda}{4a^2 e}\frac{16\mu}{9\pi^2} = \lambda\, G_8'$$

$$H_1 = (1+e^2)^2 \frac{\pi^2}{4a^2 e}\frac{16\mu}{3}\left[1 - 2\mu\left(1 - \frac{20}{3\pi^2}\right) + \mu^2\left(1 - \frac{200}{9\pi^2} + \frac{3640}{27\pi^4}\right)\right]$$

$$H_2 = (2^2+e^2)^2 \frac{\pi^4}{4a^2 e}\left[1 - \mu\left(1 - \frac{3}{8\pi^2}\right) + 0.6\mu^2\left(1 - \frac{5}{4\pi^2} + \frac{15}{32\pi^4}\right) - \frac{\mu^3}{7}\left(1 - \frac{35}{16\pi^2} + \frac{175}{64\,\pi^4} - \frac{525}{512\pi^6}\right)\right]$$

$$H_3 = (1+e^2)\frac{\pi^2}{4a^2 e}16\mu\left[1 - 2\mu\left(1 - \frac{14}{3\pi^2}\right) + \mu^2\left(1 - \frac{140}{9\pi^2} + \frac{2440}{27\pi^4}\right)\right]$$

$$H_4 = -(2^2 + e^2) \frac{\pi^2}{4a^2 e} 6\mu \left[1 - 2\mu \left(1 - \frac{3}{8\pi^2} \right) + \mu^2 \left(1 - \frac{5}{4\pi^2} + \frac{15}{32\pi^4} \right) \right]$$

$$H_5 = (2^2 + \nu e^2) \frac{\pi^2}{4a^2 e} 6\mu \left[1 - 2\mu \left(1 - \frac{3}{8\pi^2} \right) + \mu^2 \left(1 - \frac{5}{4\pi^2} + \frac{15}{32\pi^4} \right) \right]$$

$$H_6 = - \frac{\lambda}{4a^2 e} \left[1 - \frac{\mu}{3} \left(1 - \frac{3}{8\pi^2} \right) \right] = \lambda H_6'$$

$$H_7 = (1 + \nu e^2) \frac{1}{4a^2 e} 64\mu^2 \left[1 - \frac{5\mu}{3} \left(1 - \frac{20}{3\pi^2} \right) \right]$$

$$H_8 = - \frac{\lambda}{4a^2 e} \frac{16\mu}{9\pi^2} = \lambda H_8'$$

APPENDIX 5.1

COMPUTER PROGRAMME FOR THE EVALUATION OF MODAL LOSS FACTOR

```
    DIMENSION SIA(10),COA(10)
    OUTPUT   FORMAT
 50 FORMAT(E20.6,4F8.3,F10.5)
    INPUT   FORMAT
 10 FORMAT(3F4.1,3F8.3,2F10.5,2E12.3)
    PI=3.14159265
    X=1./32.
    X1=1./16.
    DO 200 I=1,8
    PIX=PI*X
    SIA(I)=SIN(PIX)
    COA(I)=COS(PIX)
200 X=X+X1
700 READ 10,PM,PN,PNU,A,B,SN,P,H,E,SJ
    CK=1.+3.**SN+5.**SN+7.**SN
    CF=SJ*E/(84.*PI)
    CFF=CK*CF
    SN2=1./(SN-1.)
    SN6=1./SN
    SN7=(SN-2.)/SN
    CMA=PM*PM/(A*A)
    CNB=PN*PN/(B*B)
    CMN=CMA+CNB
    C=3.*P/(PI*PI*H*H*A*3*CMN*CMN)
    CMN1=CMA+PNU*CNB
    CMN2=CMA*PNU+CNB
    CMN3=CMN1*C
    CMN4=CMN2*C
    CMN5=0.7*PM*PN*C/(A*3)
 30 D=0.
    US=0.
    J=1
    K=1
```

```
  9 CXY=SIA(J)*SIA(K)
    CT=COA(J)*COA(K)
    SX=CXY*CMN3
    SY=CXY*CMN4
    ST=CT*CMN5
    C1=0.5*(SX+SY)
    C2=0.5*(SX-SY)
    C3=SQRT(C2*C2+ST*ST)
    SP11=C1+C3
    SP22=C1-C3
    SP1=ABS(SP11)
    SP2=ABS(SP22)
    IF(SP1-SP2)40,60,60
 60 RP=SP2/SP1
    SED=SP1*(1.+RP)
    SEDD=SP1*SP1*(1.-2.*PNU*RP+RP*RP)
    GO TO 75
 40 RP=SP1/SP2
    SED=SP2*(1.+RP)
    SEDD=SP2*SP2*(1.-2.*PNU*RP+RP*RP)
 75 IF(J-K) 300,400,300
400 DED=SED**SN
    USD=SEDD
    GO TO 500
300 DED=2.*(SED**SN)
    USD=2.*SEDD
500 D=D+DED
    US=US+USD
    J=J+1
    IF(J-8)9,9,21
 21 K=K+1
    J=K
    IF(I-8)9,9,23
 23 ETA=CFF*D/US
    ETAP=ETA**SN1
    PRINT 50,ETAP,PM,PN,A,B,H
    GO TO 700
    STOP
    END
```

APPENDIX 5.2

COMPUTER PROGRAMME FOR THE EVALUATION)F FUNDAMENTAL MODE

LOSS FACTOR FOR A LINEARLY VARYING THICKNESS PLATE --

ONE TERM GALERKIN SOLUTION

```
      DIMENSION SIA(10),COA(10),ALPX(20)
C     OUTPUT   FORMATS
   55 FORMAT(2E16.6,2F8.3)
   95 FORMAT(2F10.4,2E16.6,2F12.4)
C     INPUT   FORMATS
   20 FORMAT(F5.2,F15.5)
   30 FORMAT(F10.5,E16.6)
   50 FORMAT(F4.1,3F10.5,2E12.3)
      READ 50,PNU,SN,P,H,E,SJ
      A=59.06
      PI=3.14159265
      SN1=SN-2.
      SN2=1./(SN-1.)
      SN6=1./SN
      SN7=SN1/SN
      CK=1.+3.**SN+5.**SN+7.**SN
      CF=SJ*E/(84.*PI)
      CFF=CK*CF
      PI2=PI*PI
      PI4=PI2*PI2
      A4=A**4.
      AB1=1./(A*A)
      X=1./32.
      X1=1./16.
      DO 200 I=1,8
      PIX=PI*X
      SIA(I)=SIN(PIX)
      COA(I)=COS(PIX)
      X=X+X1
  200 CONTINUE
```

```
 10 READ 30,AR,ETAC
    B=A/AR
    AB2=1./(B*B)
    AB=AB1+AB2
    ABSQ=AB*AB
    AB11=AB1+PNU*AB2
    AB22=PNU*AB1+AB2
    JJ=1
700 READ 20,ALPH,FP
    ALPH2=ALPH*ALPH
    ALPH3=ALPH*ALPH2
    C11=1.+1.5*ALPH+ALPH2*(1.-1.5/PI2)+0.25*ALPH3*(1.-3./PI2)
    C12=PI4*0.25*A*B*ABSQ*C11
    C13=1.5*PI2*ALPH2*AB*(1.+0.5*ALPH)/AR
    CC2=0.25*A*B*(1.+ALPH*0.5)
    C14=6.*PI2*AB11*ALPH2*CC2*AB1
    CC1=C12+C13-C14
    FPN=CC1*A4/CC2
    ERROR=100.*(FPN-FP)/FP
    PRINT 95,ALPH,AR,CC1,CC2,FPN,ERROR
    X=1./32.
    X1=1./16.
    DO 900 I=1,16
    ALPX(I)=1.+ALPH*X
    X=X+X1
900 CONTINUE
    CMN3=0.75*P*PI2/(H*H*CC1)
    CMN4=0.7*CMN3/(A*B)
    CMN5=CMN3*AB11
    CMN6=CMN3*AB22
    D=0.
    US=0.
    J=1
    K=1
  9 CXY=ALPX(J)*SIA(J)*SIA(K)
    CT=ALPX(J)*COA(J)*COA(K)
    SX=CMN5*CXY
    SY=CMN6*CXY
    ST=CMN4*CT
    C1=0.5*(SX+SY)
    C2=0.5*(SX-SY)
    C3=SQRT(C2*C2+ST*ST)
```

```
      SP11=C1+C3
      SP22=C1-C3
      SP1=ABS(SP11)
      SP2=ABS(SP22)
      IF(SP1-SP2)40,60,60
   60 RP=SP2/SP1
      SED=SP1*(1.+RP)
      SEDI =SP1*SP1*(1.-2.*PNU*RP+RP*RP)
      GO TO 75
   40 RP=SP1/SP2
      SED=SP2*(1.+RP)
      SEDI =SP2*SP2*(1.-2.*PNU*RP+RP*RP)
   75 IF(J-K) 300,400,300
  400 M=17-J
      Z1=ALPX(J)+ALPX(M)*((ALPX(M)/ALPX(J))**SN)
      Z2=ALPX(J)+ALPX(M)*((ALPX(M)/ALPX(J))**2.)
      DED=(SED**SN)*Z1
      USD=SEDD*Z2
      GO TO 500
  300 M=17-J
      N=17-K
      Z3=ALPX(J)+((ALPX(K)/ALPX(J))**SN)*ALPX(K)
      Z4=((ALPX(M)/ALPX(J))**SN)*ALPX(M)+((ALPX(N)/ALPX(J))**SN)*ALPX(N)
      Z5=ALPX(J)+((ALPX(K)/ALPX(J))**2.)*ALPX(K)
      Z6=((ALPX(M)/ALPX(J))**2.)*ALPX(M)+((ALPX(N)/ALPX(J))**2.)*ALPX(N)
      DED=(SED**SN)*(Z3+Z4)
      USD=SEDD*(Z5+Z6)
  500 D=D+DED
      US=US+USD
      J=J+1
      IF(J-8)9,9,21
   21 K=K+1
      J=K
      IF(K-8) 9,9,23
   23 ETA=CFF*D/US
      ETAP=ETA**SN2
      RATIO=ETAP/ETAC
      PRINT 55,ETAP,RATIO,ALPH,AR
      JJ=JJ+1
      IF(JJ-8)700,700,10
      END
```

APPENDIX 5.3

COMPUTER PROGRAMME FOR THE EVALUATION OF FUNDAMENTAL MODE

LOSS FACTOR FOR A LINEARLY VARYING THICKNESS PLATE---

TWO TERM GALERKIN SOLUTION

```
      DIMENSION SIA(10),COA(10),ALPX(20),SIB(10),COB(10)
C     OUTPUT   FORMATS
    1 FORMAT(6E13.5)
    2 FORMAT(5E16.6)
    3 FORMAT(2F8.3,2E16.6)
    4 FORMAT(2E16.6,2F10.2)
C     INPUT   FORMATS.
   20 FORMAT(F5.2,F15.5)
   30 FORMAT(F10.5,E16.6)
   50 FORMAT(F4.1,3F10.5,2E12.3)
      READ 50,PNU,SN,P,H,E,SJ
      PI=3.14159265
      A=59.06
      SN1=SN-2.
      SN2=1./(SN-1.)
      SN3=SN+1.
      SN6=1./SN
      SN7=SN1/SN
      CK=1.+3.**SN+5.**SN+7.**SN
      CF=SJ*E/(84.*PI)
      CFF=CK*CF
      PI2=PI*PI
      PI4=PI2*PI2
      A4=A**4.
      AB1=1./(A*A)
      BO=E*(H**3.)/10.92
      CMN1=0.75*BO*PI2/(H*H)
      PII=1.5/PI2
      PIJ=2.*PII
      X=1./32.
      X1=1./16.
      DO 200 I=1,8
      PIX=PI*X
      SIA(I)=SIN(PIX)
      COA(I)=COS(PIX)
      PIXX=2.*PIX
      SIB(I)=SIN(PIXX)
      COB(I)=COS(PIXX)
      X=X+X1
  200 CONTINUE
```

```
10 READ 30,AR,ETAC
   B=A/AR
   AB2=1./(B*B)
   AB11=AB1+PNU*AB2
   AB22=PNU*AB1+AB2
   AB33=4.*AB1+PNU*AB2
   AB44=4.*PNU*AB1+AB2
   CMN2=CMN1*0.7/(A*B)
   Z1=1./(A*A*AR)
   Z2=0.25*Z1
   ARS=AR*AR
   Z3=1.+ARS
   Z4=4.+ARS
   Z5=Z3*Z3*PI4*Z2
   Z6=Z4*Z4*PI2*Z2
   Z7=Z3*Z1*PI2*1.5
   Z8=-8.*PI2*Z2*Z4
   Z9=-6.*PI2*Z2*(1.+0.3*ARS,
   Z11=Z3*Z3*Z2*PI2/3.
   Z12=Z4*Z4*PI4*Z2
   Z13=-Z3*Z2*PI2*8.
   Z14=Z4*Z2*PI2*6.
   Z15=-6.*PI2*(4.+0.3*ARS)*Z2
   Z16=32.*Z2*(4.+0.3*ARS)/3.
   Z17=32.*Z2*(1.+0.3*ARS)/3.
   JJ=1
700 READ 20,ALPH,FP
   X=1./32.
   X1=1./16.
   DO 900 I=1,16
   ALPX(I)=1.+ALPH*X
   X=X+X1
900 CONTINUE
   ALPH2=ALPH*ALPH
   ALPH3=ALPH*ALPH2
   ALPC=1.+0.5*ALPH
   AL=ALPC*ALPH2
   ALL=1.+ALPH
   G1=Z5*(1.+1.5*ALPH+ALPH2*(1.-PII)+0.25*ALPH3*(1.-PIJ))
   G2=Z6*(-16.*ALL*ALPH/3.+ALPH3*(320./(9.*PI2)-8.)/3.)
   G3=AL*Z7
   G4=Z8*(ALPH *(52./(9.*PI )-1.)-2.*ALL)*ALPH
   G5=AL*Z9
   G6=-ALPC*Z2
   G7=Z16*ALPH3
   G8=Z2*ALPH*16./(9.*PI2)
   H1=Z11*(ALPH3*(320./(9.*PI2)-8.)-16.*ALPH*ALL)
   H2=Z12*(1.+1.5*ALPH+ALPH2*(1.-PII/4.)+0.25*ALPH3*(1.-PIJ/4.))
   H3=Z13*ALPH*(2.*ALL+ALPH2*(1.-28./(9.*PI2)))
   H4=AL*Z14
   H5=AL*Z15
   H6=G6
   H7=Z17*ALPH3
   H8=G8
```

```
      A1=H1+H3+H7
      A2=H2+H4+H5
      B1=G1+G3+G5
      B2=G2+G4+G7
      B4=P/BO
      F1=B1+H6
      F2=A2+H6
      F3=A1+H8
      F4=B2+H8
      XF1=H6*H6-H8*H8
      XF2=H6*(A2+B1)-H8*(A1+B
      XF3=B1*A2-A1*B2
      XF4=-XF2/(2.*XF1)
      XF5=XF2*XF2-4.*XF1*XF:
      XF6=ABS(XF5)
      XF7=SQRT(XF6)/(2.*XF1)
      FP1=XF4+XF7
      FP2=XF4-XF7
      F1=B1+H6*FP2
      F2=A2+H6*FP2
      F3=A1+H8*FP2
      F4=B2+H8*FP2
      F6=A2*F1+B1*F2-A1*F4-B2*F3
      A11=B4*F2/F6
      A21=-B4*F3/F6
      ERROR=100.*(FP2-FP)/FP
      PRINT 1,A1,A2,B1,B2,A11,A21
      PRINT 2,F1,F2,F3,F4,F6
      PRINT 3,AR,ALPH,FP2,ERROR
      D=0.
      US=0.
      J=1
      K=1
      NN=1
      MM=1
    9 CXY1=A11*SIA(J)*SIA(K)
      CXY2=A21*SIB(J)*SIA(K)
      CT1=A11*COA(J)*COA(K)
      CT2=2.*A21*COB(J)*COA(K)
   11 CT=CT1+CT2
      SX=ALPX(J)*(CXY1*AB11+CXY2*AB33)*CMN1
      SY=ALPX(J)*(CXY1*AB22+CXY2*AB44)*CMN1
      ST=ALPX(J)*CMN2*CT
      C1=0.5*(SX+SY)
      C2=0.5*(SX-SY)
      C3=SQRT(C2*C2+ST*ST)
      SP11=C1+C3
      SP22=C1-C3
```

```
      SP1=ABS(SP11)
      SP2=ABS(SP22)
      IF(SP1-SP2)40,50,60
   60 RP=SP2/SP1
      SED=SP1*(1.+RP)
      SEDD=SP1*SP1*(1.-2.*PNU*RP+RP*RP)
      GO TO 75
   40 RP=SP1/SP2
      SED=SP2*(1.+RP)
      SEDD=SP2*SP2*(1.-2.*PNU*RP+RP*RP)
   75 DED=ALPX(J)*(SED**SN)
      USD=SEDD*ALPX(J)
      D=D+DED
      US=US+USD
      IF(J-K)300,400,300
  400 NN=NN+1
      IF(NN-2)15,12,15
   12 J=17-J
      CXY2=-CXY2
      CT1=-CT1
      GO TO 11
  300 MM=MM+1
      IF(MM-2)17,16,17
   16 DED=DED*((ALPX(K)/ALPX(J))**SN3)
      USD=USD*((ALPX(K)/ALPX(J))**2.)
      D=D+DED
      US=US+USD
      J=17-J
      CXY2=-CXY2
      CT1=-CT1
      GO TO 11
   17 N=17-K
      DED=DED*((ALPX(N)/ALPX(J))**SN3)
      USD=USD*((ALPX(N)/ALPX(J))**2.)
      D=D+DED
      US=US+USD
   15 J=17-J
      J=J+1
      MM=1
      IF(J-8)9,9,21
   21 K=K+1
      J=K
      NN=1
      IF(K-8) 9,9,23
   23 ETA=CFF*D/US
      ETAP=ETA**SN2
      RATIO=ETAP/ETAC
      PRINT 4,ETAP,RATIO,ALPH,AR
      JJ=JJ+1
      IF(JJ-8)700,700,10
      END
```

APPENDIX 5.4

COMPUTER PROGRAMME FOR THE EVALUATION OF RADIATION

EFFICIENCY FOR THE PLATE VIBRATING UNDER COMPLEX

NON-RESONANCE CONDITION (SUPERPOSITION OF 175 MODES)

```
      DIMENSION U(5),R(5)
      DIMENSION PM(175),PN(175),FRQ(175),UMN(175),RFS(175),GP(175)
      DIMENSION AMP(175,25),DELT(175,25),BNP(175,25),GAM(175,25)
C     OUTPUT FORMATS
  100 FORMAT(/6HEXFRQ=F8.2,2X,4HFRQ=F8.2,2X,4HVEL=E16.4,2X,5HVELT=E16.4)
  200 FORMAT(3HPM=F4.0,1X,3HPN=F4.0,1X,4HRFS=E12.4,4HR'JU=E12.4,5X,4HSPR=
     1E16.4)
  400 FORMAT(2HI=I3,2X,4HRE1=E12.4,2X,4HRE2=E12.4,2X,3HRE=E12.4,2X,5HTSP
     2R=E15.4)
C     INPUT FORMATS
   10 FORMAT(2F10.3,3F10.6,F10.2,I5)
   20 FORMAT(F10.2)
   30 FORMAT(I5)
   40 FORMAT(2F5.0,20X,F20.10,30X)
      PI=3.14159265
      PII=PI*0.25
      PIJ=PI**4.
      PIK=PI*0.5
      PIL=2.*PI
C     GAUSS 5-POINT INTEGRATION COEFFICIENTS
      U(1)=0.
      U(2)=0.26923465
      U(3)=-0.26923465
      U(4)=0.45308992
      U(5)=-0.45308992
      R(1)=64./225.
      R(2)=0.23931433
      R(3)=0.23931433
      R(4)=0.11846344
      R(5)=0.11846344
```

```
      READ 10,A,B,RHO,P,H,C,NG
      C2=2.*P/(PI*A*B*RHO*H)
      READ 30,MODE
      READ 40,(PM(I),PN(I),FRQ(I),I=1,MODE)
   90 READ 20,EXFRQ
      WNK=PIL*EXFRQ/C
      WA=WNK*A
      WB=WNK*B
      C1=16.*WA*WB/PIJ
      PROD=EXFRQ*EXFRQ
      SIGMA=0.
      I=1
      RU=0.
      II=1
      JJ=1
      RV=0.
   70 PMS=PM(I)*PM(I)
      PNS=PN(I)*PN(I)
      TERM=FRQ(I)*FRQ(I)
      CMN=EXFRQ/(TERM-PROD)
      UMN(I)=C2*CMN
      USQ=UMN(I)*UMN(I)
      VEL=USQ/8.
      SIGMA=SIGMA+USQ
      VELT=SIGMA/8.
      PRINT 100,EXFRQ,FRQ(I),VEL,VELT
      PMP=PM(I)*PI
      PNP=PN(I)*PI
      N=JJ+1
      DO 95 M=II,JJ
   95 GP(M)=0.
      GS=0.
      JK=1
C     NUMERICAL  INTEGRATION  BY  GAUSS  QUADRATURE  METHOD
      DO 50 J=1,NG
      T1=SIN(PIK*U(J)+PII)
      DO 50 K=1,NG
      T2=PIK*U(K)+PII
      A1=WA*T1*COS(T2)
      B1=WB*T1*SIN(T2)
```

```
      AC=COS(0.5*A1)
      BC=COS(0.5*B1)
      T3=AC*AC*BC*BC*T1
      AMP(I,JK)=A1/PMP
      DELT(I,JK)=AMP(I,JK)*AMP(I,JK)-1.
      BNP(I,JK)=B1/PNP
      GAM(I,JK)=BNP(I,JK)*BNP(I,JK)-1.
      GAUS=T3/(DELT(I,JK)*DELT(I,JK)*GAM(I,JK)*GAM(I,JK))
      GUU=GAUS*R(J)*R(K)
      GS=GS+GUU
      IF(I-1)50,50,60
   60 DO 65 M=II,JJ
      GAUP=T3/(DELT(M,JK)*DELT(N,JK)*GAM(M,JK)*GAM(N,JK))
      GVV=GAUP*R(J)*R(K)
   65 GP(M)=GP(M)+GVV
   50 JK=JK+1
   55 CONTINUE
      RFS(I)=C1*GS/(PMS*PNS)
      SPR=RFS(I)*VEL
      RUU=RFS(I)*USQ
      RU=RUU+RU
      PRINT 200,PM(I),PN(I),RFS(I),RUU,SPR
      IF(I-1)15,15,25
   25 DO 75 M=II,JJ
      C3=2.*UMN(M)*UMN(N)
      C4=PM(M)*PM(N)*PN(M)*PN(N)
      RFP=C1*C3*GP(M)/C4
   75 RV=RV+RFP
   85 CONTINUE
      RE1=RU/SIGMA
      RE2=RV/SIGMA
      RE=RE1+RE2
      TSPR=RE*VELT
      PRINT 400,I,RE1,RE2,RE,TSPR
      JJ=JJ+1
   15 I=I+1
      IF(I-MODE)70,70,80
   80 GO TO 90
      STOP
      END
```

-168-

BIBLIOGRAPHY

1. Appl, F.C., and Byers, N.R., 'Fundamental Frequency of Simply Supported Rectangular Plates of Linear Varying Thickness", J.Appl.Mech., V32, N.1,p.163,1965.

2. Bailey, J.R. and Fahy, F.J., 'Radiation and Response of Cylindrical Beams excited by Sound', Trans.ASME., Ser.'B', V94, N1, p.139,1972.

3. Beranek, L.L., 'The Transmission and Radiation of Acoustic Waves by Structures', Proc. I.Mech.E.,V.173, p.12, 1959.

4. Chan, C.M.P. and Anderton, D. 'The Correlation of Machine Structure Surface Vibration and Radiated Noise', Inter-Noise 72 Proc. Washington, D.C. p.261,1972.

5. Cochardt, A.W., 'A Method for Determining Internal Damping of Machine Members', J.Appl. Mech., V,76, p.257, 1954.

6. Crandall,S.H., 'The Role of Damping in Vibration Theory', J.S. and V., V.11, N1, p.3, 1970.

7. Cremer, L., 'Calculation of Sound Propagation in Structures,' Acoustica, V.3, p.317, 1953.

8. Cremer, L. and Schwantke, G., 'Zum problem der abstrahlung von biegewellen', Acustica, V7, p.329, 1957.

9. Crocker, M.J. and Price, A.J., 'Sound Transmission Using Statistical Energy Analysis", J.S and V., V9, N3, p.469, 1969.

10. Crocker, M.J.and Price,A.J., 'Damping in Plates', Letter, J.S and V, V9, n3, p.501, 1969.

11. Donato,R.J., 'Direct Derivation of Radiation Resist-
    ance of a Vibrating Panel', J.S. and V., V.28, N1,
    p. 87, 1973.

12. Dym, C.L., 'A more Direct Derivation of Radiation
    Resistance of a Panel', J. S and V., V.32, N.2,p.279,
    1974.

13. Fahy, F.J. and Wee, R.B.S., 'Some Experiments with
    Stiffened Plates under Acoustic Excitation', J.S. and
    V., V7, p.431, 1968.

14. Fahy, F.J., Reply to Letter 'Damping in Plates',
    J.S and V., V.9, N.3, p.506, 1969a

15. Fahy, F.J., 'Structural-Acoustic Interaction', Adv.
    Course in Noise and Vib., ISVR, University of Southampton,
    Ch.20, 1973.

16. Feit , D., 'Pressure Radiated by Point Excited
    Elastic Plate', J.Acoust.Soc.Am., V.40,p.1489,1966.

17. Gomperts, M.C., 'Sound Radiation from a Thin Infinite
    Plate Excited by a Harmonic Line Force, Point Force or
    Moment near the Critical Frequency', Proc.7th Int.Cong.
    Acoust.Budapest, 1971.

18. Gösele, K., 'Schallabstrahlung von platten,die zu
    biegeschwingungen angeregt sind', Acustica, V.3, p.243,
    1953.

19. Gösele, K., 'Abstrahlverhalten von wanden', Acustica,
    V.6, p.94, 1956.

20. Greene, D.C., 'Vibration and Sound Radiation of damped and undamped flat plates', J.Acoust.Soc.Am., V.33, N.10, p.1315, 1961.

21. Gutin, L.Y., 'Sound Radiation from an Infinite Plate Excited by a Normal Point Force', Sov.Phy.Acoust., V10, N.4, p.331, 1965.

22. Hamme, R.N., 'Materials and Techniques for Damping Vibrating Panels', Noise Control, p.23, March 1957.

23. Heckl, M., 'Schallabstrahlung von platten bei punkt-formiger anregung', Acustica, V.9, p.371, 1959.

24. Heckl, M., 'Measurements of Absorption Coefficients on Plates', J.Acoust.Soc.Am., V34, p.803, 1962.

25. Hooker, R.J., 'Equivalent Stress for Representing Damping in Combined Stress,' J.S. and V., V.10, N.1, p.62, 1969.

26. Ivanov, V.S. and Romanov, V.N., 'Determination of the Sound Pressure near the Surface of an Infinite Plate Driven by a Point Source,' Sov.Phy.Acoust., V.16, N.4, 1971.

27. Jain, R.K. and Soni, S.R., 'Free Vibrations of Rectangular Plates of Parabolically Varying Thickness', Indian Jr. of Pure and App.Maths, V.4, N.3, p.267, 1973.

28. Johnston, R.A. and Barr, A.D.S., 'Acoustic and Internal Damping in Uniform Beams', Jr.Mech.Engg. Sci., V.11, N2, p.117, 1969.

29. Junger, M.C. and Feit, D., 'Sound, Structures, and their Interaction', The MIT Press, 1972.

30. Kantorovich, L.V. and Krylov, V.I., 'Approximate Methods of Higher Analysis', 3rd ed., Inter Science Pub.Inc.New York, 1964.

31. King, A.J., 'Vibration and Noise of Mechanisms and machines- Causes and Remedies, ' Engineering, V.183, p.716, 1957.

32. Kurtze, G. and Bolt, R.H., 'On the Interaction between Plate Bending Waves and their Radiation Load', Acustica, V.9, p.238, 1959.

33. Lazan, B.J. and Demer, L.J., 'The Damping, Elasticity and Fatigue Properties of Temperature Resistant Materials', Proc. ASTM, V.51, p.611, 1951.

34. Lazan, B.J., 'Effect of Damping Constants and Stress Distribution on the Resonance Response of Members', J.Appl. Mech., V.20, p.201, 1953.

35. Lazan, B.J., 'Energy Dissipation Mechanisms in Structures, with Particular Reference to Material Damping', Structural Damping, J.E.Ruzicka, Ed., ASME, Sec.1,1959.

36. Lazan, B.J., and Goodman, L.E., 'Material and Interface Damping', Shock and Vibration Handbook, C.M. Harris and C.E.Crede, Eds., McGraw Hill, Chap.36, 1961.

37. Lazan, B.J., 'Damping of Materials and Members in Structural Mechanics', Pergamon, 1st ed., 1968.

38. Leissa, A.W., 'Vibration of Plates', NASA, SP-160, 1969.

39. Lyamshev, L.M., 'Theory of sound radiation by thin elastic shells and plates', Sov.Phys.Acoust., V.5,N.4, p.431, 1960.

40. Lyon, R.H. and Maidanik, G., 'Power Flow between Linearly Coupled Oscillators', J.Acoust.Soc.Am., V.34, p.623,1962.

41. Lyon, R.H., 'Sound Radiation from a beam attached to a Plate,' J.Acoust.Soc.Am., V.34, p.1265, 1962.

42. Maidanik, G., 'Response of Ribbed Panels to Reverberant Acoustic Fields', J.Acoust.Soc.Am., V.34, p.809, 1962.

43. Maidanik, G. and Kerwin,Jr.E.M., 'Influence of Fluid Loading on the Radiation from Infinite Plates below the Critical Frequency', J.Acoust.Soc.Am., V.40, p.1034, 1966.

44. Maidanik, G., 'The Influence of ^{F}luid Loading on the Radiation from Orthotropic Plates', J.S. and V.,V3, N.3, p.288, 1966.

45. Mangiarotty, R.A., 'Acoustic Radiation Damping of Vibrating Structures', J.Acoust.Soc.Am., V.35, p.369, 1963.

46. Manning, J.E. and Maidanik, G., 'Radiation Properties of Cylindrical Shells', J.Acoust.Soc. Am., V.36, p.1691, 1964.

47. Marin, J. and Stulen, F.B., 'A New Fatigue Strength-Damping Criterion for the Design of Resonance Members,' Trans.ASME, 69, A-209,1947.

48. Mazzola, C.J., 'Acoustic Radiation from an Infinite Plate with a Baffle Normal to its Surface', J.S. and V., V.13, N.2, p.163, 1970.

49. Mead, D.J., 'Criteria for Comparing the Effectiveness of Damping Treatments', Noise Control, p.27, May-June 1961.

50. Mead, D.J., 'The Practical Problems of Assessing Damping Treatments', Jr. S. and V., V.1, N.3,p.270,1964.

51. Mentel, T.J. and Fu, C.C. 'Damping Energy Dissipation at Support Interfaces of Square Plates', WADC Tech.Rept. 59-96, June 1959.

52. Mentel,T.J., 'Vibration Energy Dissipation at Structural Support Junctions', Structural Damping, J.E.Ruzicka,Ed., ASME, Sect.4, 1959.

53. Mentel, T.J. and Chi, S.H., 'Experimental Study of Dilatational Versus Distortional-Straining Action in Material-Damping Production', J.Acoust. Soc. Am., V.36, p.357, 1964.

54. Meyer, E., 'Messungen zur korperschallubertragung an hand von modellen', Acustica, V.6, p.51, 1956.

55. Myklestad, N.O., 'The Concept of Complex Damping', J.Appl.Mech.V.19, No.3, p.284, 1952.

56. Nigam, S.P. and Grover, G.K., 'Evaluation of Fundamental Mode Loss Factor for a Rectangular Plate', Proc. 19th Congress, ISTAM, 1974.

57. Nigam, S.P.,Grover, G.K. and Lal,S., 'Loss Factor for a Simply Supported Rectangular Plate of Variable Thickness', accepted for publication in AIAA.

58. Nikiforov, A.S., 'Radiation from a Plate of Finite Dimensions with Arbitrary Boundary Conditions', Sov. Phy. Acoust. V.10, N.2, p.178, 1964.

59. Plahkov, D.D., 'Near Sound Field of an Infinite Plate Driven by a Point Force', Sov.Phy.Acoust., V.13, p.264, 1967.

60. Rao, B.V.A., Rama Bhat, B., and Sastry, R.V.R., 'Determination of Natural Frequencies and Modal Patterns of Vibrating Structures by Acoustic Measurements', 15th Cong. ISTAM, India.p.21, 1970.

61. Robertson, J.M. and Yorgiadis, A.J., 'Internal Friction in Engineering Materials', Trans.ASME, 68, A-173, 1946.

62. Scarborough, J.B., 'Numerical Mathematical Analysis', Oxford and IBH, 6th ed. Ch.8,1966.

63. Skudrzyk, E.J., 'Vibrations of a System with a Finite or an Infinite Number of Resonances,' J.Acoust. Soc., Am., V.30, N.12, p.1140, 1958.

64. Skudrzyk, E.J., 'Sound Radiation of a System with a Finite or an Infinite Number of Resonances', J.Acoust.Soc.Am., V.30, No.12, p.1152,1958.

65. Skudrzyk, E.J., 'Theory of Noise and Vibration Insulation of a System with Many Resonances,' J.Acoust. Soc.Am., V.31, N.1, p.68, 1959.

66. Smith, Jr. P.W., 'Response and Radiation of Structural Modes Excited by Sound', J.Acoust. Soc.Am.,V.34, p.640, 1962.

67. Smith, Jr..P.W., 'Coupling of Sound and Panel Vibration below the Critical Frequency, 'J.Acoust.Soc.Am., V.36, p.1516,1964.

68. Snowdon, J.C., 'Vibration and Shock in Damped Mechanical Systems', Wiley, 1968.

69. Soni, S.R., 'Vibrations of Elastic Plates and Shells of Variable Thickness', Ph.D.Thesis, University of Roorkee, 1972.

70. Timoshenko, S., and Woinowsky-Krieger, S., 'Theory of Plates and Shells', McGraw-Hill, New York, 1959.

71. Ungar, E.E.,   'Maximum Stresses in Beams and Plates Vibrating at Resonance',Trans.ASME, Ser.B., V.84, p.149, 1962.

72. Ungar, E.E.,   'Damping of Panels', Noise and Vibration Control, L.L. Beranek, Ed., McGraw-Hill,Ch.14,1971.

73. Ver, I.L., and Holmer, C.I.,   'Interaction of Sound Waves with Solid Structures', Noise and Vibration Control, L.L.Beranek, Ed., McGraw Hill, Ch.11,1971.

74. Volterra, E. and Zachmanoglou,E.C.,   'Dynamics of Vibrations', Charles, E., Merrill Books, Inc., 1965.

75. Wallace, C.E.,   'Radiation Resistance of a Baffled Beam', J.Acoust.Soc.Am., V.51,N.3(II), p.936,1972.

76. Wallace, C.E.,   'Radiation Resistance of a Rectangular Panels', J.Acoust.Soc.Am., V.51, N.3(II),p.946,1972.

77. Waller, M.D.,   'Concerning Combined and Degenerate Vibration of Plates', Acustica, V.3, p.370, 1953.

78. Waller, M.D.,   'Critical Review of Earlier Chladni Figures', Acustica, V.4, p.677, 1954.

79. Warburton, G.B.,   'The Vibration of Rectangular Plates', Proc. I.Mech.E., V.168, p.371, 1954.

80. Westphal, W.,   'Zur schallabstrahlung einerzu biegeschwingungen angeregten wand', Acustica, V.4, p.603,1954.

81. Whittier, J.S.,   'Phenomenological Theories of hysteretic material damping with application to the vibrations of Circular Plates', ASD Tr.61-264, Nov.1961.

82. Whittier, J.S., 'Hysteretic Damping of Structural Materials under Biaxial Dynamic Stresses', Expl.Mech. V2, p.321, 1962.

83. Yorgiadis, A.J., 'Damping Capacity of Materials', Prod.Engg., V.25, p.164, 1954.